EFFECT OF MODERATE CONFINEMENT ON FLEXURE BEHAVIOR OF REINFORCED CONCRETE BEAMS

By

Muhammad Haris Hameed

(2011-NUST-MS Ph.D-Str-18)

This thesis is submitted in partial fulfilment of the requirements for the degree of

Master of Science

In

Structural Engineering

NUST Institute of Civil Engineering (NICE)
School of Civil & Environmental Engineering (SCEE)
National University of Sciences and Technology (NUST)
Islamabad, Pakistan

2015

This is to certify that

Thesis entitled

EFFECT OF MODERATE CONFINEMENT ON FLEXURE BEHAVIOR OF REINFORCED CONCRETE BEAMS

Submitted by

Muhammad Haris Hameed

Has been accepted towards the partial fulfillment

of

the requirements

for

Master of Science in Civil Engineering

_____

Brigadier (Retired) Dr. Khaliq-ur-Rashid Kayani

National Institute of Civil Engineering

School of Civil and Environmental Engineering

National University of Sciences and Technology, Islamabad.

DEDICATED

TO

MY PARENTS, TEACHERS

AND

WELL WISHERS

ACKNOWLEDGEMENTS

All praise to Almighty Allah who gave the courage and power to the author for completing this research work.

I am heartily thankful to my supervisor **Brig. (Retd.) Prof. Dr. Khaliq ur Rashid Kayani**, for giving me time and support from initial to final level made it possible for me to complete this work especially in the compilation of this manuscript and discussions.

I must not forget the supporting role of my friends and especially to **Engr. Sajjad Ahmad**, **Engr. Ali Raza Khalid** & **Engr. Umar Farooq** students of Ms. Structural engineering at NICE, NUST and laboratory staff at NICE, for providing the technical assistance and cooperation during the reported research work.

Thanks to **Lt. Col (Retd.) Farooq Ahmad** and **Engr. Yousaf Anwar Khan** for providing their great help in casting and experimentation phase of this research project. Without them this was not easily possible for us to complete this phase.

I appreciate the support provided to me by my parents and my family as this research work would not have completed without their prayers and whole hearted encouragement and support.

ABSTRACT

It is well known that confined concrete has better stress- strain behavior in compression than unconfined concrete. This concept has traditionally been applied to columns where compression concrete is confined through better arrangement of longitudinal as well as lateral steel for improved strength and ductility. On the other hand, failure of compression concrete in reinforced concrete beams is avoided, being brittle in nature, by imposing restriction on amount of longitudinal reinforcement so that the failure should be governed by yielding of steel for ductility requirements. The design of over-reinforced concrete beams is therefore, not permitted by codes of practice. The research on confinement of compression concrete in beams has already been initiated to explore the possibility of improved behavior in terms of strength and ductility. Ten reinforced concrete beams were tested, which included four traditionally designed beams and six confined beams. Flexural span of confined beams was provided with steel stirrups extending to half beam depth for confinement. Both over-reinforced and under-reinforced beams were tested. Experimental results indicated that ductility of confined beam is improved with the confinement especially in over-reinforced beams. The result also lead to the requirement of revision in maximum allowable longitudinal reinforcement in codes if adequate confinement stirrups are provided.

TABLE OF CONTENTS

LIST OF FIGURES

LIST OF TABLES

1. INTRODUCTION

1.1 Historical Overview

Over the last 50 years the strength of concrete used in structures has been gradually increasing. With passage of time each successive development and corresponding strength increase, the definition of “high strength” was revised. In early 1940’s the achieved compressive strength of concrete was around 25 MPa (3625 psi) which had an increment up to about 35 MPa (5075 psi) in 1950. In the 1970’s concrete mixtures showed compressive strength in excess of 41 MPa (6000 psi) or more at 28-days and were designated as high-strength concrete by American Concrete Institute (ACI) [1]. Over the period of time, concrete strength grew to about 131 MPa (19000 psi) have been batched by few ready mix producers and have been used in many major structures around the globe [2] .The full benefits of this technology have yet to be utilized, due to an insufficient understanding of the concrete. The brittle nature of concrete is a major obstacle in its widespread use, as any benefits in terms of reduced member size are negated by the need for an increased factor of safety to prevent brittle failure. Previous research has revealed that the incorporation of confining reinforcement in concrete increases its ductility.

The brittleness of concrete is significant when used in concrete structures, in other words using concrete without preventing the brittle failure is risky and unacceptable. When a material or structural element demonstrates excessive plastic deformation without significant loss in strength, its behavior is marked as ductile. [3]. Large deformations under overload conditions ensure adequate warning before failure. Confinement of concrete is believed to improve strength and ductility and is an important aspect that needs to be considered while designing structural concrete members, especially in areas of seismic activity and other accidental loads such as blast effects or vehicle crashes. Not only the strength but also the ductility needs to be enhanced in many cases to improve the structural performance particularly under seismic loads. Confinement of concrete has been proven to be an effective technique in

increasing the ductility of the concrete members and to a lesser degree, in improving their strength [4].

1.2 Confinement and Flexural Behavior

The confinement of concrete in compression is a complicated phenomenon, but extensive research is being carried out to understand its behavior. Confinement is mainly of two types, active and passive. Active confinement occurs when concrete is subjected to a pressure such as confining fluid, while passive confinement occurs when lateral reinforcement (confinement bars or ties) applies a confining reaction to laterally expanding concrete. Due to compressive load, the concrete in the confined area will expand but the confinement stirrups resist expansion due to passive confining pressure, and is called passive confinement. The confinement effects depends on different aspects such as spacing and yield strength of confining steel[8].

In this research, we will focus on the passive confinement where concrete is confined by the rectangular ties. Concrete expands laterally under a load but the confinement will resist the expansion and it will reduce the tendency of internal cracking, which increases the strength and ductility. If proper confinement is used, brittle failure can be avoided, by restraining lateral expansion and ductility of concrete in compression can be enhanced[8]. Most of the studies about confinement of concrete is based on test on concrete columns, while the idea of confinement of concrete in beams is a recent activity. Research on the effect of confining reinforcement in beams has revealed that the addition of confining reinforcement could significantly improve the flexural ductility of beams, regardless of the concrete strength [9, 10].One of the purpose of this study is to understand the confinement of concrete in beams as reported in studies as reflected earlier.

The majority of published research on confinement has been related to seismic loading conditions. The ductility resulting from confinement is used to maintain the ultimate flexural capacity of columns under the large deformations experienced during earthquakes. On the other hand, the design approaches adopted by Codes of Practice require beams to be under-reinforced in order to prevent brittle compression failures under static loading conditions. The ductile beam design concept approach larger size beams where large ductility requirements are to be met.

Although concrete confinement is widely regarded to improve flexural behavior of beams, yet, attempts to utilize this beneficial effect in the design of beams under static loading conditions are minimal. The enhancing influence of the confinement stirrups on compression concrete modifies the balanced conditions and suggests that the limit on longitudinal reinforcement ratio specified in Codes of Practice should be reconsidered. Confinement of compression concrete with closed steel stirrups enables to prevent the brittle failure of over-reinforced beams. It is well known that the behavior of confined concrete depends upon the level of confinement[11].

1.3 Research Objectives

Although it is generally accepted that confined concrete shows increased ductility and strength there is a difference of opinion on both the enhancement of ductility and strength in confined concrete strength. This opinion will be confirmed by this research which is being carried out in this thesis.

The objective is to improve our understanding of how RC beam (under and over-reinforced) behave when confined with confinement stirrups. Flexural capacity and ductility of confined beams will be investigated. It is therefore necessary to provide experimental data to facilitate the study of effect of confinement on flexural strength and ductility.

The aim of performing this research was also confirmation of the existing knowledge and obtaining new ones on confinement effect on flexural strength and ductility of concrete beams. This thesis will addresses the need to collect sufficient experimental data, in order to understand the effects of confining reinforcement, on the properties of concrete beams.

1.4 Methodology

The literature review focusing on available research on flexural behavior of confined RC beams has been carried out. The experimental study based on the review has been devised. Ten full scale beams having moderate longitudinal reinforcement were cast and tested. In this ten beams included two each over and under-reinforced reference beams. Moreover three each over and under-reinforced confined beams in the central portion are included.

2. CONFINEMENT OF CONCRETE & ITS APPLICATION

2.1 General

It is important for a designer to design a structure that it should ensure a ductile failure, in order to allow deflection and other warning signs before complete failure of structure. The reduction in ductility can lead to catastrophic failure of structural member which then could lead to loss of human lives. Concrete is a brittle material it fails abruptly at ultimate load, in order to ensure relative ductile failure the technique used is confinement of concrete. When the concrete is confined (in compression region), especially when the beam is designed as over-reinforced beam, the failure is the abrupt and without warning , in order to ensure the failure to be in a ductile manner confinement are added to the compression region. Ductile structures are generally able to dissipate significant amounts of energy during cyclic deformations. These two attributes (inelastic deformation and energy dissipation) are essential in earthquake-resistant structures, since they must survive high deformations with no loss of strength and dissipate the high input of energy [13, 14].

Under overload conditions before failure of a structure large deflection are ensured by ductility, this large deflections warns of impending failure. Ductility is an important requirement when designing structures subjected to earthquake loading. Ductility of RC members changes with size of member as well as strength of concrete.

Proper reinforcement detailing of structural members as per the provision of Codes of Practice ensure enough ductility. Therefore, the detailing rules provided in these codes should be respected. Ductility of the structural elements depends directly on the plastic rotation's capacity of the critical sections which can be achieved through choice of suitable (ductile) steel, adequate design of section ensuring that the position of the neutral axis at failure is small and provision of proper confinement through transverse reinforcement.

Most of the research on beam confinement is based on the results of the research on columns, because this concept is recently being applied to beams.

2.2 Flexural Theory

The normal stress due to bending are called flexure stresses**.** When transverse load is applied on the beam, compressive and tensile forces are developed along the length of the beam. The maximum tensile and compressive forces are observed on the extreme points of the section. Since the variation of stress along the section is linear, there comes a point where stresses are zero called neutral axis.

The classic formula for determining the bending stress in a beam under simple bending is:

$$\sigma_x = \frac{My}{I_x} \qquad \text{(Eq. 2.1)}$$

where;

- σ is the bending stress
- M - the moment about the neutral axis
- y - the perpendicular distance to the neutral axis
- I_x - the second moment of area about the neutral axis *x*.

2.2.1 Basic Assumptions in Flexure Theory

Five basic assumptions are made:

1. Plane sections remains plane before and after bending.

2. Strain in concrete is the same as in reinforcing bars at the same level, provided that the bond between the steel and concrete is sufficient to keep them acting together under the different load stages i.e., no slip can occur between the two materials.

3. The stress- strain behavior of both material (Steel and Concrete) is known.

4. The tensile strength of concrete can be ignored.

5. At ultimate stage the strain at extreme compression fiber of section is assumed as 0.003, as per ACI Code

The assumption of plane sections remaining plane means that strains vary linearly from one extreme fiber to other, these are proportional to the distance from the neutral axis, Fig. 2.1.

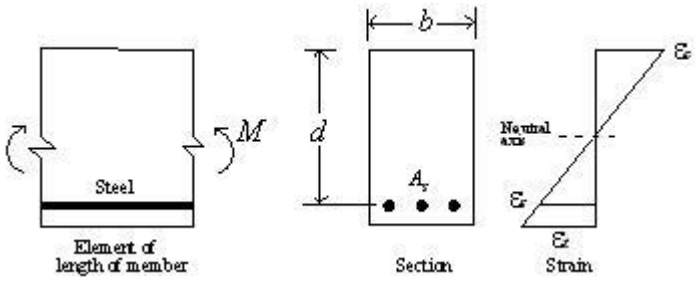

2.3 Failure Modes in Beams

This topic discusses the brief possible failure of beams under transverse loads. The fig 2.2 shows most of the failure modes of beams.

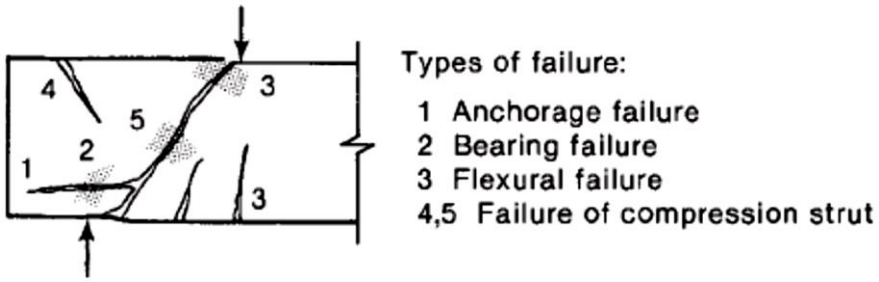

Figure 2-1.2 *Types of Failure cracks in beam*

2.3.1 Diagonal Failure

Diagonal failure is caused due to a combination of shear force and the bending moment. Several structural concrete members like slabs, columns and beams etc. have also been reported to have failed due to shear distress or diagonal failure. Mechanism of transfer of shear in all members is believed to be the same, however, cracking pattern may vary.

2.3.2 Diagonal Tension Failure

The diagonal crack initiates from the last flexural crack formed. In case of slender beams (a/d between 2.5 and 6), failure occurs within the shear span. The crack penetrates in the beam and reaches the compression zone of the beam at failure

loadings, it is likely to fail as a result of splitting of concrete, which is in a brittle manner as shown in Figure 2.2.

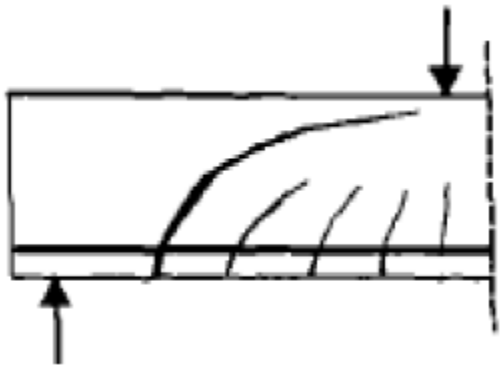

Figure 2.2-2: Diagonal Tension Failure

2.3.3 Shear Tension Failure

In this case too, the shear crack penetrates in a same way through the beam but is not likely to cause the failure at its own. Loss of bond between concrete and longitudinal steel can also cause failure due to splitting cracks developing in this region (Figure 2.3). Splitting of compression concrete is a phenomenon for this type of failure at ultimate stages of load.

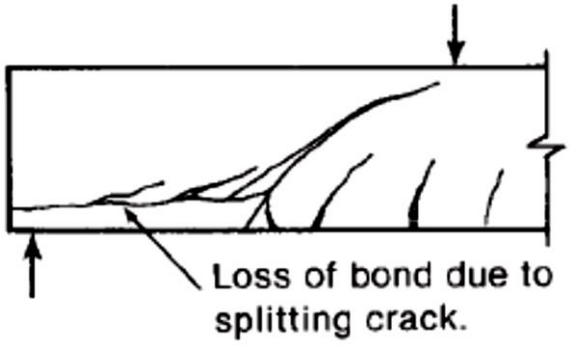

Figure 2.2-3 : Shear Tension Failure

2.3.4 Shear Compression Failure

Contrary to shear tension failure, if splitting cracks do not appear and the failure is caused merely due to diagonal shear crack propagating through the beam, it is termed as a shear compression failure (Figure 2.4). This failure mode mainly occurs to deep beams. In short beams, due to presence of arch action, the ultimate load causing failure can be much higher.

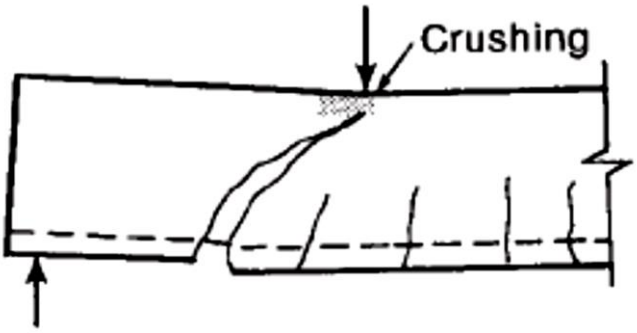

Figure 2.2-4: Shear Compression Failure

2.3.5 Flexural Failure

In beams at maximum bending region vertical cracks are developed. Eventually, these cracks cause failure of the beams as shown in Figure 2.2. The failure is due to either excessive yielding of longitudinal reinforcement or crushing of the compression concrete above flexural crack.

2.3.6 Anchorage Failure

Anchorage failure may be described as a slip or loss of bond of the longitudinal reinforcement with the concrete (Figure 2.2). It can be linked to dowel action where the aggregates interlocking resistance around the bar has failed resulting in splitting of the concrete.

2.3.7 Bearing Failure

When bearing stresses exceed the bearing capacity of the concrete, it results in failure of the support. If size of bearing plate is too small, it will result in failure if concrete at the support as shown in Figure 2.2.

2.4 Confinement State

Confinement of compression region of concrete is a complicated phenomenon, but extensive research is carried out internationally to understand its behavior. There are two types of confinement i.e. active and passive confinement. Active confinement occurs when concrete is subjected to the pressure such as confining fluid and passive confinement is that when a reaction is applied to the concrete by lateral reinforcement.

When compressive load is increased which will result in expansion of compression concrete but the lateral confinement will resist the expansion. Thus this confinement is called passive confinement. Various factors affects this confinement such as spacing, yield strength of the confining reinforcement.

This thesis focus only on passive confinement confined by transverse reinforcement via a rectangular tie shown in Fig 2.6. Concrete expands laterally under a compressive load in compression region but passive confinement resist the expansion reducing the tendency of penetrating cracks in compression region resulting in increase of strength capacity and ductility. Using proper confinement can avoid the brittle failure, this confinement restrains lateral expansion and increase strength and ductility of concrete. The research on confinement of beams is a recent research, earlier the confinement of beam was related to the confinement studied by confinement of columns. On this base, more data is needed on the behavior of confined beams. Base and Read (1965) showed through experimental testing confinement enhances the strength and ductility of beams with high tensile longitudinal steel percentage.

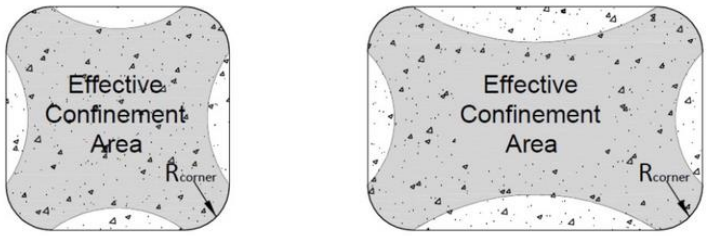

Figure 2.2-5: Confined and Unconfined Concrete in Tie Confinement

2.5 Efficient Confinement

Design codes recommend to design the beams as under-reinforced section which avoids the brittle failure (failure in compression). However, if longitudinal reinforcement is increased more than the limit the flexural capacity of beam is increased but it creates the brittle failure of beam, which is the reason that design codes does not allow this approach because ductility is an important factor related to human safety. Confinement of concrete has been proven to be an effective technique in increasing the ductility of the concrete members and to a lesser degree, in improving their strength. The confined area in a beam is shown in longitudinal direction in Fig 2-1 (Appendix-II).

Kwan et al. (2004) came to a conclusion that using a higher grade steel increases the flexural strength but the ductility is compromised. On the other hand using a higher grade of steel in compression zone of the beam may help in increasing the flexural capacity but not helps to increase the flexural ductility.

There are few ways to improve the ductility of concrete in compression, providing longitudinal compression reinforcement, using randomly oriented steel fibre, or installing a helical or tie confinement in the compression zone.

To find the most effective way a brief comparison is presented. Shan and Rangan (1970) tested 24 group of beam to compare the ductility. Their result showed that confinement with stirrup enhances ductility more than the compression reinforcement and the steel fibres. Based on experimental results they concluded that confinement in compression zone of a beam is more efficient than steel fibres or compression reinforcement.

Also, most of the literature in research, such as Park and Paulay (1975), Sheikh and Uzumeri (1980), Sheikh and Yeh (1986), Hatanaka and Tanigawa (1992) and Cusson and Paultre (1994) proved that helical confinement is more effective than rectangular tie confinement.

Circular spirals confine concrete much more effectively than rectilinear ties, and the mechanism of concrete confinement for circular spiral is better understood than for ties. But their relative ease in detailing makes use of ties more attractive than spiral.

2.6 Confinement Models

Almost all the confinement models are based on experimental investigations. In most of the tests the ratio of the area of the confined core to the gross area of the specimen was small compared with the values commonly used in practice. There are different models presented by different researchers such as Chan, Kent and Park, Roy and Sozen, Sargin, Sheikh and Uzumeri, Soliman and Yu, and Vellenas, Bertero and Popov.

The model presented by Sheikh and Uzumeri (1980) was further extended by Shamim A. Sheikh and C.C Yeh (1986) by incorporating the flexural effect in confinement. The equation proposed in relation to this model is as follow:

$$K_s = 1 + \frac{BH}{P_{occ}}\left[\left(1 - \frac{\sum_{i=1}^{n} c_i^2}{\alpha A_{co}}\right)\left(1 - \frac{0.5stan\theta}{B}\right)\left(\left(1 - \frac{0.5stan\theta}{H}\right)\right)\right]\beta(\rho_t f_{sv})^{\gamma} \quad \text{(Eq 2.2)}$$

$$f_{cc} = \eta K_s f_{cp} \quad \text{(Eq 2.3)}$$

$$\varepsilon_{s1} = 0.0022K_s \quad \text{(Eq. 2.4)}$$

In equation, $\alpha = 5.5$, $\beta = \frac{1}{140}$, $\theta = 45°$, $f_{sv} = f_{yv}$ and $\gamma = 0.5$

where：

A_{co}= the area of the core measured from c to c of the perimeter tie.

A_s= the area of the longitudinal steel.

B = is the core size (width) measured from the centre to centre of the perimeter tie.

H = is the core size (depth) measured from the centre to centre of the perimeter tie.

c = the distance between laterally supported longitudinal bars.

f_{cp} = is the strength of unconfined concrete in the structural concrete member and is equal to $K_p f_c'$.

K_p = the ratio of unconfined concrete strength in the structural concrete member to f_c'

$P_{occ} = K_p f_c'$(Aco — A,), unconfined strength of the concrete core

s= is the tie spacing *(s_v)*

ρ_t = is the ratio of the volume of the tie steel to the volume of the core.

ε_o = is the strain corresponding to the maximum stress in the unconfined concrete.

2.6 Beam Confinement

The majority of the research carried out in confinement is the behavior in dynamic loadings. The ductility achieved due to confinement enable large deflection at ultimate loadings experienced in the dynamic loads. On the other hand, codes recommend that the design of beam should be under-reinforced so that the failure should be ductile .When increased ductility due to confinement is provided these limitations are believed to be too restrictive.

It is widely acknowledged that confinement plays an influential role in enhancing flexural behavior of beams, however, no effort has been made to utilize this influential role in the design of beams under static loading conditions. In an attempt to

utilize the enhancing influence of the confining stirrups, it is suggested that the longitudinal reinforcement ratio should be allowed to exceed the maximum value specified in Codes of Practice. The brittle failure in (over-reinforced) beams can be prevented by providing confinement stirrups in compression region. Pam et al (2001), it was found that beams could fail in a brittle manner if they were provided with excessive amounts of tension steel [23].

It is generally accepted that confinement increases the strength and ductility of concrete. Confinement reinforcement increases the ductility and compressive strength of concrete under compression by resisting lateral expansion due to Poisson's effect. In this study confined stirrup reinforcement is used in the compression zone of under and over-reinforced beams. The effectiveness of confinements depends on spacing and diameter of confining reinforcement. Adding confinement to an over-reinforced beam section has no effect on the flexural stiffness, but slightly increases the flexural strength of the reinforced beam before the peak resisting moment. At the post-peak stage the confining stresses dramatically increase the residual moment resisting capacity of the beam, increasing flexural ductility [22].

Lot of significant work has been done on modelling of confined concrete [24], models existed so far are based on limited amount of tests. As far as strength is concerned, considerable work has been done [25, 26]; however, concrete was typically considered as unconfined, and steel data were almost exclusively drawn from tests on 'traditional' reinforcing bars. In order to analyze the flexural ductility of beams, post-peak nonlinear moment curvature analysis is needed [27, 28]. The flexural ductility of beams is dependent not only on the ductility of the concrete but also on the amount of steel reinforcement. Hadi and Elbasha [29] also investigated the effect of the tensile reinforcement ratio upon the ductility of concrete beams. It was found that yield load increased as the tensile reinforcement ratio increased [30, 31]. The post yield ultimate load showed the opposite behavior and decreases as the tensile reinforcement ratio increased.

2.7 Ductility & Mechanism of Confinement

It has long been recognized that transverse steel in the form of rectangular hoops can increase the strength, and in particular the deformation capacity (ductility) of reinforced concrete members [16]. According to Xie et al, (1994), tensile ratio, amount

of reinforcement in compression zone, the lateral steel ratio and strength of concrete are the factors which play an influential role in deformability. Brittleness or ductility is a function of the state of compressive stresses, unconfined concrete strength, volumetric expansion, and concrete softening [12]. In earthquake-resistant design, the capability of a system or structural element to undergo large amplitude cyclic deformations, under a given ground motion, without excessive strength deterioration is typically given by the available ductility ratio, μ [17, 18]. A convenient measure of the ductility of a section subjected to flexure or combined flexure and axial load is the ductility ratio μ of the ultimate curvature attainable without significant loss of strength, Øu, to the curvature corresponding to first yield of the tension reinforcement, Øy, as shown in following equation.

$$\mu = \frac{\text{Øu}}{\text{Øy}} \qquad \text{Eq. 2.5}$$

As discussed earlier, due to Poisson's effect, the lateral expansion is arrested by the confining reinforcement which results increase in ductility and strength. The behavior of confined concrete depends on the lateral reinforcement spacing, strength and bar diameter. This confinement effect come into action after a time when load is applied and Poisson's ratio is reached. Initially confinement does not increase the strength and ductility, but when the stress is increased up to 60% of the maximum cylinder strength, the concrete is effectively confined [19]. However, there is no additional confinement effect when the confining steel reaches its yield strength. Spalling is quite visible when the concrete is confined. This is caused by the closely spaced confinement stirrups physically separating the concrete cover from the core, causing an early failure of the cover [11, 15, 20].

Confinement in concrete is achieved by the suitable placement of transverse reinforcement. Transverse reinforcement is hardly active at low stress level, at this level unconfined and confined level behaves the same. At stresses close to the uniaxial strength of concrete dilates due to the internal fracturing and bear out against the transverse reinforcement which then causes a confining action in concrete. This phenomenon of confining concrete causes a significant increase in the ductility of concrete [21].

2.8 Factors affecting confinement

The behavior of concrete confined with stirrups at maximum strains depends on the confining pressure, which affects the several factor. The following are the main factors that affect the confinement of compression concrete:

2.8.1 Lateral Reinforcement Ratio

Lateral reinforcement ratio is the ratio of the volume of lateral reinforcement to the volume of core concrete. The confining pressure is increased on the core concrete when lateral reinforcement is increased on the same way ductility is also enhanced.

2.8.2 Characteristics of Confined Steel

The stress strain relationship of confining steel and its grade affects the confining pressure. The concrete expands without restraint and crack begins to appear when lateral confinement reinforcement yields. However the reinforcement with high strength and strain hardening stress strain relationship retains expansion until either the stage at which concrete fails to take more load or up to the tension failure of confinement steel (Sheikh,1978). However, Muguruma et al. (1979) said that high strength of steel stirrups provide higher degree of confinement.

2.8.3 Lateral Reinforcement Spacing/Pitch

The spacing of confinement steel significantly affects the strength and ductility of concrete members. Razvi and Saaticioglu (1994) stated that spacing is more effective in columns with a relatively high volumetric ratio of steel.

2.8.4 Size of Confining Reinforcement

This factor minimum effects the strength and ductility of concrete members but it affects the spalling off the concrete cover because the size of confinement steel separates the core concrete from cover concrete. Thus as the confinement bar size increases the concrete spall of earlier. However, in some cases when spacing of confinement bars is high the increase in diameter of confinement bar may not affect the concrete at all. In these kind of cases the spacing between the confining steel is reduced to increase the performance of concrete. (Bayrak,1998)

2.9 Research Investigation on Confinement of Beams

2.9.1 Base and Read (1965)

Base and Read tested 13 concrete and 3 pre stressed beams with a total of 16 beams. The cross section of the beams was 152 x 208 mm and about 3 m of length. The beam were tested by using single point load test. There were three types of beam i.e. under-reinforced, over-reinforced and beams with balanced steel ratio. The confinement of beams were of two types one type was in which only rectangular stirrups are used and the other was confined with rectangular stirrup with 50 and 203 mm od spacing and helical reinforcement having pitch of 25 and 50 mm diameters of 6.35 and 4.76mm. The confined size of concrete was 82mm. In this investigation they concluded that failure of beams can be changed from sudden to ductile when confinement is provided. Moreover, the helical confinement increases the ductility of rectangular pre-stressed concrete beams.

2.9.2 Shah and Rangan (1970)

Shah and Rangan tested 24 groups of beams with two similar beams in each group. The cross section dimension of beam were 50.8 x 76.2 and length of 914.4mm. This experiments were performed in order to compare their ductility. The test was carried as two point load test to have a constant moment zone. This zone contain different volume of closed stirrups, different amount of steel fibers or different amount of compression longitudinal reinforcement. Based on experimental investigation Shah and Rangan concluded that confinement by compression zone of a beam is more efficient than steel fibers or longitudinal compression reinforcement.

2.9.3 Issa and Tobaa (1994)

Issa and Tobaa tested twenty five specimens confined by continuous square and circular spirals to study the stress strain characteristics of confined concrete under concentric axial compression.

2.9.4 Ziara et al (1995)

Ziara investigated the confinement experimentally. A total of twelve beams were tested in which four beams were without confinement and remaining eight beam with confinement in compression zone. The dimension detail of the beams were 200 x 300 x3500 mm. The tie spacing were 35 and 60 mm which were provided in the compression zone of beam. The main purpose was to study the flexural effect of beam

by confinement. He concluded that confinement in compression zone did not significantly increased the flexural capacity but their ductility was increased.

2.9.5 Mansur et al (1997)

Mansur tested eleven HSC beams having length of 3.30 m. The cross section details of the beam were 170 x 250 mm. All but one beam was over-reinforced, and the compression zone of the beams was confined with either ties or fibers, or left unconfined. Test results indicate that the brittle type of failure in over-reinforced concrete beams can be arrested by introducing transverse ties or discrete steel fibers in the compression zone. Ductility increases with increase in volume of confining ties, but up to a certain limit. Whitney's rectangular stress block can be used in the strength design of high-strength concrete flexural members

2.9.6 Hadi and Schmidt (2002)

Seven no of beams were tested in this research having dimensional details as 200 x 300 x 4060 mm. The objective of investigation was to study the ductility of beams using helical reinforcement in the compression region of beam. They concluded that beam was very brittle in its failure without helix confinement.

2.9.7 Nuri M. Elbasha (2005)

Elbasha tested 20 beams to study the behavior of over-reinforced HSC helically confined beams. The size of the beam tested were 200 x 300 mm. The length of the beams was 4000mm. The helical pitch and diameter was variable. The helical pitch were 25, 50, 75,100 and 150 mm having diameter of 8 and 10 mm. The main objective was to study the effect of helical confinement in over-reinforced HSC beams. In addition to this it the efficiency of helical confinement was compared with other shaped confinement stirrups. They concluded that confinement increases ductility and overall performance of HSC beams. He also concluded that provision of helical confinement in the compression zone of over-reinforced beams makes it fail in a ductile manner.

2.9.10 M N. S. Hadi and Nuri M. Elbasha (2008)

Tested 10 helically confined beams under four point load. The cross section used in experiment was 200 x 300 x 4000 mm. The helical diameter and pitch was changed. The helical diameter was 8 and 12 mm & pitch 25, 50, 75,100 to 160 mm. They concluded that displacement ductility index increases as the helical pitch decreases and that the confinement effect is negligible when the helical pitch is equal to or greater than the core diameter for helically confined beams.

2.9.11 M. N. S. Hadi and R. Jeffry (2010)

Tested 5 HSC beams (200 x 300 x 4000 mm) with varying tensile reinforcement and different shapes of confinement stirrups under four point load, with emphasis placed on the mid-span deflection. Results showed that placing helixes with the right diameter and pitch in the compression zone of reinforced concrete beams improve their strength and ductility.

3 EXPERIMENTAL PROGRAM

3.1 General

An experimental program was devised where a no of simply supported beams reinforced with shear stirrups in addition to the longitudinal reinforcement designed to study the confinement of compression concrete. This confinement was to be provided by additional stirrups up to mid depth of beams from the top (Fig 3.4, Appendix III). Experimental investigation was carried in National University of Sciences and Technology on full scale beams to study the confinement effect on flexural capacity and ductility of over-reinforced and under-reinforced beams. Eight beams 3350 mm long by 200mm wide and 300mm deep were subjected to two point loading. The confinement stirrups were installed in the compression zone of beams having no shear stresses. The confinement stirrups having depth of about 150 mm were provided in flexural span of beam specimens. The concrete cover for all the beams was maintained at 25 mm.

3.2 Detail of Beams

All ten beams were casted in a single concrete batch. The cross section of beams were 200x 300 mm. The beam specimens were 3350 mm (11 feet) with an effective span of 3000 mm. The details of beam is shown in fig 3.4. The specimen were of following three types:

Reference beams were traditionally designed with shear stirrups at spacing of 127 mm (5 inch). The longitudinal reinforcement for under-reinforced beam specimens was 2 No 25 bars while for over-reinforced beams specimens was 2 No 25 and 1 no 29. The confined under and over-reinforced beams were same as the reference beams except the flexural spans of these beams were provided with confinement stirrups at a distance of 63 mm center to center.

The alphanumeric i.e. **R-UR-1** is used to represent the name of the beam, in which R stands for Reference beam, UR means Under-reinforced beam and 1 is specimen. For Confined beam specimens R is replaced by C. The details and sections are given in Table 3.8 & Fig 3-4 in Appendix III.

3.3 Fabrication of Beam Samples

3.3.1 Formwork

The formwork was constructed using plywood having thickness of 25 mm. The dimension of formwork was the same as for beam i.e. 300mm height, 200 mm width and 3350mm of length (Shown in Figure 3-5 Appendix-III). The formwork was constructed strictly and bracing was fixed in it so that the wood should not be misaligned from its place. The formwork was used to cast eight beams at a time. The inner walls of formworks was cleaned and properly oiled so that bond is avoided between concrete and wood.

3.3.2 Reinforcement Cages

The cages for beams depends on three types of beam which were casted. Firstly the reference beams having hanger bars and shear stirrups of 10mm dia with 127mm spacing throughout the length. The longitudinal reinforcement for under-reinforced reference beams contains 2 bars of 25 mm dia and in over-reinforced reference beam there were 2 nos of 25 mm and one of 29 mm dia bar (Shown in Figure 3-6, Appendix III). All the longitudinal bars are extended upwards hooks to around 100mm from corners on both sides. The confinement stirrups which are only confining the compression region of over and under-reinforced beam are spread only in flexural span of beam which is the central 1000 mm span of beam, remaining portion is provided with conventional stirrups. Further the confinement stirrups are tied with bar present at the level of neutral axis of beam to restrain the confinement stirrups.

3.3.3 Casting and Curing of Beams

The cages were placed inside the formwork with a gap of 25 mm between it to maintain clear cover of concrete with steel. This adjustment of cages is very important to maintain cover. The concrete in the cages was placed in layer form and each layer was properly compacted through vibrators. Precautions were taken while pouring of concrete (Shown in Figure 3-8, Appendix III) in central regions of beam where strain gages were fixed (Shown in Figure 3-7, Appendix III), so that it should not be damaged while placing and compacting of concrete. A no of cylinders were casted during pouring

of concrete. After pouring pool of water was formed on the top surface of beams to ensure proper curing.

3.4 Variable Examined

The variable studied in this experiment is the longitudinal reinforcement ratio of beams classified as under-reinforced and over-reinforced beam. The effect of confinement stirrups was also the part of investigation for under and over-reinforced beam and its results are compared with respective reference beams.

3.5 Instrumentation

The testing beams were instrumented appropriately. Strain gauges were tested for continuity prior to pouring of concrete. Wires attached with the gauges were connected to the Structural Load Analysis and Automation System. The measurements were recorded through software.

Three electrical strain gages were pasted and fixed on each beam in the central flexure portion. The length of the strain gages was 6 mm. The strain gages were product of Vishay Micro Measurements (origin USA). The specification of foil strain gages type is EA-06-240LZ-120/E, these gauges had 120.0+ 0.3% grid resistance in ohms with gauge factor 2.080 ± 0.5 at 24 °C and are manufactured with self-temperature compensation characteristics to minimize thermal output. The EA series gauges are a general purpose family of constant alloy strain gauges widely used in experimental stress analysis. They are constructed with a 0.03-mm tough, flexible polyamide film backing. Strain gauges were soldered and checked for continuity with the help of digital multi-meter. One gage was pasted of the longitudinal reinforcement to monitor the elongation of steel in tension region, second gage was pasted on the hanger bar of beam to monitor the compressive strain at mid of beam and the last gage was pasted on the confinement stirrup to check the effect of lateral strain on beam during bending.

Dual mechanism for recording of deflections was adopted. Electronic as well as Mechanical LVDTs were installed for each specimen. Measurements from electronic LVDTs were recorded through the computer and were noted physically by observation from mechanical LVDTs. Mid-span deflection and one-fourth position of beam within the region of pure bending between the two loading points was measured by linear

variable differential transformer (LVDT). The LVDT was fixed with its stand and was placed on the table below the beam. The Fig Shows the LVDT

The load was manually increased by a constant load interval and all the data was recorded by the data logger through program named LabVIEW installed in personal PC.

3.6 Testing

3.6.1 Test Setup

The applied on beam is two point load scheme. A load cell apply the load to a very stiff steel girder which is rested to the testing beams by two supports, having a pure bending and no shear stress region between two points of steel girder. Figure 3-9, Appendix III, shows that the beam were tested under two point load test in the strong floor of Civil Engineering laboratory at National University of Sciences and Technology.

3.6.2 Test Procedure

The cylinders were tested before testing the beams to have an exact value of compressive strength. The LVDTs and all other electronic devices were calibrated before testing. The load was applied at regular load interval and this load was continued till the beam was unable to sustain more load. At each step the deflection and strain are recorded through data logger in the PC. Finally every data was saved in the computer's hard disk and documented with the photographs.

3.7 Mix Design

In the study the concrete strength was decided and selected as 28MPa (4000psi). The mix design is given in Table 3.1 (Appendix III)

3.8 Materials

3.8.1 Cement

The Type I cement conforming to ASTM C 150–04 was used. Results of the tests carried out to ascertain the properties of cement are presented in Table 3.2 – Appendix III. Variation in the chemical composition and physical properties of the cement affect concrete compressive strength more than variations in any other single material.

3.8.2 Fine Aggregate

Sand from Lawrencepur source was used. Results of the tests conducted for verification of properties of sand are tabulated in Table 3.3 – Appendix III. The gradation of the fine aggregate is tabulated in Table 3.4 -Appendix III, and graphically shown in Figure 3.1 –Appendix III.

3.8.3 Coarse Aggregate

Aggregate from Margalla crush site was used in this research. Maximum size for the aggregate was kept as 19 mm. The laboratory test results are tabulated in Table 3.5 - Appendix III. The gradation and sieve analysis was determined in accordance with ASTM C 136 – 01 and tabulated in Table 3.6 - Appendix III, and graphically illustrated in Fig 3.2-Appendix III.

3.9.10 Concrete

All the beams were constructed using ready mix concrete having maximum size of aggregate of 19mm (0.75 inch). The concrete slump was observed between 25-75 mm. A workable concrete was needed to ensure that the concrete should pass from the confinement stirrups present in the beam. The cylinders casted for concrete strength were having a dia of 150mm and 300 mm of height. The average 28 days compressive strength of concrete was 28 MPa.

3.8.5 Admixtures

P-200 (product of Ultra Chemical Company), a high performance concrete admixture based on modified polycarboxylic ether, was used in the research. The dosage was kept constant throughout the research work as 0.5% to 1.5 % by weight of cement. The technical data of product is tabulated in Table 3.7- Appendix III.

3.8.6 Reinforcement/Steel

Hot rolled deformed bar of grade 60 steel of different cross section was used for the longitudinal reinforcement, hanger bar and confinement stirrups of beams.

4 EXPERIMENTAL OBSERVATION AND RESULTS

4.1 General

Testing of all ten specimens was carried out at NUST Laboratory. The samples were loaded at two points loading systems. Load was applied in increments of (1-2) Tons. After each increment of load, cracks in the beams were observed and marked. Deflections were also noted after each increment of load.

4.2 Behavior of test specimens

Detailed behavior of each specimen is discussed under

4.2.1 Reference Under-Reinforced Beam # 1 (R-UR-1)

This specimen is the reference beam for under-reinforced beams having shear stirrups throughout the beam length and depth. At the load of 8 ton flexural cracks begin to appear in bending region of beam. The inclined shear cracks near supports and below point loads begin to appear at the load of 15 ton, these cracks begin to penetrate the depth at load of 19 ton. The beam failed at the load of 26 ton. The final failure was crushing of concrete after large deflection was observed before failure.

Load deflection data and plots are given in Table 3.9 and Figure 3-13 respectively (Appendix III). Deflected shape of the beam at various stages of loading is displayed in Figure 3-33 (Appendix III).The crack pattern of the beam is shown in the Figure 3-24 (Appendix III).

4.2.2 Reference Under-Reinforced Beam # 2 (R-UR-2)

This specimen is another reference beam for under-reinforced beams having full length stirrup throughout the length of beam. At the load of 7 ton flexural cracks begin to appear in pure flexural portion of beam. When the load reached to 15 ton the shear cracks began to be visible near supports and point load position, these cracks begin to penetrate through the depth load of 19 ton. The beam failed at the load of 27 ton. The final failure was crushing of concrete after large deflection was observed before failure.

Load deflection data and plots are given in Table 3.10 and Figure 3-10 respectively (Appendix III). Deflected shape of the beam at various stages of loading is displayed in Figure 3-35 (Appendix III). The crack pattern of the beam is shown in the Figure 3-27 (Appendix III).

4.2.3 Confined Under-Reinforced Beam # 1 (C-UR-1)

The specimen was loaded gradually and the flexural cracks were visible in the central bottom region of beam at 7.5 ton of load. The number and size of the cracks began to increase. The shear cracks were in action at the load of 10 ton. At the load of 20 ton the concrete cover spalled off following the failure of beam at 26ton.

Load deflection data and plots are given in Table 3.18 and Figure 3-14 respectively (Appendix III). Deflected shape of the beam at various stages of loading is displayed in Figure 3-34 (Appendix III).The crack pattern of the beam is shown in the Figure 3-20 (Appendix III).

4.2.4 Confined Under-Reinforced Beam # 2 (C-UR-2)

No flexural cracks were visible on the surface till load of 5 ton. After this flexural cracks began to appear till 10 ton. There was no shear crack noted till 10 ton. The shear cracks began to appear from supports to the point of application of load at load of 15ton. This shear cracks began to penetrate at the load of 20ton. Failure was observed at 24 ton.

Load deflection data and plots are given in Table 3.15 and Figure 3-12 respectively (Appendix III). Deflected shape of the beam at various stages of loading is displayed in Figure 3-40 (Appendix III).The crack pattern of the beam is shown in the Figure 3-21 (Appendix III).

4.2.5 Confined Under-Reinforced Beam # 3 (C-UR-3)

This specimen is the confined under-reinforced beam. The cracking initiated in this beam from load of 8 tons. The concrete spalling off phenomenon was noted at the load of 23 ton. A large deflected shape was visible from naked eye. The failure load of the beam was 26 Ton.

Load deflection data and plots are given in Table 3.16 and Figure 3-11 respectively (Appendix III). Deflected shape of the beam at various stages of loading is displayed in Figure 3-41 (Appendix III).The crack pattern of the beam is shown in the Figure 3-28 (Appendix III).

4.2.6 Reference Over-Reinforced Beam # 1 (R-OR-1)

Very small flexural crack began to appear at the pure bending region of beam. The flexural crack appeared at 11 ton of load. The penetration of flexural cracks towards the compression was earlier as compared to other beams. The failure of beam at 35 ton was relatively less ductile and at failure large shear cracks were observed.

Load deflection data and plots are given in Table 3.11 and Figure 3-16 respectively (Appendix III). Deflected shape of the beam at various stages of loading is displayed in Figure 3-36 (Appendix III). The crack pattern of the beam is shown in the Figure 3-22 (Appendix III).

4.2.7 Reference Over-Reinforced Beam # 2 (R-OR-2)

Very small flexural crack began to appear at the pure bending region of beam. The flexural crack appeared at 5 ton of load. The penetration of flexural cracks towards the compression was earlier as compared to other beams. The failure of beam at 38 ton was relatively less ductile and at failure large shear cracks were observed.

Load deflection data and plots are given in Table 3.13 and Figure 3-15 respectively (Appendix III). Deflected shape of the beam at various stages of loading is displayed in Figure 3-38 (Appendix III).The crack pattern of the beam is shown in the Figure 3-29 (Appendix III).

4.2.8 Confined Over-Reinforced Beam # 1 (C-OR-1)

The flexural cracks began to appear 1t 10 ton of loading, they started to increase till the load of 15 ton. After this the shear cracks began to appear from shear region of beam and directed towards the point of application of loads. The concrete began to spall of near supports at load of 27 ton. At this stage the flexural crack propagation decreased and shear cracks began to penetrate and their size was increased. The concrete spalled of from compression region of beam following with the abrupt failure of load at 35ton.

Load deflection data and plots are given in Table 3.12 and Figure 3-17 respectively (Appendix III). Deflected shape of the beam at various stages of loading is displayed in Figure 3-37 (Appendix III).The crack pattern of the beam is shown in the Figure 3-23 (Appendix III).

4.2.9 Confined Over-Reinforced Beam # 2 (C-OR-2)

The flexural cracks began to appear 1t 10 ton of loading, they started to increase till the load of 15 ton. After this the shear cracks began to appear from shear region of beam and directed towards the point of application of loads. The concrete began to spall of near supports at load of 27 ton. At this stage the flexural crack propagation decreased and shear cracks began to penetrate and their size was increased. The concrete spalled of from compression region of beam following with the failure of load at 35ton.

Load deflection data and plots are given in Table 3.14 and Figure 3-18 respectively (Appendix III). Deflected shape of the beam at various stages of loading is displayed in Figure 3-39 (Appendix III).The crack pattern of the beam is shown in the Figure 3-25 (Appendix III).

4.2.10 Confined Over-Reinforced Beam # 3 (C-OR-3)

There were no cracks on the surface till 11 ton. The flexural crack appeared initially following by the shear cracks. The flexural crack were not increasing but prior to that the pure bending region of beam shear cracks were reaching in that region as the loading was increased gradually. The failure of beam occurred at 20 ton of load.

Load deflection data and plots are given in Table 3.17 and Figure 3-19 respectively (Appendix III). Deflected shape of the beam at various stages of loading is displayed in Figure 3-42 (Appendix III). The crack pattern of the beam is shown in the Figure 3-26 (Appendix III).

4.3 Moment Curvature Relationship

Moments and curvatures were computed from the load deflection data. Moments were determined by using measured load and test setup configuration. Curvatures were determined using following procedure:

- For each load point, moment is determined from the load.

- From the three deflection gauges placed under the beams at third points, the deflected shape has been developed for each load increment and shown from Figure 3-33 to Figure 3.42 - Appendix III.

- From the deflected shape, the radius of curve is determined.

- For curvature values at a given load point, inverse of radius is taken to have curvature at each points

Moment – curvature (M – Ø) curve are shown from Figure 3-43 to Figure 3-52 - Appendix III and details given in Table 3.19 to 3.28- Appendix III.

Ductility index of the beams were calculated using Moment – curvature curves shown in Appendix III Fig 3-54 & 3-55. The index used to define ductility is ductility index which is the ratio of curvature of beam at failure load to the ratio of curvature of beam at yielding load as discussed in Eq. 2.5.

4.4 Summary of behavior

General behavior of beams can be summarized as below:-

- Initial flexural cracks formed in under-reinforced beam were ranged in load from 5-7 tons while for over-reinforced it ranges from 8 – 10 tons.
- In under-reinforced beams initially flexural crack appeared in the central region of beam. As the load increases the cracks began to increase in size and number till load reaches to 15 ton.
- In confined beams the flexural cracks penetration rate was too low comparing with their respective reference beam. As shear cracks begins to penetrate from shear region to the bending region (support to point of application of load).
- The inclined cracks were observed mostly around 45 degrees.
- The confined beams cover spalls off before failure while no such thing was observed in unconfined beam.
- Significant deflection was observed in over-reinforced confined beam before failure. However under-reinforced beams failed in a ductile manner but deflection are low comparing with over-reinforced beams.

- The confinement of beams were clearly not allowing the flexural cracks to penetrate in to the confining region.

5 DISCUSSION AND INTERPRETATION

5.1 General

The aim of this experimental program in this study is to investigate the effect of confinement on behavior of under and over-reinforced beams. Ten reinforced concrete beams were tested, which included both over and under-reinforced beam. Two over-reinforced and two under-reinforced beams were traditionally designed, termed as reference (unconfined) beams. Three over-reinforced and three under-reinforced beams were confined using steel stirrups. The efficiency and failure mechanism of the confined beams were observed by comparing their performance with the unconfined (reference) beams.

5.1 General Behavior of Beams

The reference under-reinforced beams failed in a ductile manner and failure was caused by flexural cracks. However, the reference over-reinforced beams were failed in a brittle manner due to wide diagonal cracks formed during the tests. On reaching the peak load, sudden drop was observed in this case which indicated brittle failure.

The confined under-reinforced beams failed in a ductile manner. Flexural cracks appeared at mid span during the early stages of the loading. Additional flexural cracks appeared as the load was increased. These cracks were observed over almost the entire depth of the beam. The cracks in shear span changed their direction towards the load points (diagonally) as they propagated above the longitudinal reinforcement. It was observed that the confinement did not allow the vertical cracks in the flexural span to penetrate up beyond at half the depth of the beam. These beams behaved in more ductile manner as compared to the reference beams. The peak load remained the same in both types of beam.

The peak (ultimate) load for over-reinforced confined beams were same compared to the corresponding unconfined (reference) beams but a considerable improvement in ductility was seen. The cracking pattern of these beams was same as that of under-reinforced confined beams. The ultimate failure occurred after spalling of

cover concrete in the compression region which can be clearly seen in Fig 3-30 & 3-32, Appendix III.

5.2 Interpretation of Results

5.2.1 Load - Deflection Response

The load deflection response of under-reinforced reference and confined beams are showing ductile behavior. There was a clear warning before failure and yielding was as can be seen in the graphs shown in fig 4-6 Appendix -D. There was no significant change in the load deflection response of under-reinforced confined beams compared with respective reference beams despite provision of confinement stirrups at close spacing of 63.5 mm (2.5 inch).

The load deflection response of confined over-reinforced beams was significantly different comparing with reference beams as shown in fig 4-7 Appendix -D. The failure of reference beams was brittle and there was a rapid drop in load after reaching the ultimate values. The load deflection curve of confined over-reinforced beam beams showed a significant ductile behavior which included the spalling of the concrete compression cover prior to failure. The drop in load after the peak was not considerable depicting better ductility by these beams.

The comparison load deflection clearly show that area under the curve for confined over-reinforced beam is high compared to the reference beams employing that confined over-reinforced beams absorb more strain energy, desirable for seismic design of beams.

5.2.2 Cracking and Failure Pattern of Beams

Vertical cracks appeared in all beam specimens closer to the mid span. With the increase in load, these cracks propagated towards the neutral axis and cracks in the shear spans started getting inclined. Diagonal cracks appeared at relatively higher loads and propagated towards the loading points as is evident from the cracking pattern of the beam. The confinement in the beams did not allow the flexural crack to penetrate into the compression region, but the diagonal cracks in shear span widened and reached up to the loading point.

The cracking pattern of unconfined beam specimens (under and over-reinforced) followed conventional behavior. The vertical cracks were visible at the mid span region and inclined cracks were seen in shear span of the beam specimen. On the other hand, vertical cracks in confined beams were restricted at neutral axis due to presence of confinement while inclined crack in shear span propagated along the depth starting from support to point of application of load.

5.2.3 Moment Curvature Response

The Moment Curvature response for under-reinforced beams does not show any prominent change between unconfined and confined beams. The peak flexural moments of unconfined and confined under-reinforced beams shows did not exhibit any significant improvement. The average peak moment of unconfined under-reinforced beam is 130.845 kNm, while the peak ultimate moment for confined under-reinforced beam is 140.04 kNm. (Fig 4-4, Appendix IV)

The Moment Curvature response for over-reinforced unconfined and confined beams show considerable improvement in ductility. No increase was observed in flexural capacity of beams as the peak average moments for unconfined beams is 180.60 kNm and for confined is 173.13 kNm. (Fig 4-6, Appendix IV)

The curvature values also depict the same behavior of unconfined and confined beams as described above in flexural moments. The maximum mean curvature of under-reinforced unconfined beam is 33.37 x 10^{-6} rad/mm while the maximum mean curvature for under-reinforced confined beam is 35.14 x 10^{-6} rad/mm. This shows that ductility is not increased considerably by confining under-reinforced beams. Moreover, in case of over-reinforced beams, the maximum mean ductility of unconfined beam is 29.42 x 10^{-6} rad/mm and maximum mean ductility of confined beam is 46.57 x 10^{-6} rad/mm. This shows that ductility of over-reinforced confined beam is improved to 63 % from its reference beam. Thus increase in ductility is more pronounced in over-reinforced confined beam as compared to under-reinforced confined beams.

5.2.4 Ductility Comparison

The ductility of the unconfined and confined beams were calculated by two approaches. The area under the load deflection curve is one way to evaluate ductility. When the confined beams are compared with their unconfined (reference) beam, the ductility is improved in both under and over-reinforced confined beams. The average

value for under-reinforced unconfined (reference) beam is 4417.44 kNmm comparing with under-reinforced confined beam, which is 4677.51 kNmm. Similarly, the area for over-reinforced unconfined (reference) beams is 7262.14 kNmm as compared with confined beams with area of 7733.61 kNmm. Secondly, the ductility was calculated by ductility index calculated by ratio of curvatures (Φu/ Φy). The average ductility index of under-reinforced unconfined (reference) beam is 2.78 whereas the average ductility index for under-reinforced confined beam is 3.62. Similarly the average value of ductility index for over-reinforced unconfined beam is 2.68 comparing to 4.73, which is the average ductility index of over-reinforced confined beams.

The results show (Table 4.2, Appendix IV) that the ductility of confined beam is increased. However this increase in ductility is higher in over-reinforced beams.

5.2.5 Comparison of Predicted with Actual Flexural Moments

A comparison was made of actual moment values with predicted values using available confinement model. The predicted values for unconfined beams were calculated by following the ACI 318-11 analysis method. The predicted values for confined concrete were calculated by using Sheikh and Yeh (1986) model for confined concrete (calculation given in Section 4A, Appendix IV). A strength enhancement factor (Ks) of 1.38 was used to calculate moment capacity for the confinement configuration used and are shown in Section 4A Appendix IV. The predicted and measured average value of flexural moment for under and over-reinforced unconfined and confined beam are given in Table 4.1 (Appendix IV). The predicted and measured values of moment shows the validation of the confinement model followed.

5.2.6 Discussion on Effect of Flexural Behavior of Beam

The flexural capacity was observed for over and under-reinforced beams. It has been observed that under-reinforced beam failed due to yielding of longitudinal reinforcement. The confinement was done only in compression region of the beam specimens but they also failed due to yielding of longitudinal steel. The flexural capacity of unconfined and confined under-reinforced beam remained almost the same. The confinement effect had no effect on flexural capacity of beams.

The flexural capacity of over-reinforced confined beam also showed no increase. However there was an ample warning before failure of confined over-reinforced beams. Failure of over-reinforced beams is compression controlled and is demonstrated by concrete compression failure, due to the confinement provided in compression region better ductility is displayed.

5.2 Conclusions

The conclusions from this part of the investigation are given below:

- The flexural capacity of beams is mainly influenced by the characteristics of the longitudinal reinforcement rather than the degree of confinement of the compression concrete.
- Test results indicated that confinement stirrups in compression half of concrete beams improves the ductility. This ductility is more pronounced in over-reinforced beams indicated by their ductile failure.
- Over-reinforced beams can be made to fail in ductile manner by using confinement reinforcement
- The crack penetration in compression concrete can be delayed by its confinement.
- The dilation effect of the concrete in compression is reduced by provision of confinement stirrups.

REFRENCES

1. ACI, *High Strength Concrete, ACI 363R-92, ACI Committee 363 Report, American Concrete Institute, Detroit, 1992.*
2. Godfrey, K.A., *Concrete Strength Record Jumps 36%.* Civil Engineering—ASCE, 1987. **57**(10): p. 84-86.
3. Park, R. and D. Ruitong, *Ductility of doubly reinforced concrete beam sections.* ACI Structural Journal, 1988. **85**(2).
4. Samdani, S. and S.A. Sheikh, *Analytical study of FRP-confined concrete columns*. 2003: University of Toronto.
5. Shohana Iffat, K.M., Munaz Ahmad Noor, *Beam ductility experiment using 500 grade steel.* International Journal science & engineering investigations, 2012. **1**(1).
6. Hadi, M. and R. Jeffry, *Effect of different confinement shapes on the behaviour of reinforced HSC beams.* Asian J. Civ. Eng, 2010. **11**(4): p. 451-462.
7. Murugesan Reddiar, M.K., *Stress-Strain Model of Unconfined and Confined Concrete and Stress-block Parameters*. 2010.
8. Elbasha, N.M., *Behaviour of over-reinforced HSC helically confined beams.* 2005.
9. Kwan, A., F. Au, and S. Chau, *Effects of confinement on flexural strength and ductility design of HS concrete beams.* Structural Engineer, 2004.
10. Kwan, A., S. Chau, and F. Au, *Improving flexural ductility of high-strength concrete beams.* Proceedings of the Institution of Civil Engineers: Structures and Buildings, 2006. **159**(6): p. 339-347.
11. Ziara, M.M., *The influence of confining the compression zone in the design of structural concrete beams.* 1993.
12. Montoya, E., F.J. Vecchio, and S.A. Sheikh, *Compression field modeling of confined concrete: Constitutive models.* Journal of materials in civil engineering, 2006. **18**(4): p. 510-517.
13. Salse, E. and M. Fintel. *Strength, stiffness and ductility properties of slender shear walls*. in *Proceedings of 5th VVorld Conference on Earthquake Engineering—9WCEE, Rome, Italy*. 1973.
14. Carrillo, J. and S.M. Alcocer, *Seismic performance of concrete walls for housing subjected to shaking table excitations.* Engineering structures, 2012. **41**: p. 98-107.
15. Ziara, M., D. Haldane, and A. Kuttab, *Shear and flexural strengths resulting from confinement of the compression regions in circular section structural concrete beams.* Magazine of Concrete Research, 1993. **45**(164): p. 211-219.
16. Campione, G., *Analytical model for high-strength concrete columns with square cross-section.* Structural Engineering and Mechanics, 2008. **28**(3): p. 295-316.
17. Carrillo, J. and S.M. Alcocer, *Acceptance limits for performance-based seismic design of RC walls for low-rise housing.* Earthquake Engineering & Structural Dynamics, 2012. **41**(15): p. 2273-2288.
18. Park, R. *Ductility evaluation from laboratory and analytical testing*. in *Proceedings of the 9th World Conference on Earthquake Engineering, Tokyo-Kyoto, Japan*. 1988.
19. Sargin, M., *Stress-strain relationships for concrete and the analysis of structural concrete sections*. 1971: Solid Mechanics Division, University of Waterloo.
20. Foster, S.J., J. Liu, and S.A. Sheikh, *Cover spalling in HSC columns loaded in concentric compression.* Journal of Structural Engineering, 1998. **124**(12): p. 1431-1437.
21. Ashour, S.A., *Effect of compressive strength and tensile reinforcement ratio on flexural behavior of high-strength concrete beams.* Engineering Structures, 2000. **22**(5): p. 413-423.
22. Kwan, A., F. Au, and S. Chau, *Theoretical study on effect of confinement on flexural ductility of normal and high-strength concrete beams.* Magazine of Concrete Research, 2004. **56**(5): p. 299-309.
23. Pam, H., A. Kwan, and M. Islam, *Flexural strength and ductility of reinforced normal-and high-strength concrete beams.* Proceedings of the ICE-Structures and Buildings, 2001. **146**(4): p. 381-389.

24. Paulay, T. and M. Priestley, *Seismic Design of Reinforced Concrete and Masonry Buildings, John Wiley & Sons, New York.* 1992.
25. Grant, L.H., S.A. Mirza, and J.G. MacGregor. *Monte Carlo study of strength of concrete columns*. in *ACI Journal Proceedings*. 1978. ACI.
26. Kareem, A. and J. Hsieh, *Statistical analysis of tubular R/C sections.* Journal of Structural Engineering, 1988. **114**(4): p. 900-916.
27. Park, H., et al., *Moment–curvature relationship of flexure-dominated walls with partially confined end-zones.* Engineering structures, 2007. **29**(1): p. 33-45.
28. Kwak, H.-G. and S.-P. Kim, *Simplified monotonic moment–curvature relation considering fixed-end rotation and axial force effect.* Engineering Structures, 2010. **32**(1): p. 69-79.
29. Hadi, M.N. and N. Elbasha, *Effects of tensile reinforcement ratio and compressive strength on the behaviour of over-reinforced helically confined HSC beams.* Construction and Building Materials, 2007. **21**(2): p. 269-276.
30. Hadi, M.N. and L.C. Schmidt, *Use of helixes in reinforced concrete beams.* Structural Journal, 2002. **99**(2): p. 191-198.
31. Hadi, M.N., *Helically reinforced HSC beams reinforced with high strength steel.* International Journal of Materials and Product Technology, 2005. **23**(1-2): p. 138-148.

APPENDIX –A

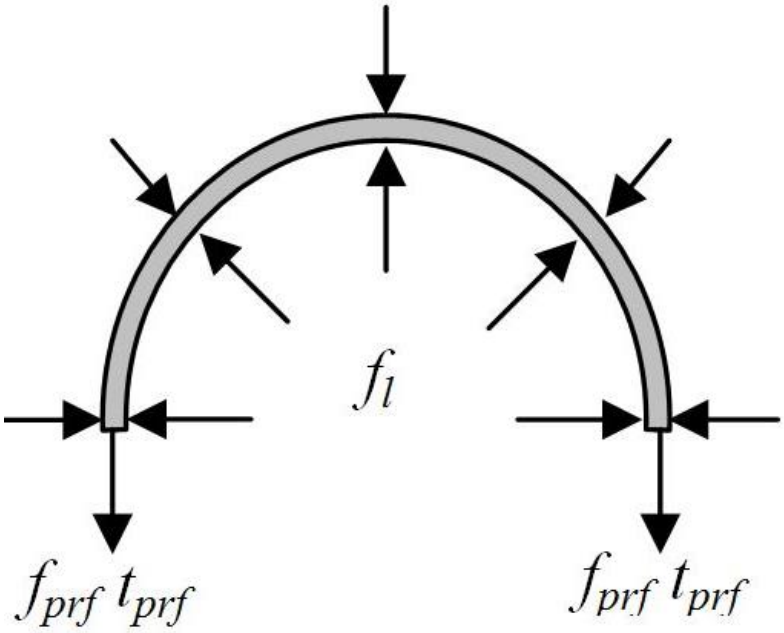

Figure A-1 Confining Mechanism

APPENDIX –B

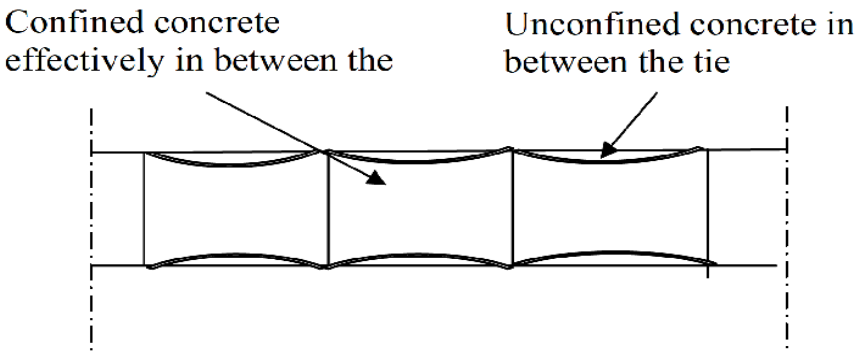

Figure 0-1: Effective confined concrete for rectangular tie

APPENDIX C

Table B-1: Mix Design

Description	Details
Cement	410 Kg / m^3
Fine Aggregate	584 Kg / m^3
Coarse Aggregate	1224 Kg / m^3
W/C ratio	0.43
Admixtures	0.5-1.5% by weight of cement
Mix ratio	1:1.48:2.96

Table B-2: Properties of Cement

Tests	Test results	Specifications
Specific gravity	3.06	ASTM C 188 – 95
Initial setting time	150 minutes at 17^0C	ASTM C 191 – 01
Final setting time	285 minutes at 17^0C	ASTM C 191 – 01

Table B-3: Properties of Fine Aggregate

Tests	Test results	Specifications
Specific gravity	2.71	ASTM C 128 – 01
Absorption	1.1%	ASTM C 128 – 01
FM	2.66	ASTM C 33 – 02

Table B-4: Gradation of Fine Aggregate

Sieve No.	Mass Retained (g)	Percent Retained	Cumulative Percent Retained	Percent Passing	
				Actual	ASTM C 33-02
3/8”	0	0	0	100	---
#4	8	1.54	1.54	98.46	95 - 100
#8	42	8.08	9.62	90.38	80 - 100
#16	108	20.77	30.39	69.61	50 - 85
#30	156	30.00	60.39	39.61	25 - 60
#50	136	26.16	86.55	13.45	5 - 30
#100	42	8.08	94.63	5.37	0 - 10
Pan	28	5.39	---	---	---
Total	520	---	---	---	---

Table B-5 : Properties of Coarse Aggregate

Detail of tests	Test results
Impact value (percent)	13.9
Crushing value(percent)	20.2
Abrasion value(percent)	15.2
Specific gravity	2.67

Table B-6 : Gradation of Coarse Aggregate

Sieve size (mm)	Mass Retained (g)	Percent Retained	Cumulative Percent Retained	Percent Passing	
				Actual	ASTM C 33-02
37.5	0	0	0	100	100
19	72	3.60	3.60	96.40	90-100
9.5	1011	50.55	54.15	45.85	40-70
4.75	877	43.85	98	2	0-15
Pan	40	2	100	0	0-5

Table B-7: Technical Data – Admixture

Description	Details
Name	P-200
Form	Viscous liquid
Color	Light brown
Specific gravity	1.08 ± 0.02 g/cm^3
pH-value	7.0 ± 1
Alkali content (%)	Less than or equal to 5.0
Chloride content (%)	Less than or equal to 0.10

Table B-8 : Summary of beam designations

Sr #	Beam Designation	28 Days Concrete Compressive Strength (MPa)	Spacing of Confinement (mm)	p/p_b	Effective Depth (mm)
UNDER-REINFORCED BEAMS					
1	R-UR-1	30	125	0.654	275
2	R-UR-2	30	125	0.654	275
3	C-UR-1	30	63	0.654	275
4	C-UR-2	30	63	0.654	275
5	C-UR-3	30	63	0.654	275
OVER-REINFORCED BEAMS					
6	R-OR-1	30	125	1.067	275
7	R-OR-2	30	125	1.067	275
8	C-OR-1	30	63	1.067	275
9	C-OR-2	30	63	1.067	275
10	C-OR-3	30	63	1.067	275

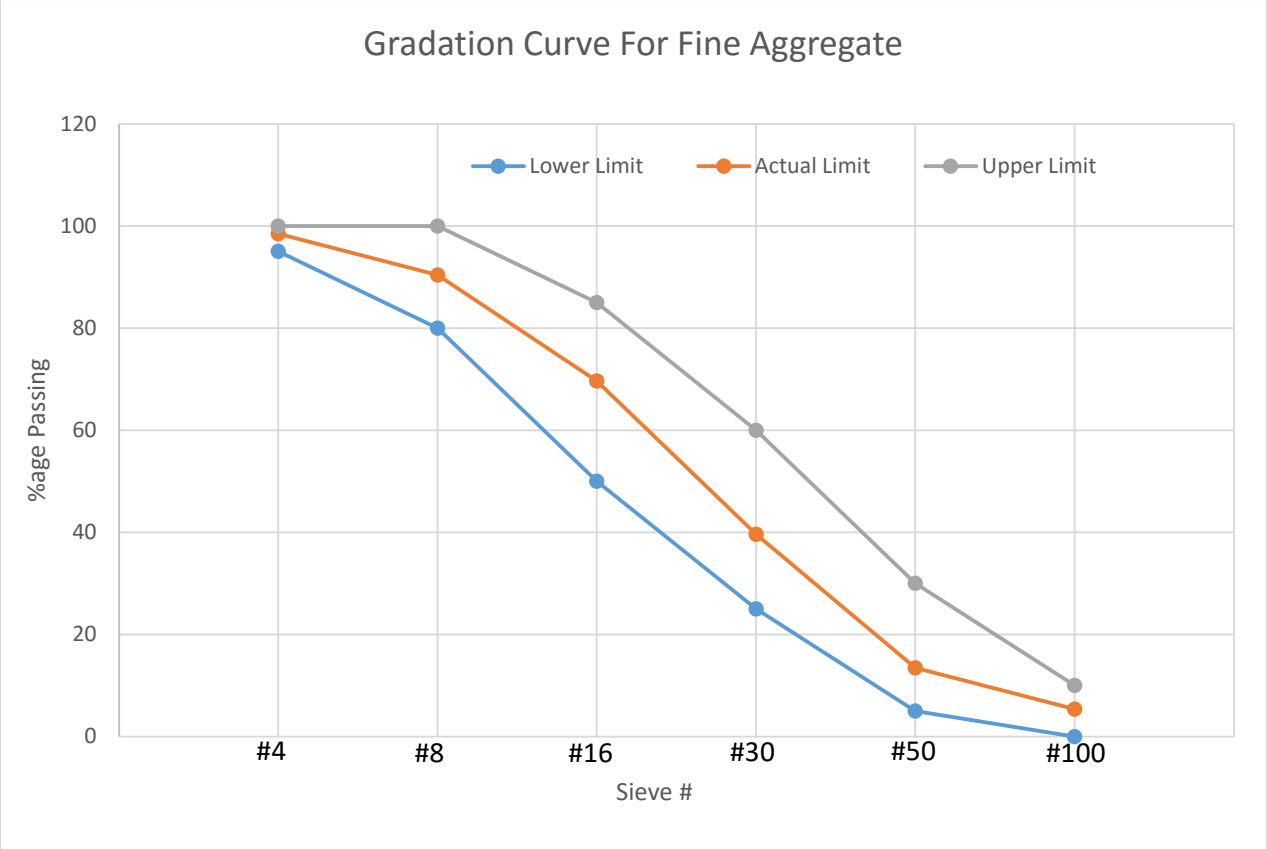

Figure B-1: Particle Size Distribution of Fine Aggregate

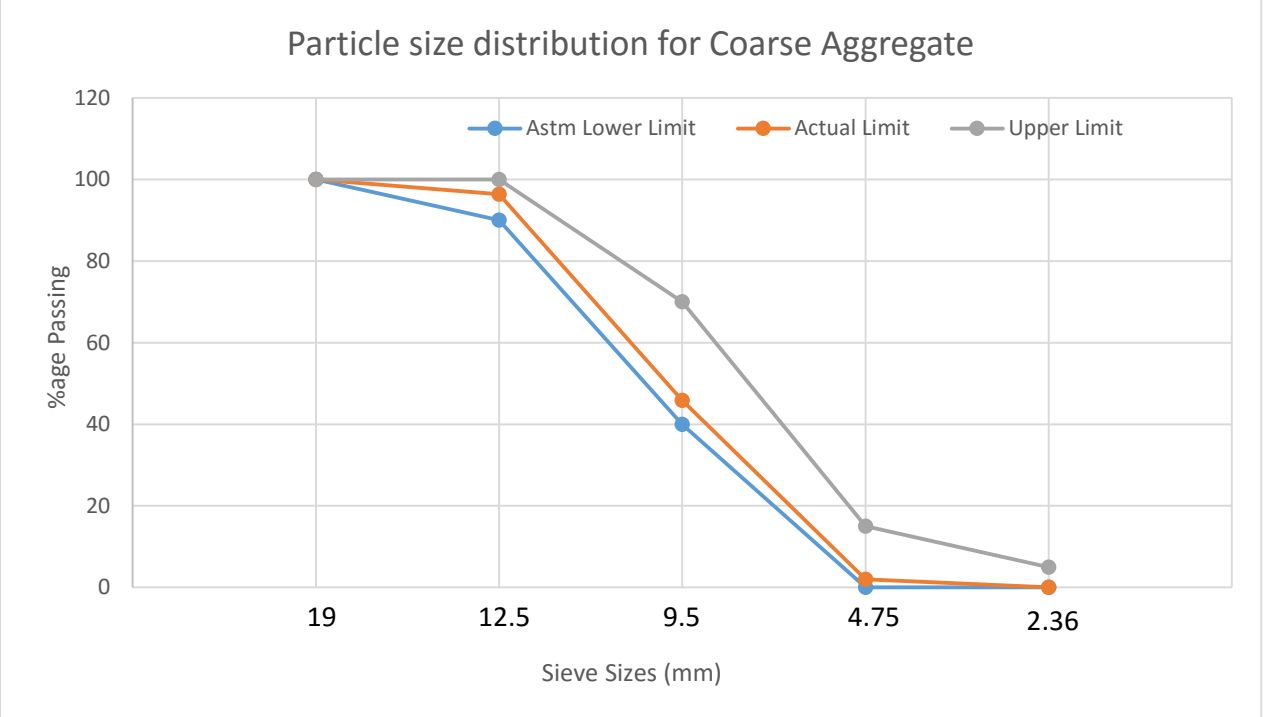

Figure B-2 : Particle Size Distribution of Coarse Aggregate.

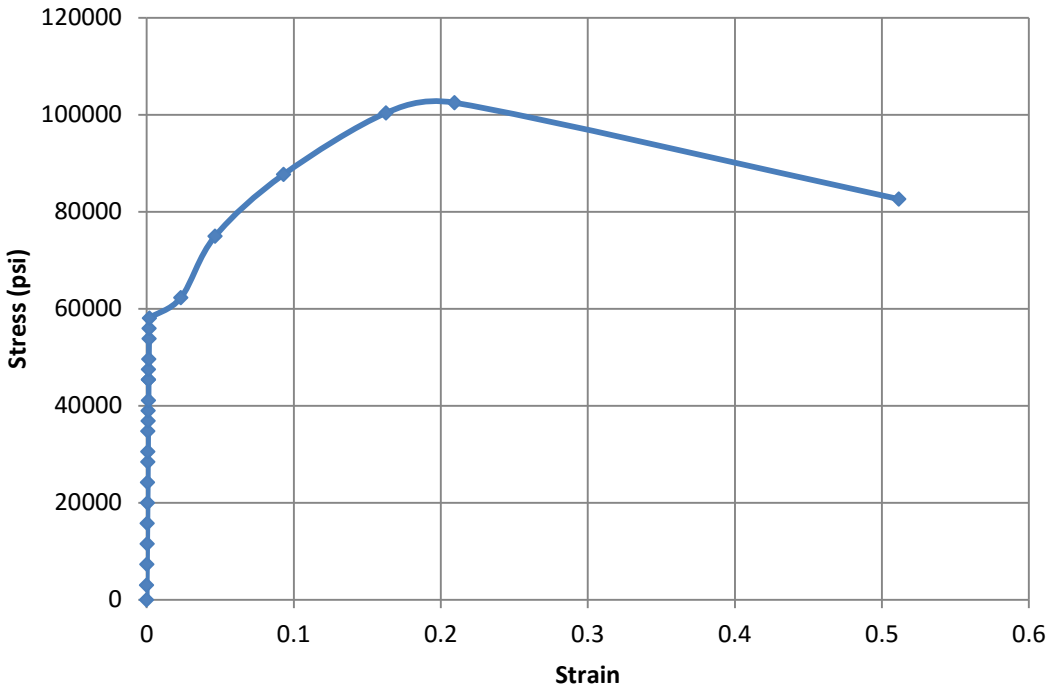

Figure C-3 : Steel Reinforcement Stress Strain Curve

Table B-9: Compressive Strength of Cylinders

Size of Cylinders (in)	Day of Testing	Compressive Strength (psi)
6x12	7	2812
		2826
	14	3238
		3807
	28	4889
		4714
		4374
		4217
		3962
		4402
		3891
		4075

Fig 3-4 Detailed Drawings of Specimen

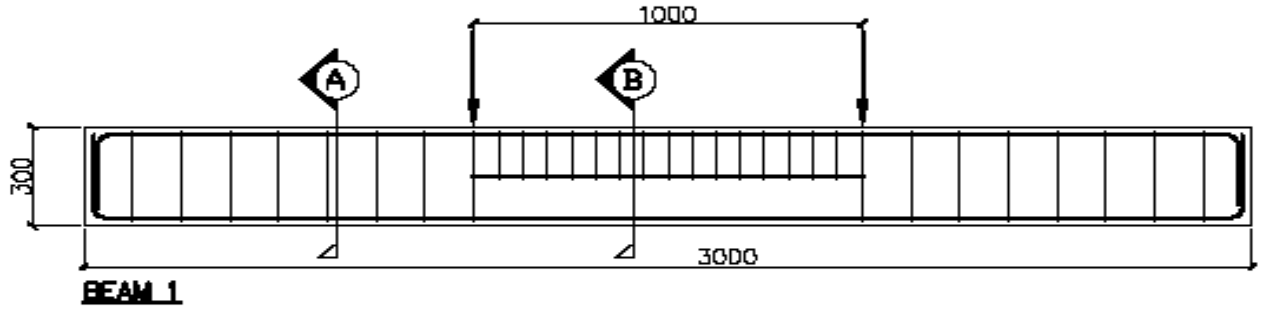

BEAM 1

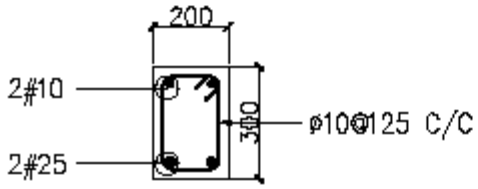

SECTION AT A

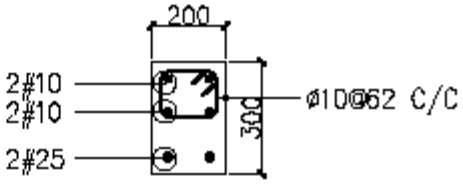

SECTION AT B

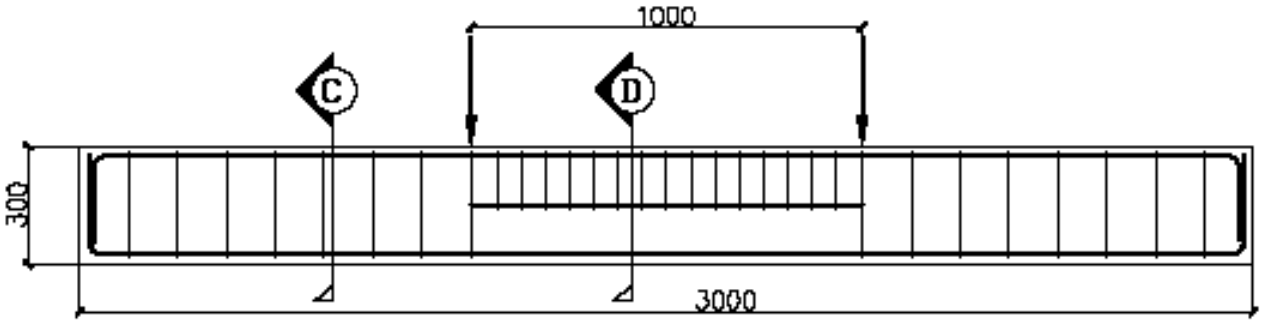

BEAM 2

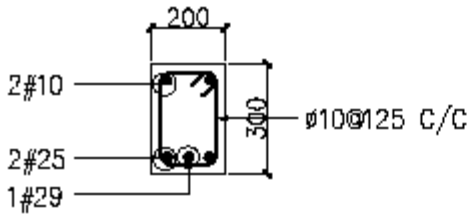

SECTION AT C

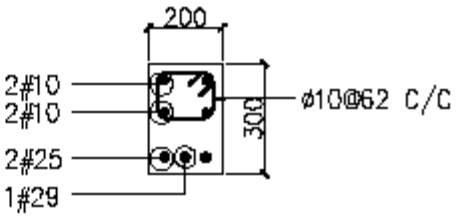

SECTION AT D

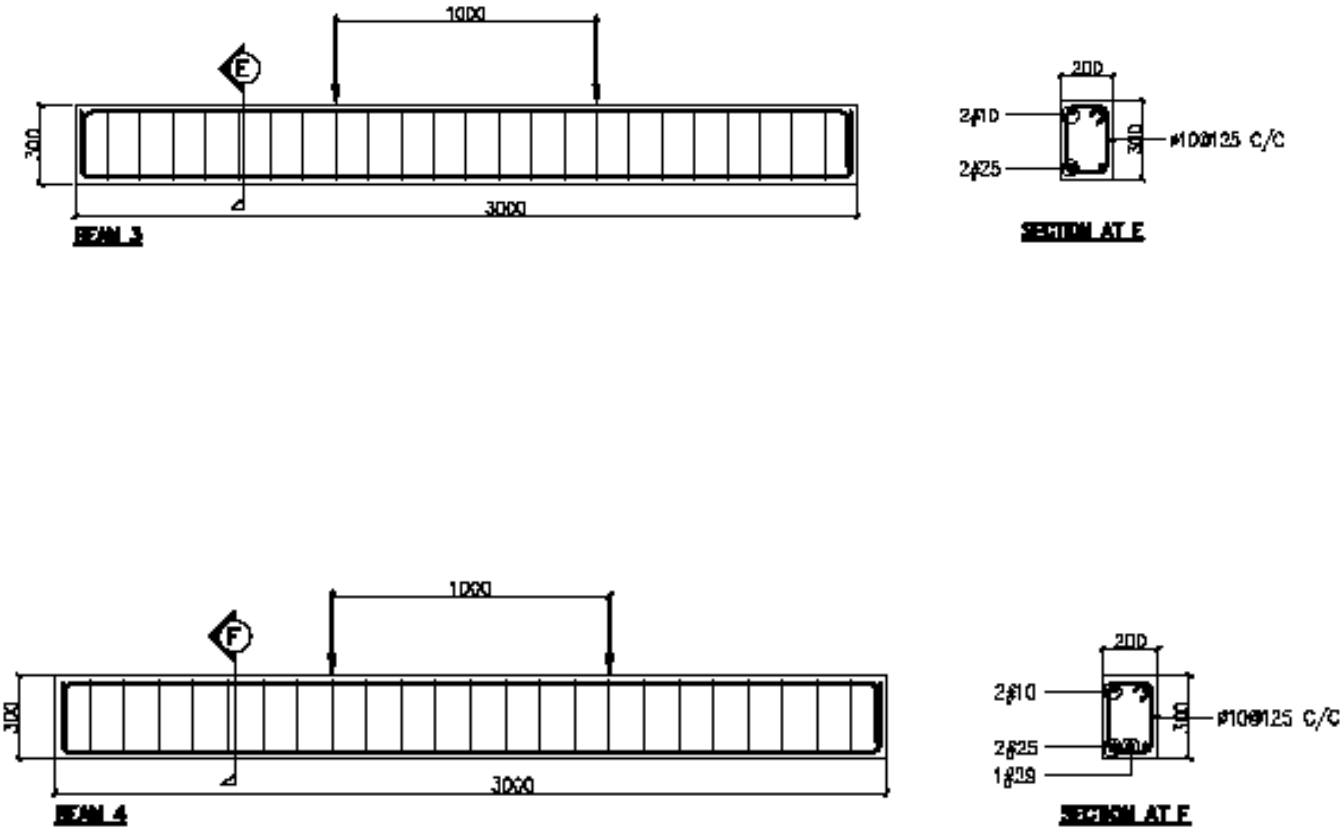

Figure B-3: Detail Drawings of Specimens

Formwork

Figure B-4: Formwork for Beams

Reinforcement Cages for Beam

Figure B-5 : Reinforcement Cages For Beams

CASTING AND CURING OF BEAMS

Figure B-6 : Form work for Beams

Figure B-7 : Pouring/Casting of Beams

Figure B-8 : Loading Arrangement

Load Deflection Data for Beams

Table B-10: Load Deflection Table for R-UR-1

Load		Deflection		
(Tons)	(KN)	Mid	Quarter Point	Quarter Point
3.25	31.90	4.57	5.41	5.41
3.22	31.54	4.58	5.43	5.43
3.19	31.28	4.59	5.45	5.45
5.76	56.50	6.53	6.80	6.80
5.17	50.76	6.69	7.03	7.03
5.03	49.38	6.73	7.09	7.09
4.94	48.48	6.75	7.13	7.13
4.88	47.86	6.77	7.16	7.16
4.83	47.36	6.78	7.19	7.19
4.79	46.96	6.79	7.20	7.20
4.75	46.60	6.80	7.22	7.22

4.72	46.30	6.81	7.24	7.24
4.69	46.02	6.82	7.25	7.25
4.67	45.78	6.82	7.26	7.26
4.64	45.56	6.83	7.27	7.27
8.29	81.35	9.71	9.18	9.18
7.81	76.60	9.80	9.34	9.34
7.64	74.95	9.84	9.41	9.41
7.54	73.94	9.86	9.45	9.45
7.46	73.14	9.87	9.48	9.48
7.40	72.56	9.89	9.51	9.51
7.34	72.04	9.90	9.53	9.53
7.30	71.59	9.91	9.55	9.55
10.38	101.86	11.81	10.97	10.97
11.74	115.15	13.50	13.03	13.03
11.48	112.58	-3.82	12.36	12.36

Table B-11: Load Deflection Table for R-UR-2

Load		Deflection		
(Ton)	(KN)	Quarter Pt	Mid Pt	Quarter Pt
3.15	30.94	0.01	0.01	0.01
5.41	53.08	1.38	1.79	1.38
5.27	51.67	1.40	1.81	1.40
5.22	51.20	1.40	1.81	1.40
7.26	71.21	2.90	3.70	2.90
7.18	70.45	2.91	3.71	2.91
10.77	105.61	5.55	7.04	5.55
10.64	104.38	5.56	7.05	5.56
10.58	103.83	5.56	7.05	5.56
15.08	147.89	8.89	11.16	8.89
14.78	144.94	8.91	11.20	8.91
14.65	143.75	8.92	11.22	8.92
15.50	152.09	9.36	11.79	9.36
16.88	165.58	10.57	13.36	10.57
16.72	164.07	10.58	13.37	10.58
18.09	177.49	11.40	14.43	11.40
18.82	184.65	12.00	15.20	12.00
18.68	183.28	12.09	15.31	12.09
21.14	207.43	13.84	17.52	13.84
20.84	204.48	13.86	17.54	13.86
23.64	231.96	16.35	20.73	16.35
23.30	228.56	16.38	20.77	16.38
25.27	247.91	18.45	23.49	18.45
24.85	243.74	18.49	23.55	1 8.49

Table B-12 : Load Deflection Table for R-OR-1

Load Cell		Deflection (mm)		
(ton)	(KN)	Quarter Pt	Mid Pt	Quarter Pt
0.25	2.47	0.17	0.13	0.17
3.23	31.73	1.56	1.63	1.56
6.19	60.69	3.04	3.41	3.04
6.05	59.37	3.05	3.42	3.05
10.87	106.66	5.65	6.65	5.65
10.77	105.65	5.66	6.66	5.66
11.97	117.45	6.22	7.37	6.22
13.85	135.90	7.23	8.63	7.23
14.17	139.02	7.43	8.87	7.43
15.13	148.39	7.85	9.40	7.85
18.19	178.40	9.56	11.56	9.56
17.83	174.94	9.60	11.59	9.60
17.79	174.50	9.62	11.63	9.62
17.69	173.50	9.63	11.64	9.63
22.29	218.68	12.47	15.15	12.47
22.11	216.87	12.49	15.17	12.49
22.00	215.86	12.50	15.18	12.50
26.23	257.32	14.92	18.24	14.92
25.82	253.34	14.96	18.29	14.96
25.60	251.11	14.99	18.32	14.99
25.46	249.76	15.00	18.34	15.00
30.18	296.10	17.95	22.04	17.95
33.98	333.35	22.91	28.28	22.91

Table B-13: Load Deflection Table for R-OR-2

Load		Deflection (mm)		
(Tons)	(KN)	Quarter Pt.	Mid Pt.	Quarter Pt.
0.68	6.66	0.25	0.37	0.25
2.31	22.65	0.65	0.99	0.65
4.85	47.54	1.31	1.97	1.31
5.65	55.47	1.63	2.45	1.63
5.61	55.00	1.63	2.45	1.63
8.01	78.63	2.48	3.62	2.48
7.94	77.93	2.48	3.62	2.48
7.90	77.54	2.48	3.62	2.48
7.88	77.29	2.48	3.62	2.48
10.03	98.39	3.21	4.64	3.21
9.93	97.41	3.21	4.64	3.21
9.88	96.92	3.21	4.64	3.21
12.59	123.47	4.28	6.10	4.28
12.56	123.19	4.28	6.10	4.28
15.53	152.37	5.18	7.34	5.18
15.11	148.20	5.20	7.36	5.20
15.02	147.34	5.20	7.36	5.20
18.24	178.94	6.25	8.86	6.25
17.70	173.59	6.26	8.91	6.26
17.59	172.58	6.26	8.91	6.26
20.32	199.37	7.14	10.26	7.14
19.95	195.69	7.15	10.27	7.15
23.37	229.23	8.45	12.20	8.45
24.23	237.69	8.81	12.74	8.81
26.40	259.02	9.75	14.14	9.75
26.22	257.19	9.76	14.15	9.76
27.95	274.22	10.42	15.23	10.42
30.04	294.67	11.33	16.57	11.33
29.73	291.62	11.35	16.58	11.35
29.57	290.08	11.37	16.59	11.37
32.33	317.13	12.45	18.17	12.45
31.76	311.54	16.99	22.90	16.99
37.12	364.13	20.06	27.40	20.06
36.27	355.79	20.16	27.51	20.16

Table B-14 : Load Deflection Table for C-OR-2

Load		Deflection (mm)		
(Tons)	(KN)	Quarter Pt.	Mid Pt.	Quarter Pt.
0.04	0.35	0.00	0.00	0.00
3.13	30.68	0.59	1.12	0.59
6.96	68.26	1.58	2.76	1.58
9.57	93.83	2.34	4.03	2.34
10.17	99.76	2.62	4.51	2.62
10.09	99.02	2.62	4.51	2.62
12.28	120.44	3.32	5.68	3.32
12.19	119.57	3.32	5.68	3.32
15.12	148.29	4.27	7.19	4.27
14.92	146.34	4.28	7.19	4.28
17.39	170.56	4.98	8.33	4.98
18.02	176.78	5.40	9.00	5.40
18.57	182.14	5.56	9.26	5.56
20.19	198.10	6.21	10.29	6.21
20.06	196.77	6.21	10.29	6.21
23.08	226.44	7.40	12.15	7.40
22.92	224.87	7.41	12.16	7.41
25.87	253.79	8.59	14.03	8.59
25.61	251.21	8.60	14.04	8.60
30.10	295.27	10.40	16.90	10.40
29.58	290.16	10.42	16.93	10.42
33.25	326.17	12.14	19.69	12.14
35.37	346.97	13.23	21.50	13.23

Table B-15: Load Deflection Table for C-UR-2

Load		Deflection (mm)		
(Tons)	(KN)	Quarter Pt.	Mid Pt.	Quarter Pt.
1.78	17.45	0.49	0.66	0.49
1.76	17.30	0.49	0.66	0.49
2.01	19.76	0.56	0.78	0.56
4.07	39.91	1.16	1.83	1.16
6.26	61.42	2.09	3.45	2.09
6.17	60.51	2.10	3.45	2.10
7.78	76.35	2.79	4.66	2.79
7.71	75.62	2.79	4.66	2.79
7.67	75.21	2.79	4.65	2.79
9.77	95.84	3.64	6.12	3.64
9.64	94.52	3.64	6.12	3.64
9.58	93.99	3.64	6.12	3.64
9.54	93.60	3.64	6.12	3.64
13.14	128.93	5.13	8.67	5.13
12.87	126.30	5.14	8.68	5.14
12.79	125.46	5.14	8.68	5.14
14.93	146.44	6.00	10.13	6.00
14.62	143.37	6.01	10.16	6.01
14.51	142.39	6.01	10.16	6.01
14.45	141.74	6.01	10.17	6.01
14.41	141.32	6.01	10.17	6.01
14.37	140.94	6.01	10.17	6.01
16.38	160.72	7.08	12.11	7.08
16.23	159.26	7.08	12.13	7.08
16.15	158.43	7.09	12.13	7.09
16.10	157.90	7.09	12.14	7.09
16.04	157.35	7.09	12.15	7.09
19.83	194.58	9.73	17.19	9.73
19.63	192.55	9.74	17.22	9.74
19.51	191.44	9.74	17.23	9.74
19.44	190.69	9.75	17.24	9.75
19.38	190.10	9.75	17.25	9.75
20.73	203.37	11.25	20.60	11.25
20.47	200.85	11.25	20.65	11.25
21.30	208.96	14.95	30.17	14.95

Table B-16 : Load Deflection Table for C-UR-3

Load		Deflection (mm)		
(Tons)	(KN)	Quarter Pt.	Mid Pt.	Quarter Pt.
0.03	0.34	0.02	0.04	0.02
5.14	50.46	1.44	2.29	1.44
5.07	49.71	1.45	2.30	1.45
5.03	49.38	1.45	2.30	1.45
8.34	81.78	2.96	4.70	2.96
8.19	80.32	2.97	4.71	2.97
8.13	79.78	2.97	4.70	2.97
10.18	99.85	3.84	6.03	3.84
11.76	115.41	4.79	7.46	4.79
11.68	114.61	4.79	7.46	4.79
11.64	114.15	4.79	7.46	4.79
11.60	113.82	4.79	7.46	4.79
15.56	152.64	6.80	10.47	6.80
15.43	151.40	6.80	10.47	6.80
15.38	150.83	6.80	10.47	6.80
19.02	186.57	8.54	13.07	8.54
18.85	184.95	8.54	13.08	8.54
18.77	184.15	8.55	13.08	8.55
18.71	183.58	8.55	13.08	8.55
23.41	229.70	10.68	16.39	10.68
23.17	227.32	10.70	16.42	10.70
23.06	226.20	10.70	16.43	10.70
27.05	265.32	12.62	19.71	12.62
26.13	256.31	12.88	20.35	12.88
25.92	254.32	12.89	20.38	12.89

Table B-17: Load Deflection Table for C-OR-3

Load		Deflection (mm)		
(Tons)	(KN)	Quarter Pt.	Mid Pt.	Quarter Pt.
1.53	14.97	-0.15	0.00	-0.15
3.90	38.30	0.69	1.07	0.69
7.16	70.25	2.36	3.32	2.36
11.39	111.69	4.83	6.67	4.83
11.30	110.86	4.84	6.68	4.84
11.25	110.40	4.84	6.68	4.84
11.22	110.09	4.85	6.69	4.85
11.20	109.84	4.85	6.69	4.85
11.18	109.64	4.85	6.69	4.85
14.34	140.64	6.60	8.92	6.60
14.23	139.59	6.61	8.93	6.61
14.92	146.40	6.94	9.36	6.94
16.09	157.80	7.67	10.35	7.67
15.97	156.62	7.68	10.36	7.68
17.91	175.67	8.71	11.75	8.71
17.66	173.29	8.74	11.78	8.74
20.22	198.36	10.02	13.57	10.02
19.81	194.34	10.06	13.62	10.06
24.55	240.79	12.89	17.43	12.89
24.55	240.79	13.29	17.94	13.29
24.37	239.05	13.31	17.96	13.31
27.01	264.96	15.19	20.74	15.19
26.60	260.99	15.22	20.81	15.22

Table B-18 : Load Deflection Table for C-OR-2

Load		Deflection (mm)		
(Tons)	(KN)	Quarter Pt.	Mid Pt.	Quarter Pt.
1.53	14.97	-0.15	0.00	-0.15
3.90	38.30	0.69	1.07	0.69
7.16	70.25	2.36	3.32	2.36
11.39	111.69	4.83	6.67	4.83
11.30	110.86	4.84	6.68	4.84
11.25	110.40	4.84	6.68	4.84
11.22	110.09	4.85	6.69	4.85
11.20	109.84	4.85	6.69	4.85
11.18	109.64	4.85	6.69	4.85
14.34	140.64	6.60	8.92	6.60
14.23	139.59	6.61	8.93	6.61
14.92	146.40	6.94	9.36	6.94
16.09	157.80	7.67	10.35	7.67
15.97	156.62	7.68	10.36	7.68
17.91	175.67	8.71	11.75	8.71
17.66	173.29	8.74	11.78	8.74
20.22	198.36	10.02	13.57	10.02
19.81	194.34	10.06	13.62	10.06
24.55	240.79	12.89	17.43	12.89
24.55	240.79	13.29	17.94	13.29
24.37	239.05	13.31	17.96	13.31
27.01	264.96	15.19	20.74	15.19
26.60	260.99	15.22	20.81	15.22

Load Deflection Graphs for the beams

Under Reinforced Beams

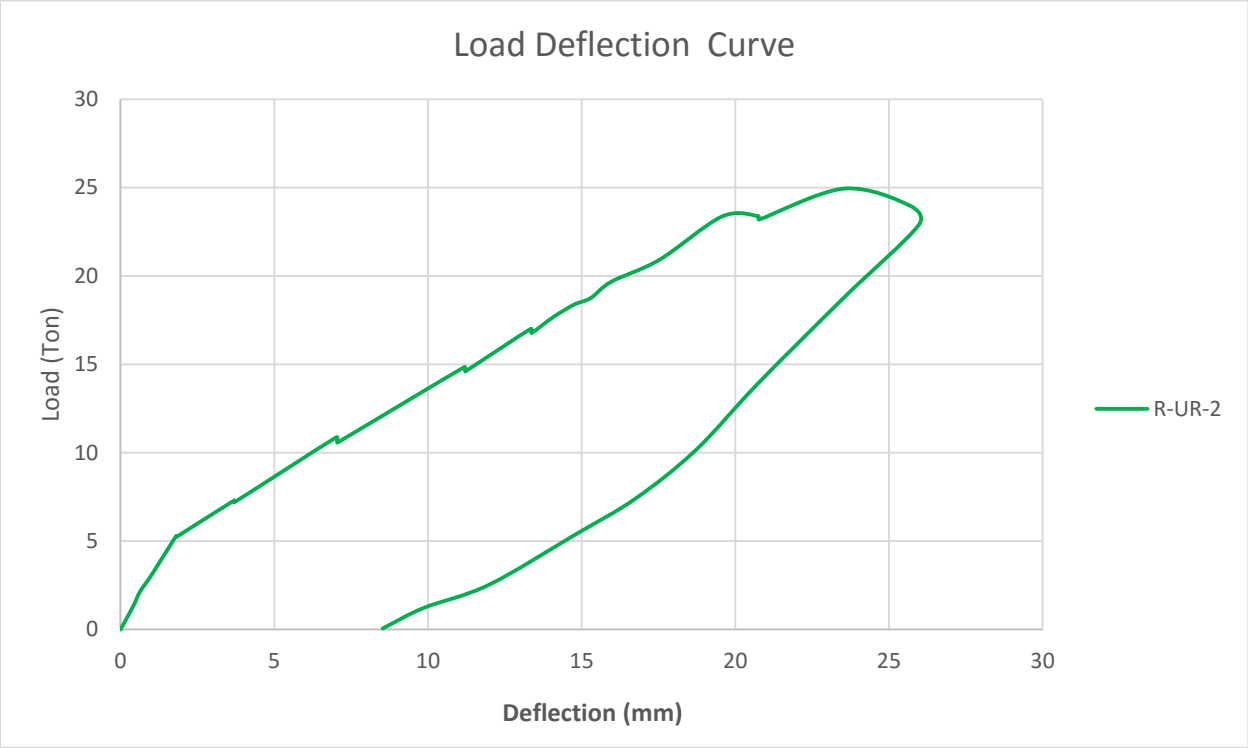

Figure B-9 Load- Deflection Curve for R-UR-2

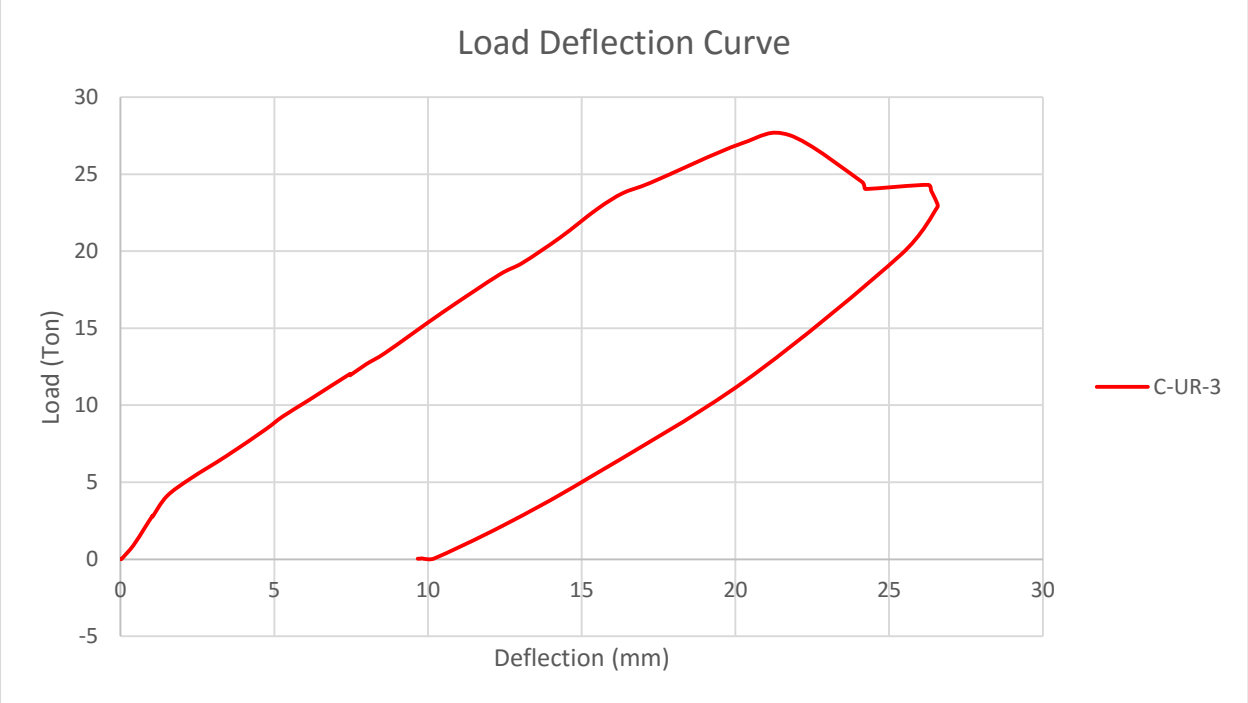

Figure B-10 Load Deflection Curve for C-UR-3

Figure B-11 Load Deflection curve For C-UR-2

Figure B-12 Load Deflection Curve for R-UR-1

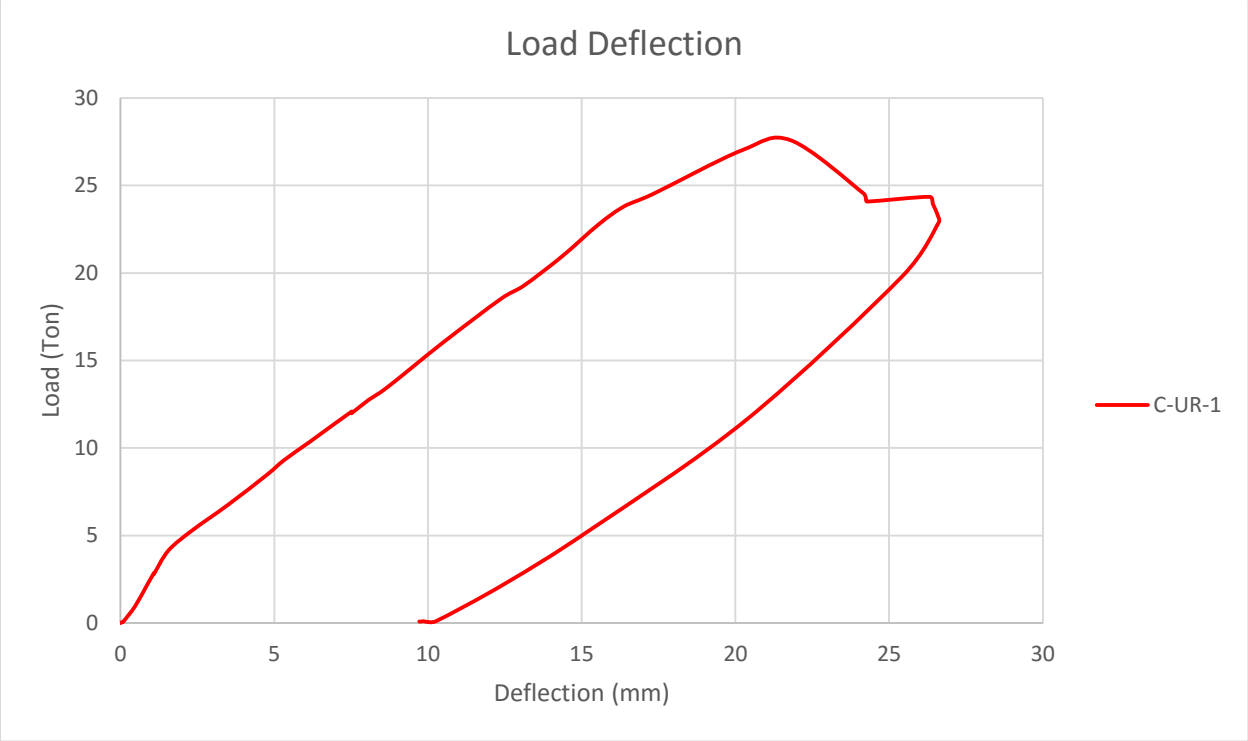

Figure B-13 Load Deflection Curve for C-UR-1

Load Deflection Curves For Over Reinforced Beams

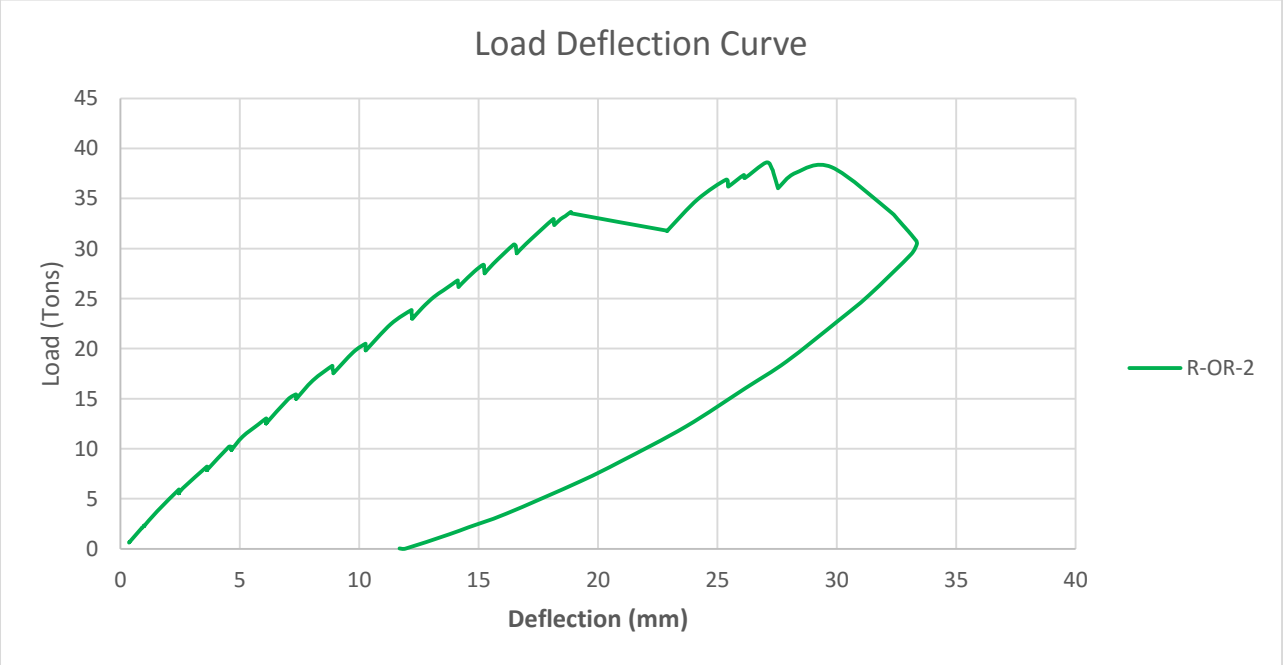

Figure B-14 Load Deflection Curve for R-OR-2

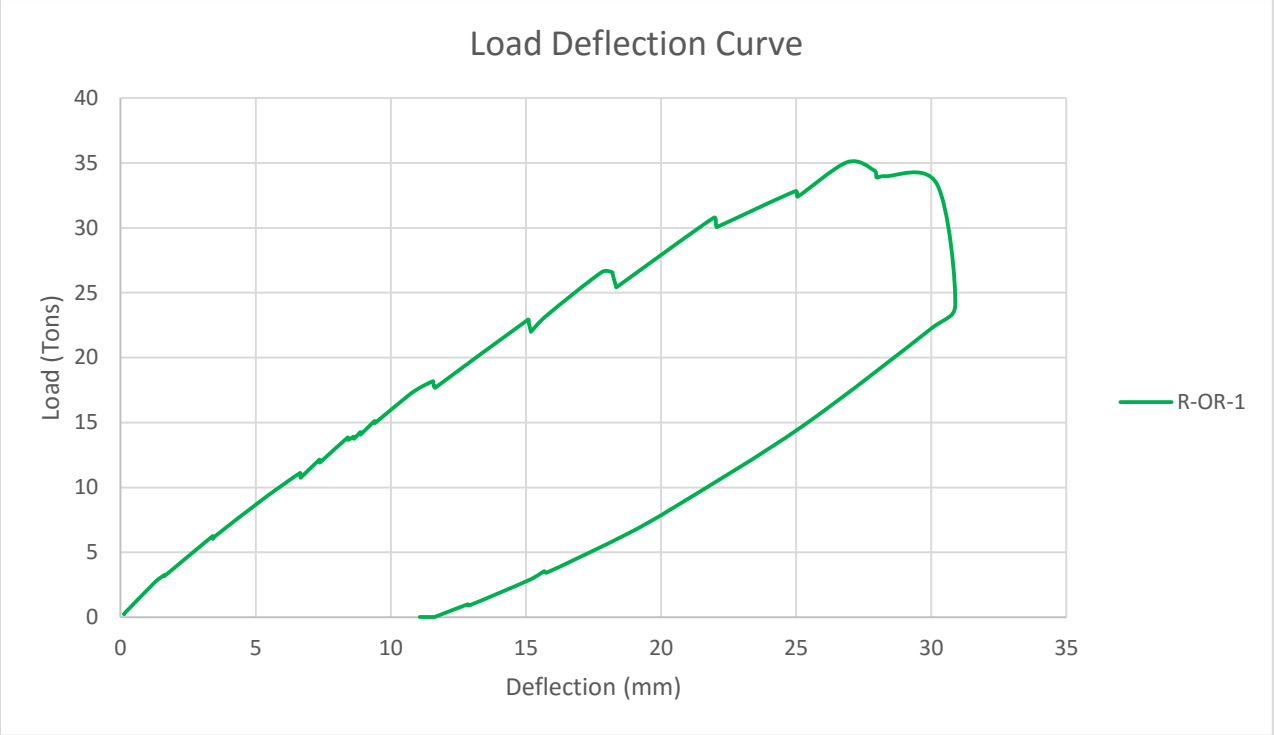

Figure B-15 Load Deflection Curve for R-OR-1

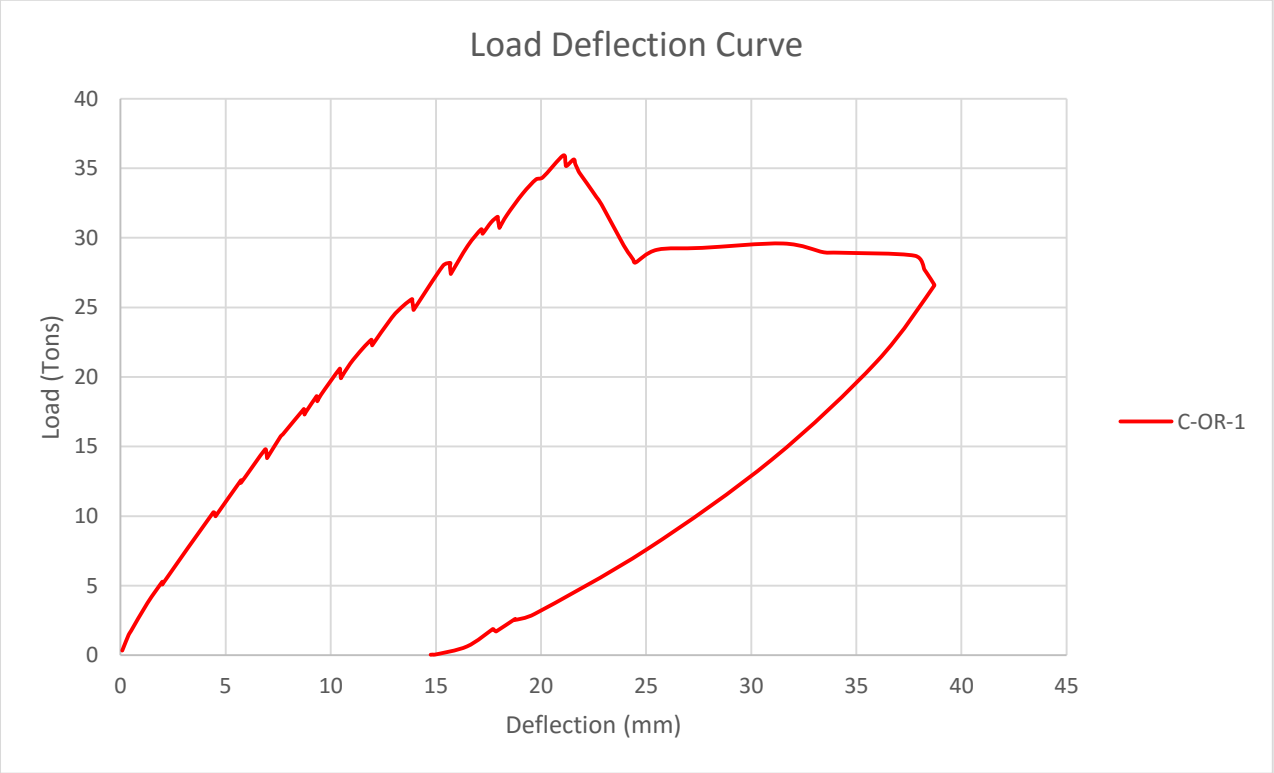

Figure B-16 Load Deflection Curve for C-OR-1

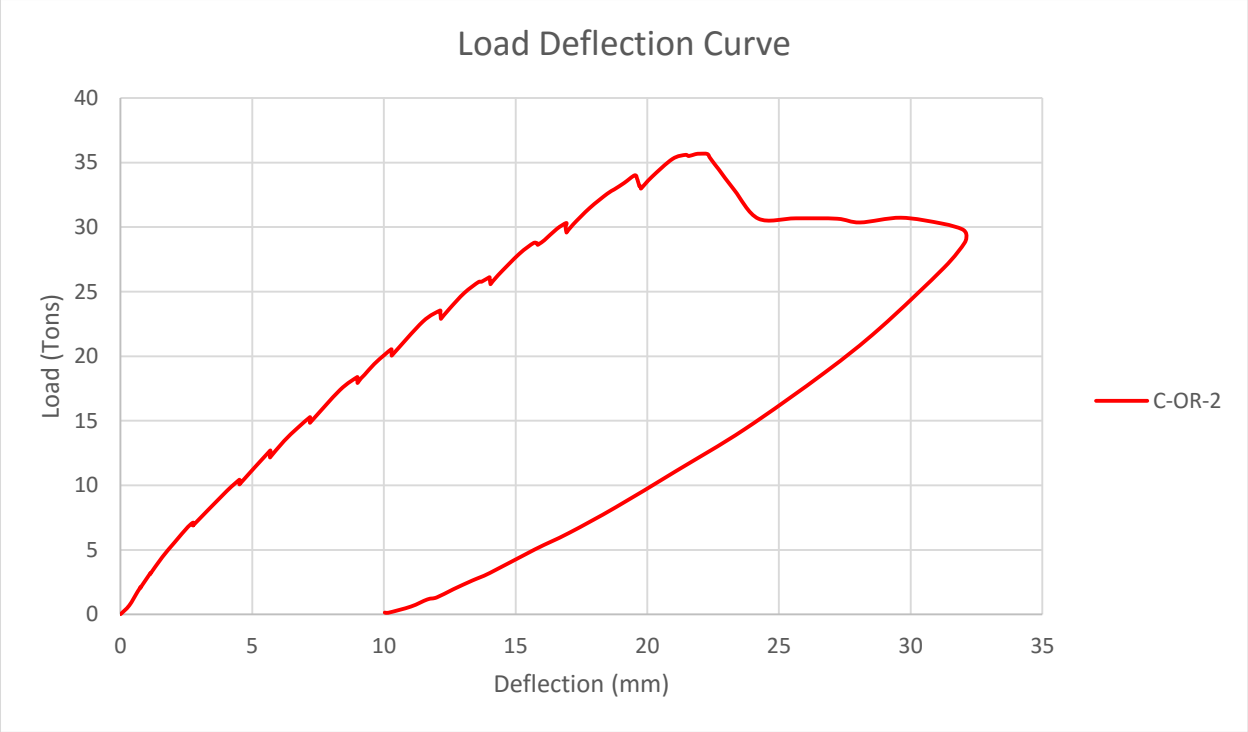

Figure B-17 Load Deflection Curve for C-OR-2

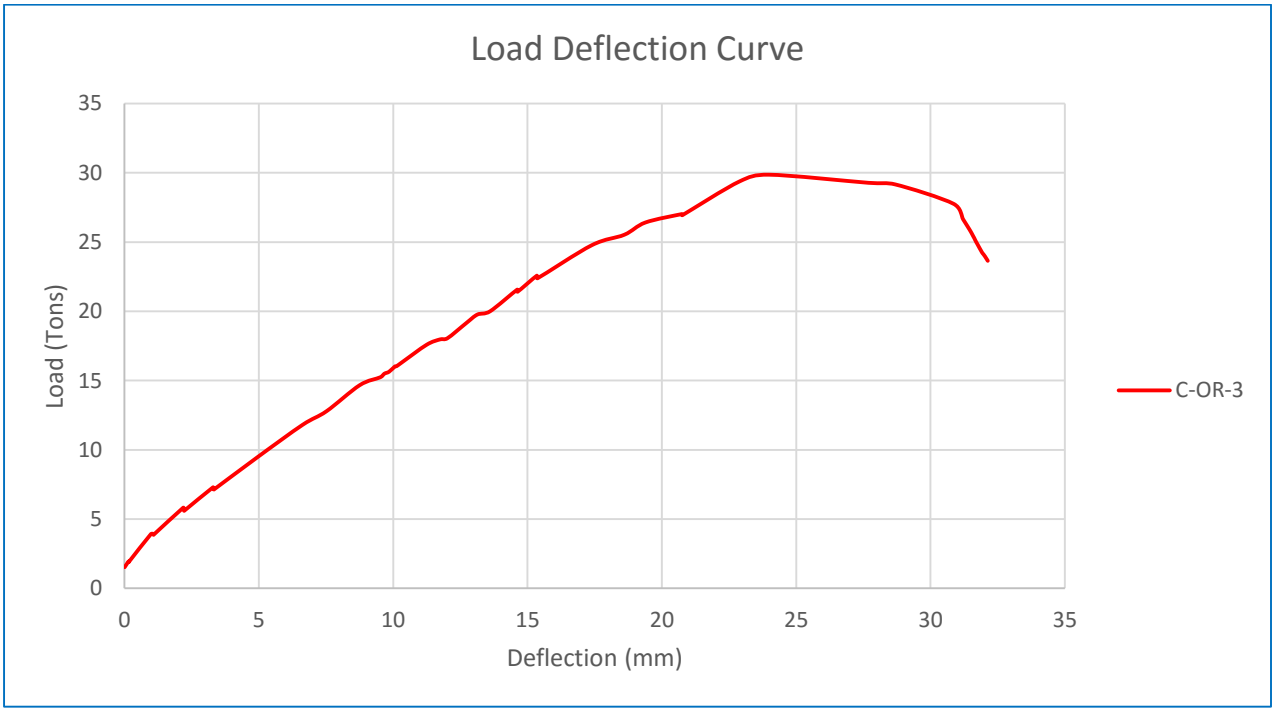

Figure B-18 Load Deflection Diagram for C-OR-3

Failure Patterns of Beams

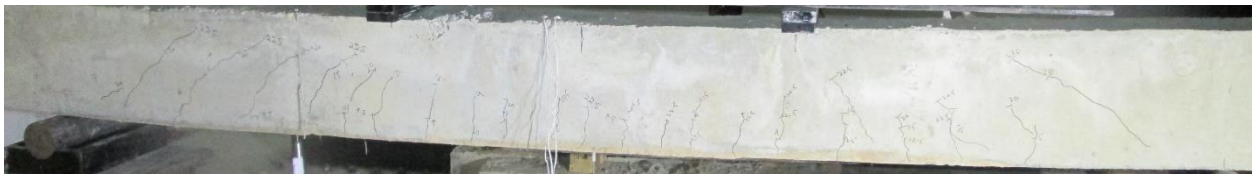

Figure B-19 : Cracking Pattern of C-UR-1

Figure B-20 : Cracking Pattern of C-UR-2

Figure B-21 : Cracking Pattern of R-OR-1

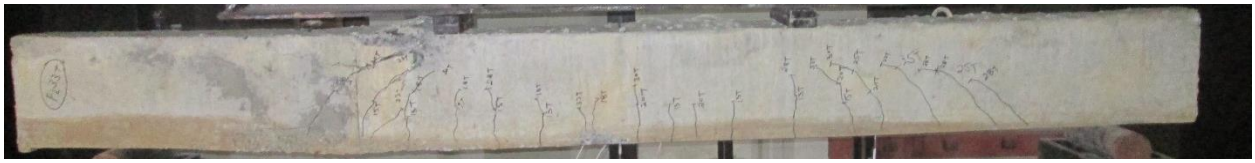

Figure B-22 : Cracking Pattern of C-OR-1

Figure B-23 : Cracking pattern of R-UR-1

Figure B-24 : Cracking Pattern of C-OR-2

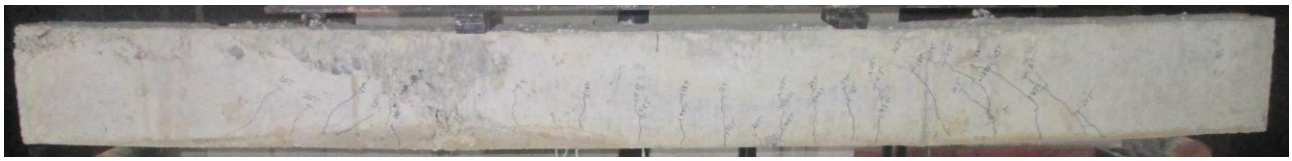

Figure B-25 : Cracking Pattern of C-OR-3

Figure B-26 : Cracking Pattern of R-UR-2

Figure B-27 : Cracking Pattern of C-UR-3

Figure B-28 : Cracking Pattern of R-OR-2

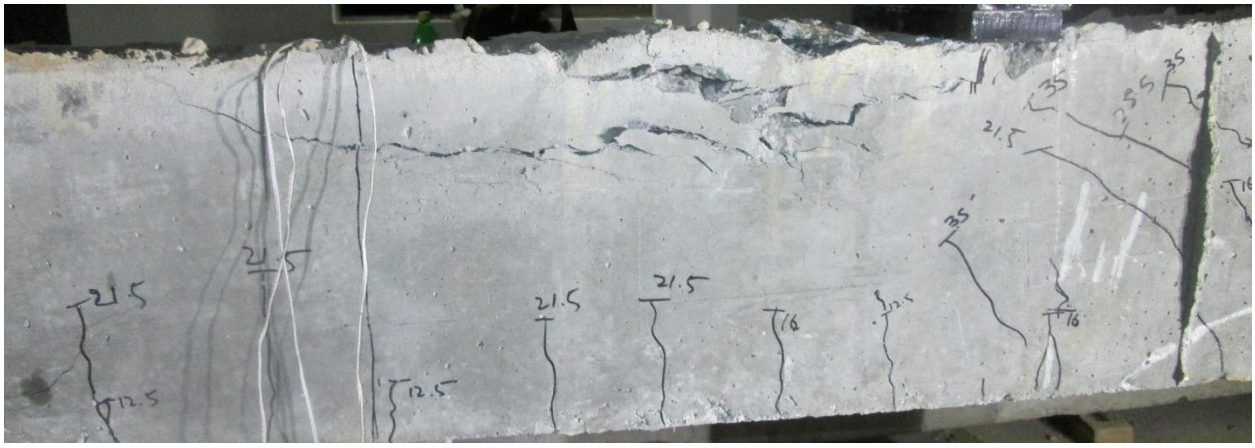

Figure B-29 : Failure Pattern of Over Reinforced Confined Beam

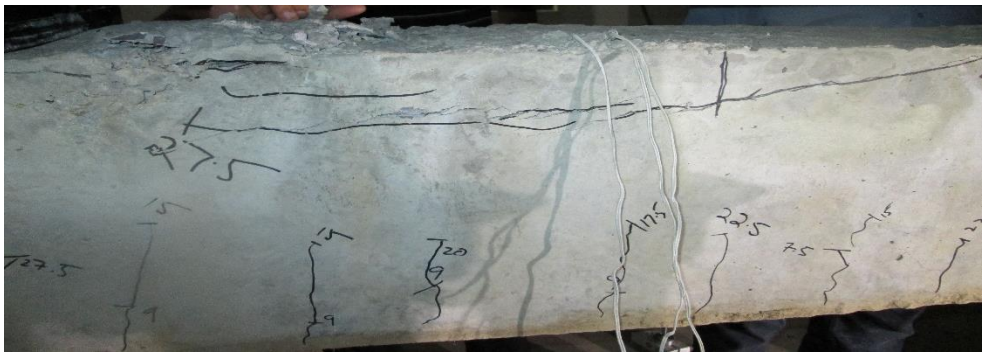

Figure B-30 : Failure Pattern of Confine UR Beam (Spalling)

Figure B-31 : Typical failure of Confined Beam (Spalling of cover)

Elastic curve of Beams (Over and Under Reinforced)

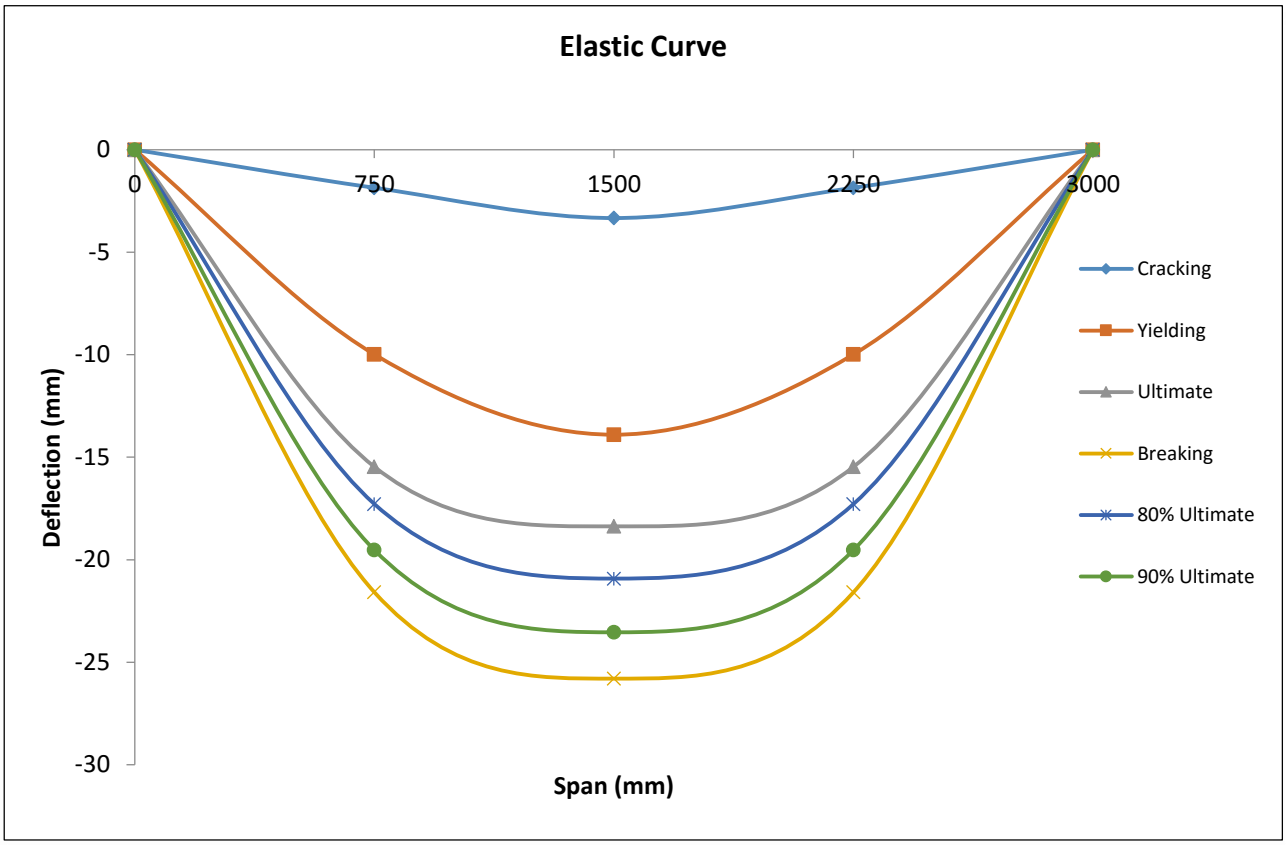

Figure B-32 Deflection at various stages for R-UR-1

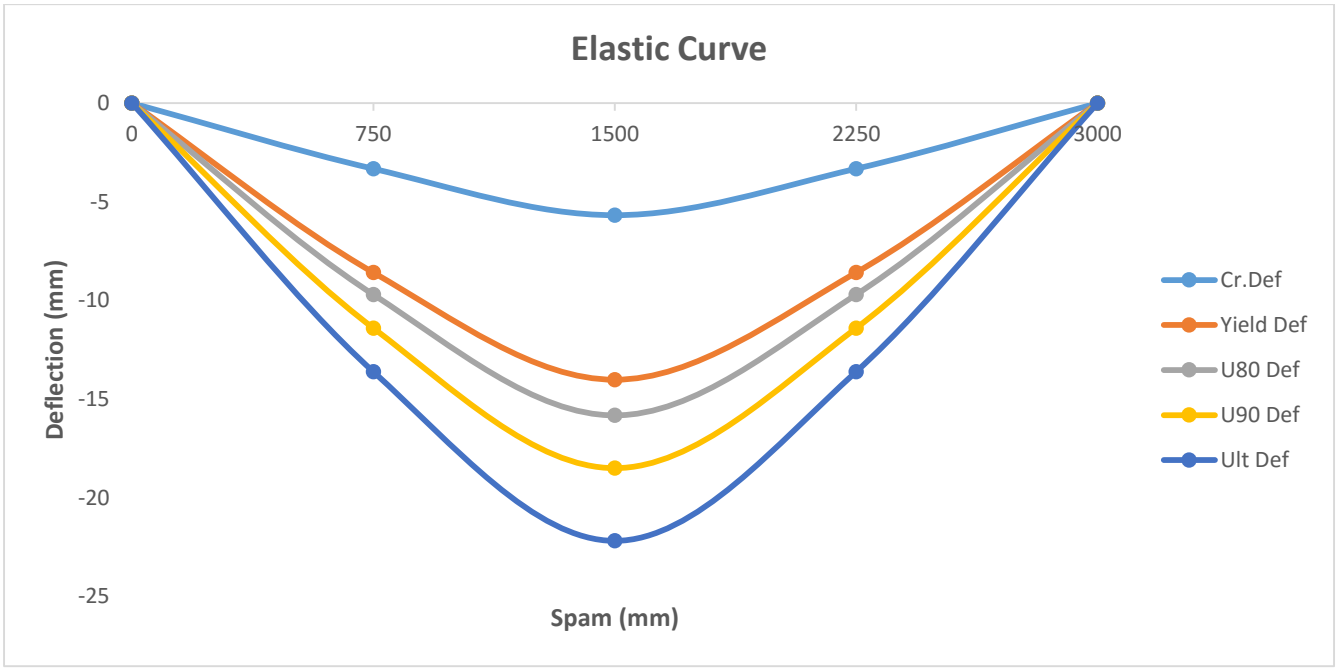

Figure B-33 Deflection at various stages for C-OR-2

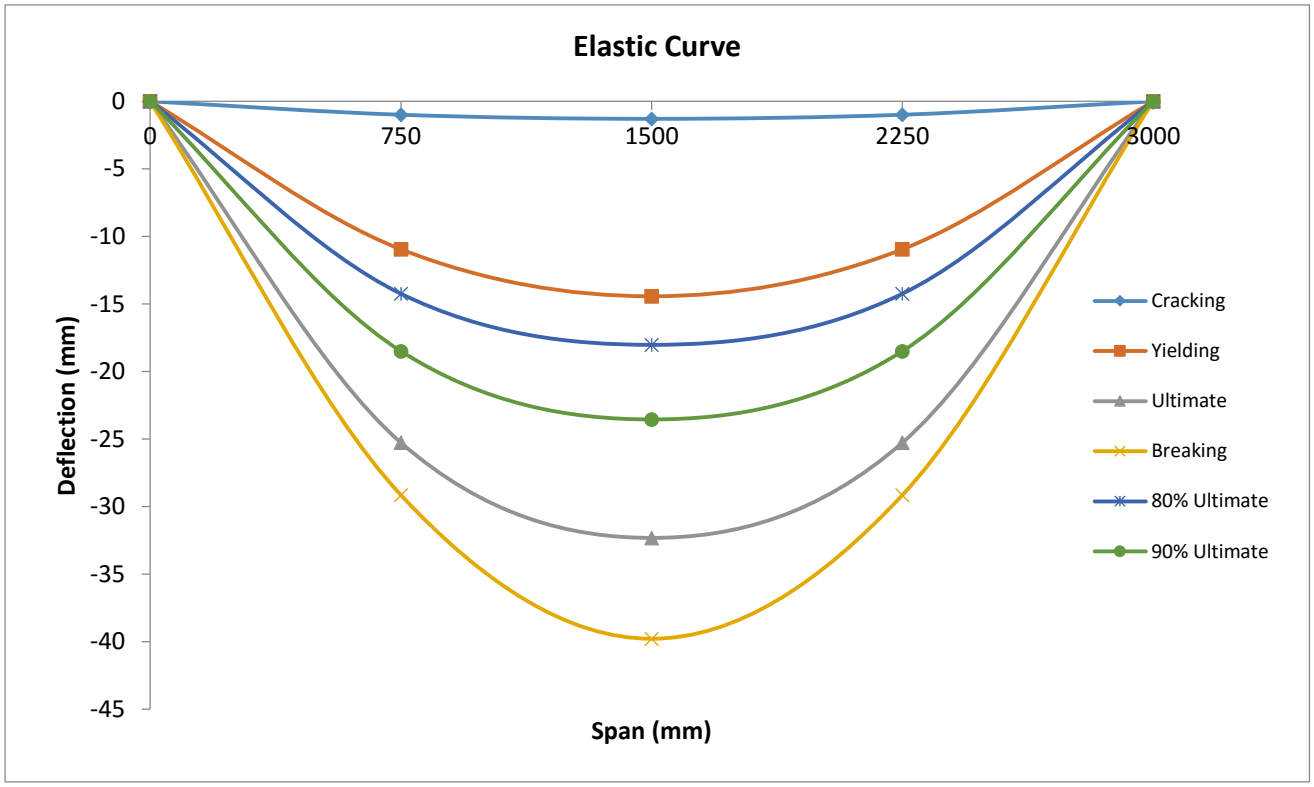

Figure B-34 : Deflection at various stages for R-UR-2

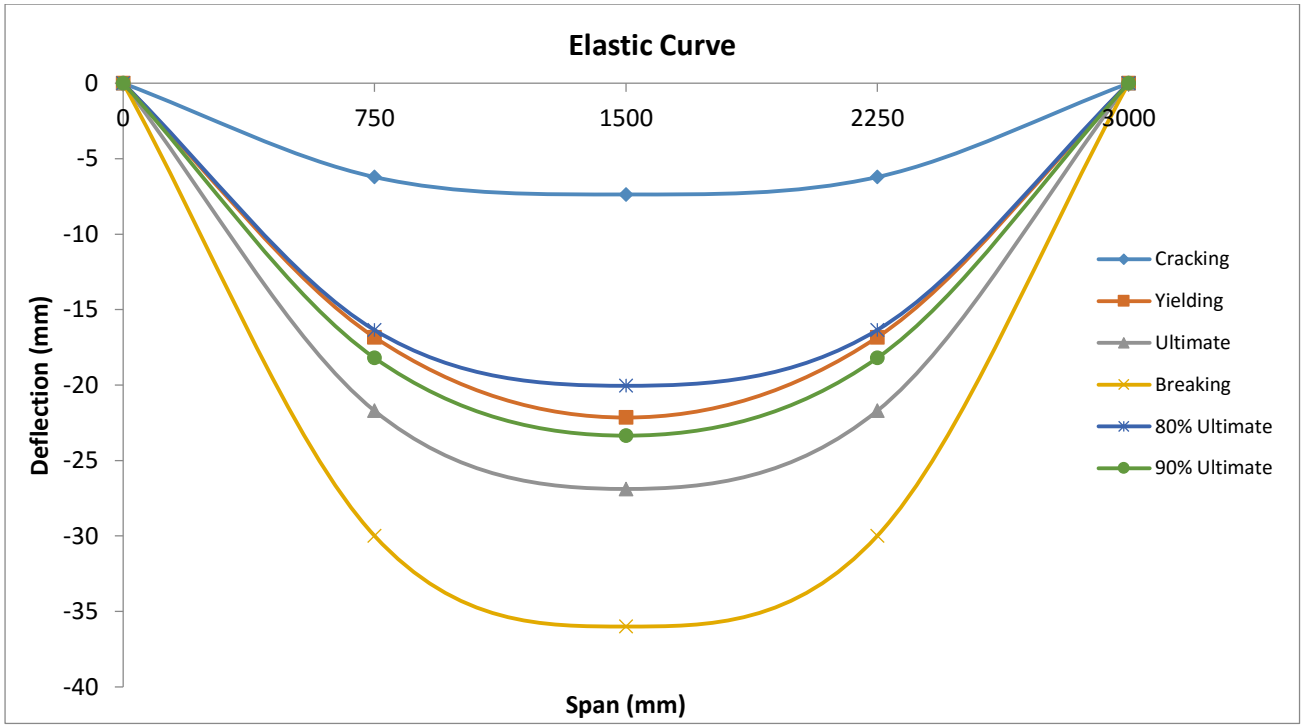

Figure B-35 : Elastic Curve at various Stages for R-OR-1

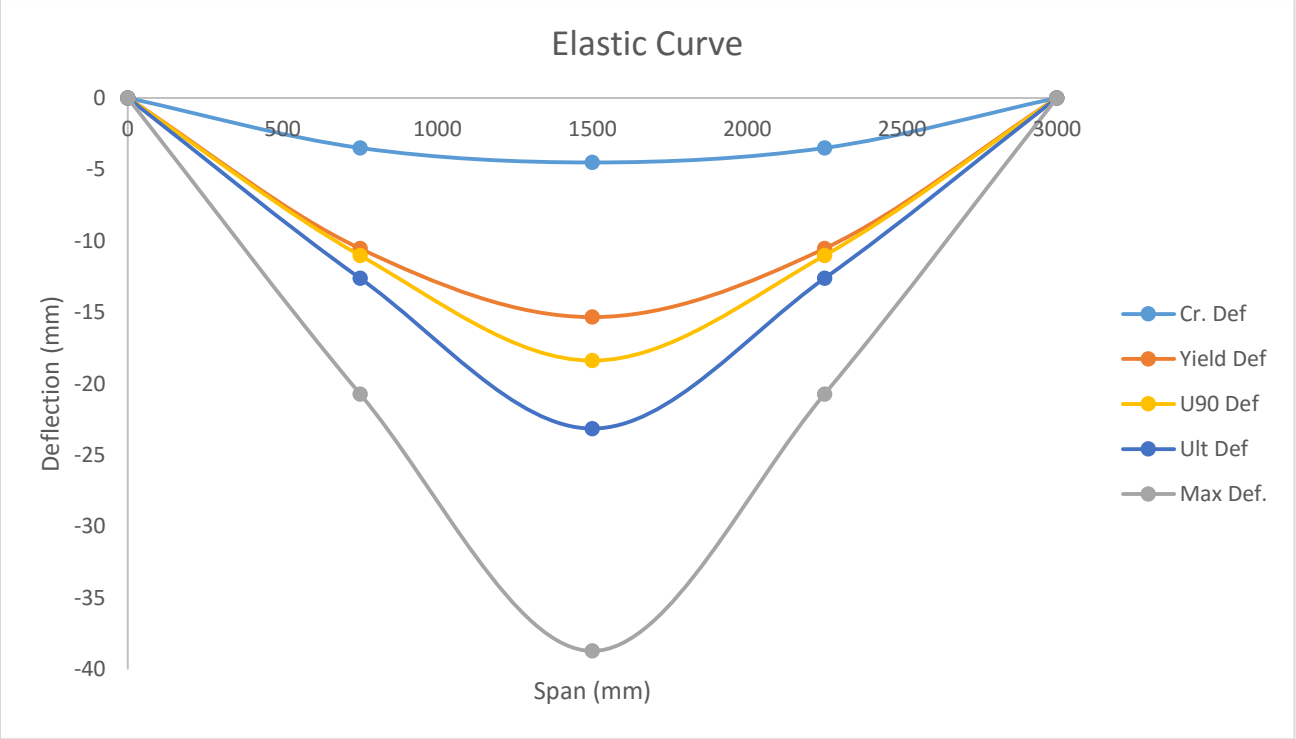

Figure B-36 : Elastic Curve at various Stages for C-OR-1

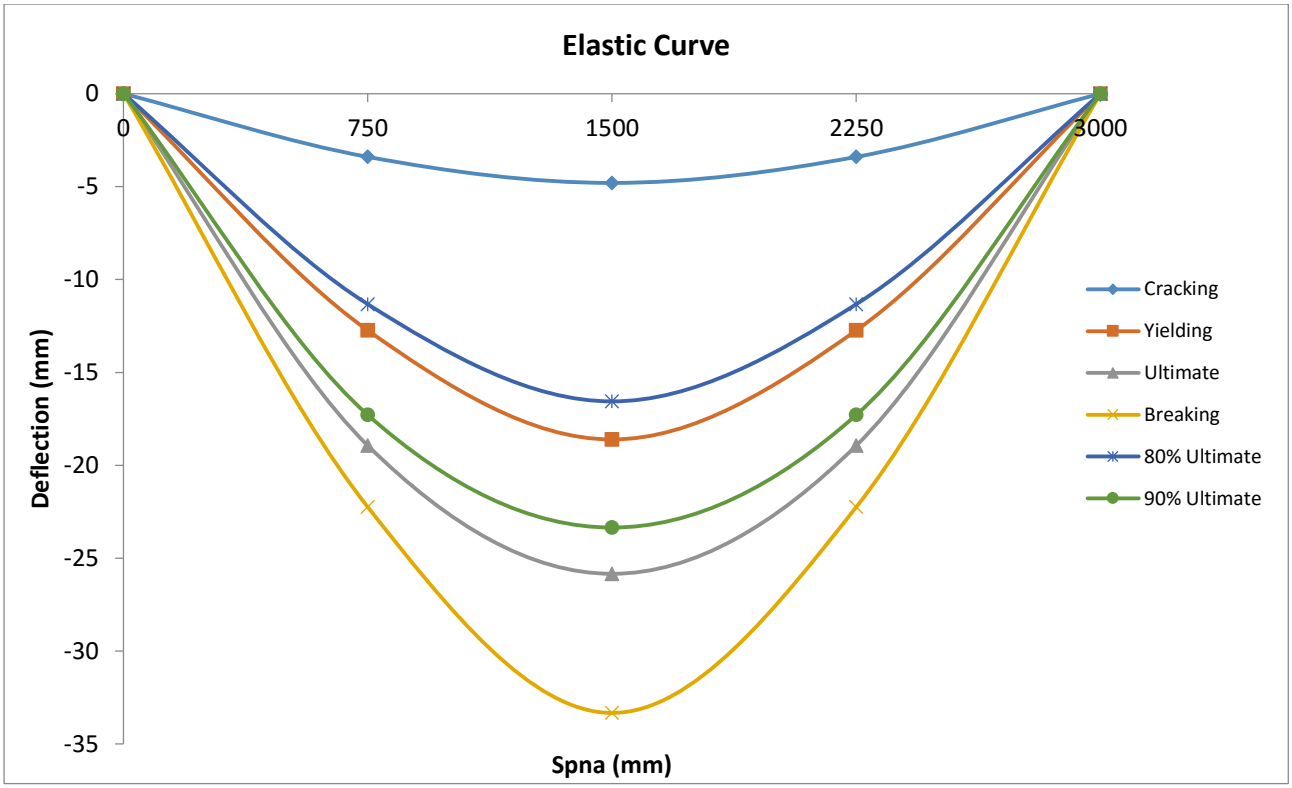

Figure B-37 : Deflection at various Stages for R-OR-2

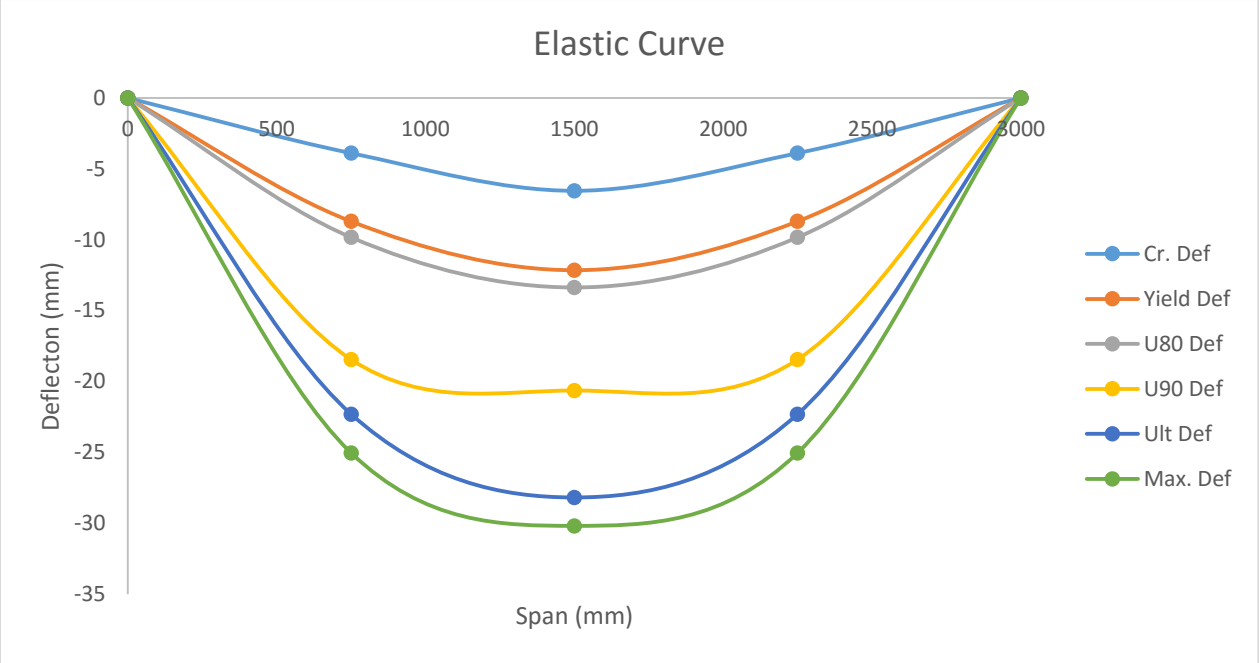

Figure B-38 : Deflection at various Stages for C-UR-2

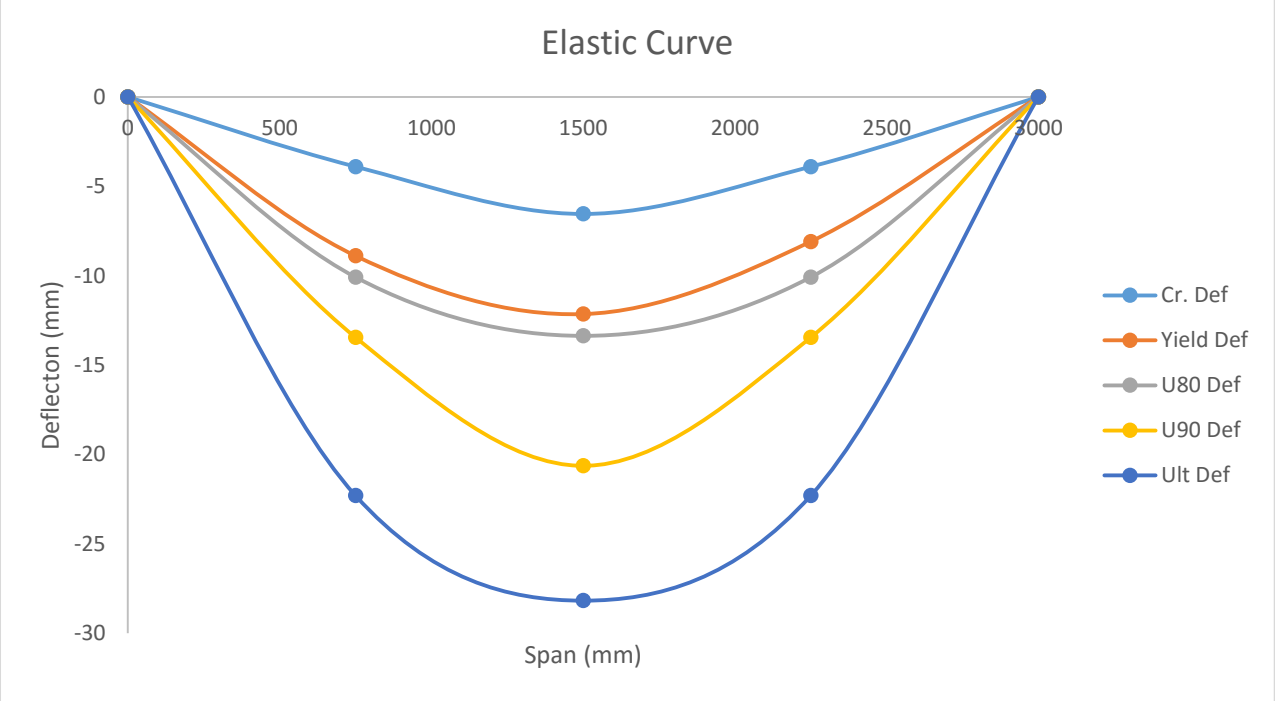

Figure B-39 : Deflection at various stages for C-UR-1

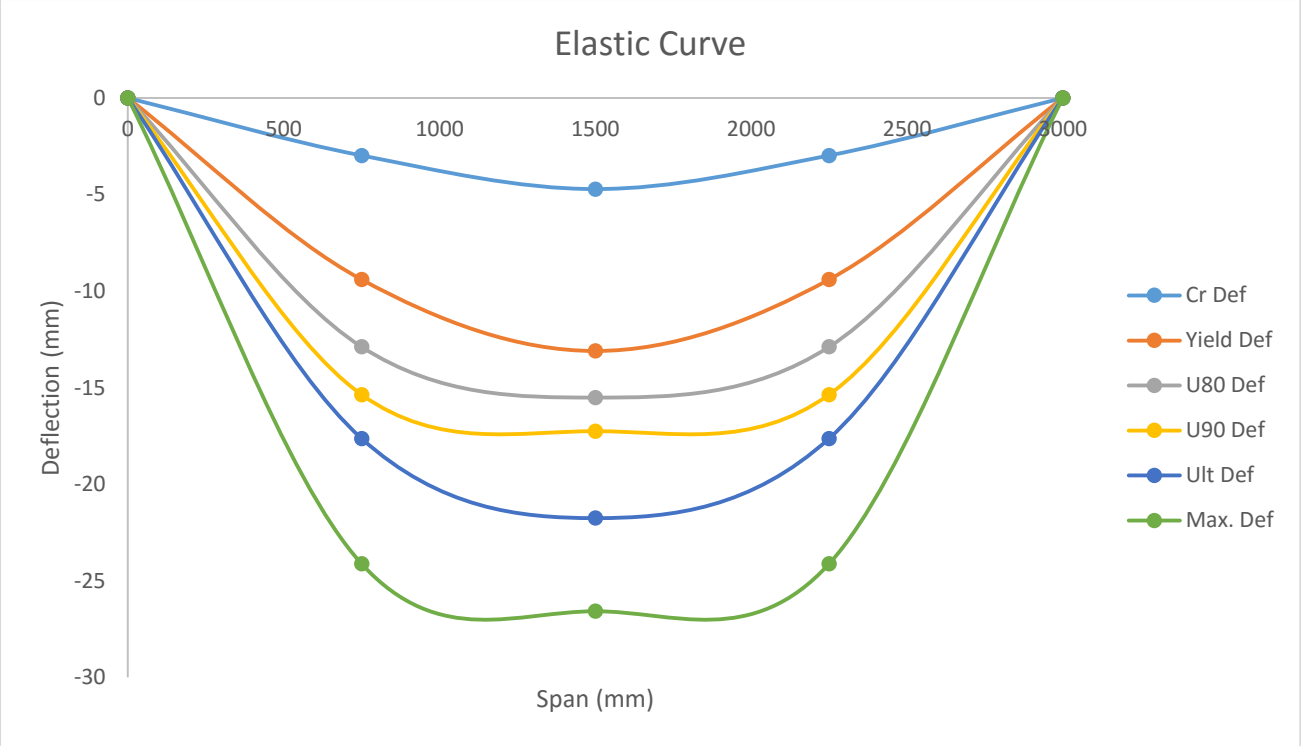

Figure B-40 : Deflection at various stages for C-UR-3

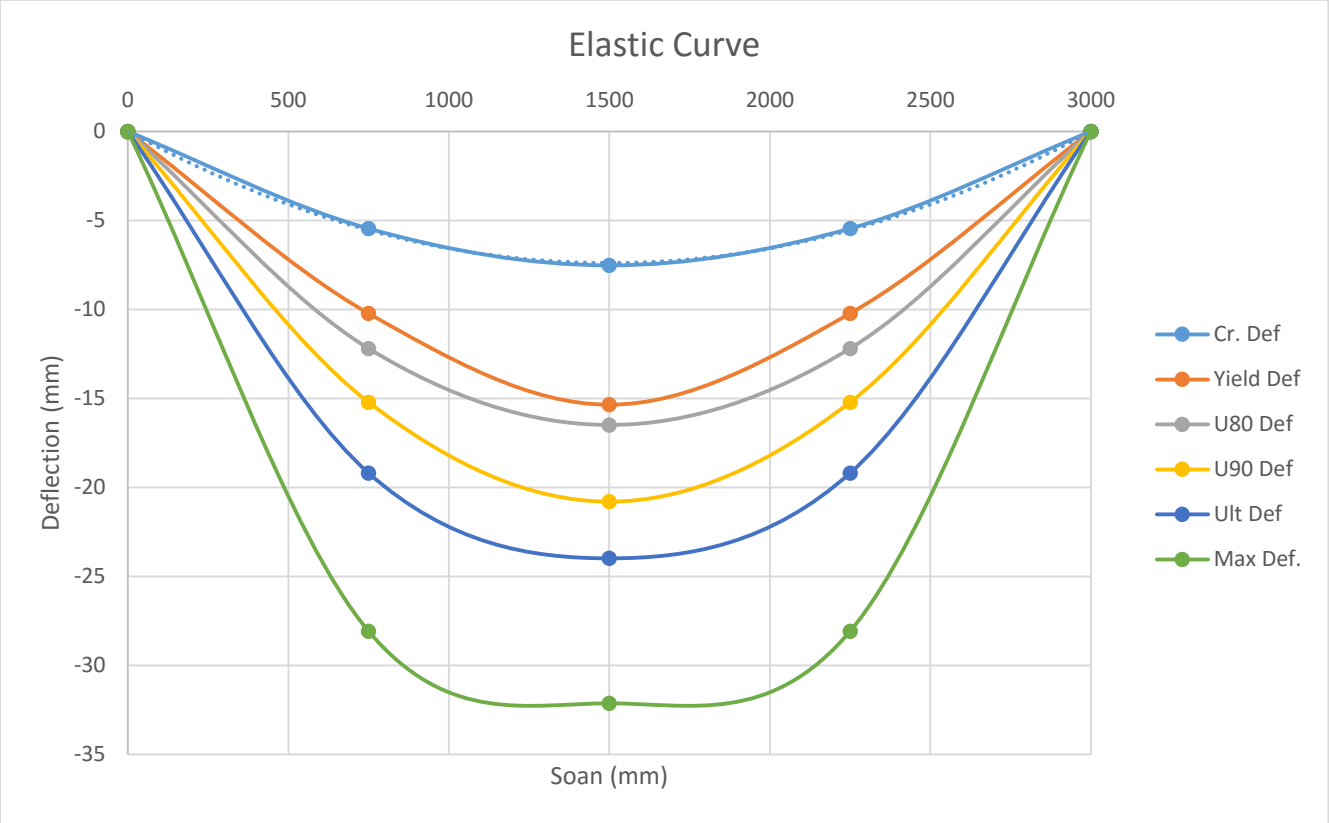

Figure B-41 : Deflection at various stages for C-OR-3

Moment Curvatures Curves for Beams

Under Reinforced Beams

Table B-19 : M-Phi Table for C-UR-2

Moment (KN.m)	Curvature (rad/mm)
0.00	0.0E+00
75.65	2.2E-06
122.87	1.00E-05
136.93	1.12E-05
150.01	2.89E-05
129.12	3.15E-05

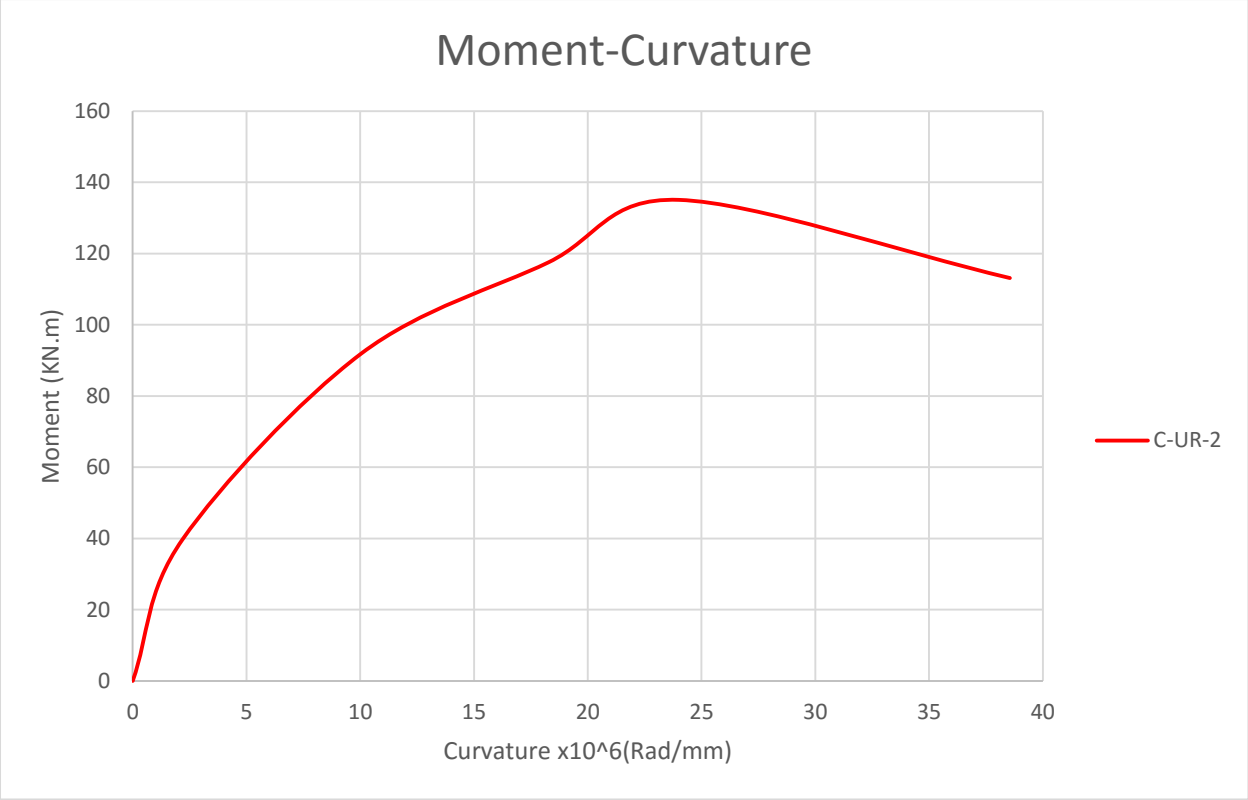

Figure B-42 : M-Phi Curve for C-UR-2

Table B-20 : M-Phi Table for Beam C-UR-3

Moment (KN.m)	Curvature (rad/mm)
0.00	0.0E+00
39.79	1.21E-05
91.78	1.83E-05
111.54	2.0E-05
135.06	2.4E-05
113.13	3.13E-05

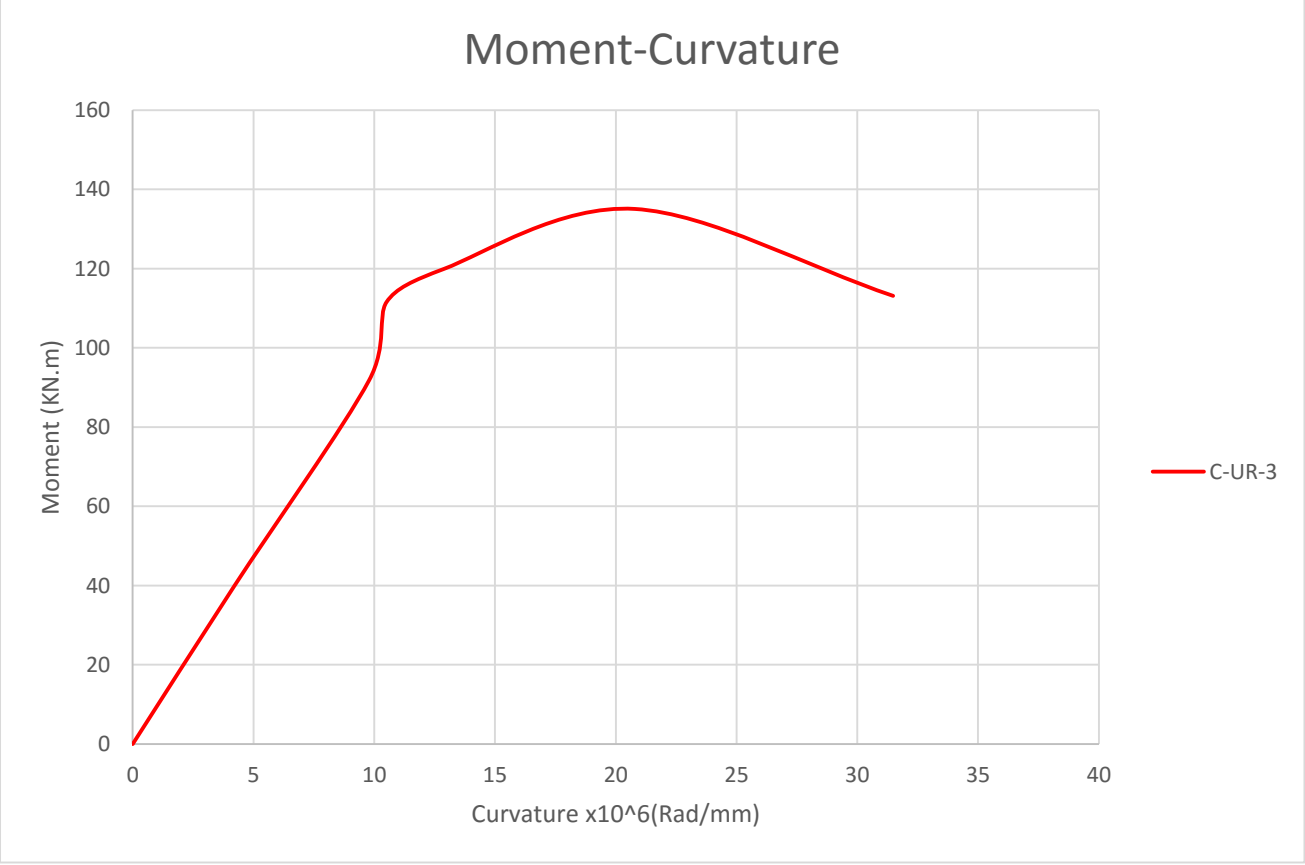

Figure B-43 : M-Phi Curve for Beam C-UR-3

Table B-21 : M-Phi Table for C-UR-1

Moment (KN.m)	Curvature (rad/mm)
0.00	0.00E+00
39.79	9.00E-06
91.78	9.51E-06
111.54	10.01E-06
119.91	1.09E-05
135.06	2.08E-05
113.13	2.55E-05

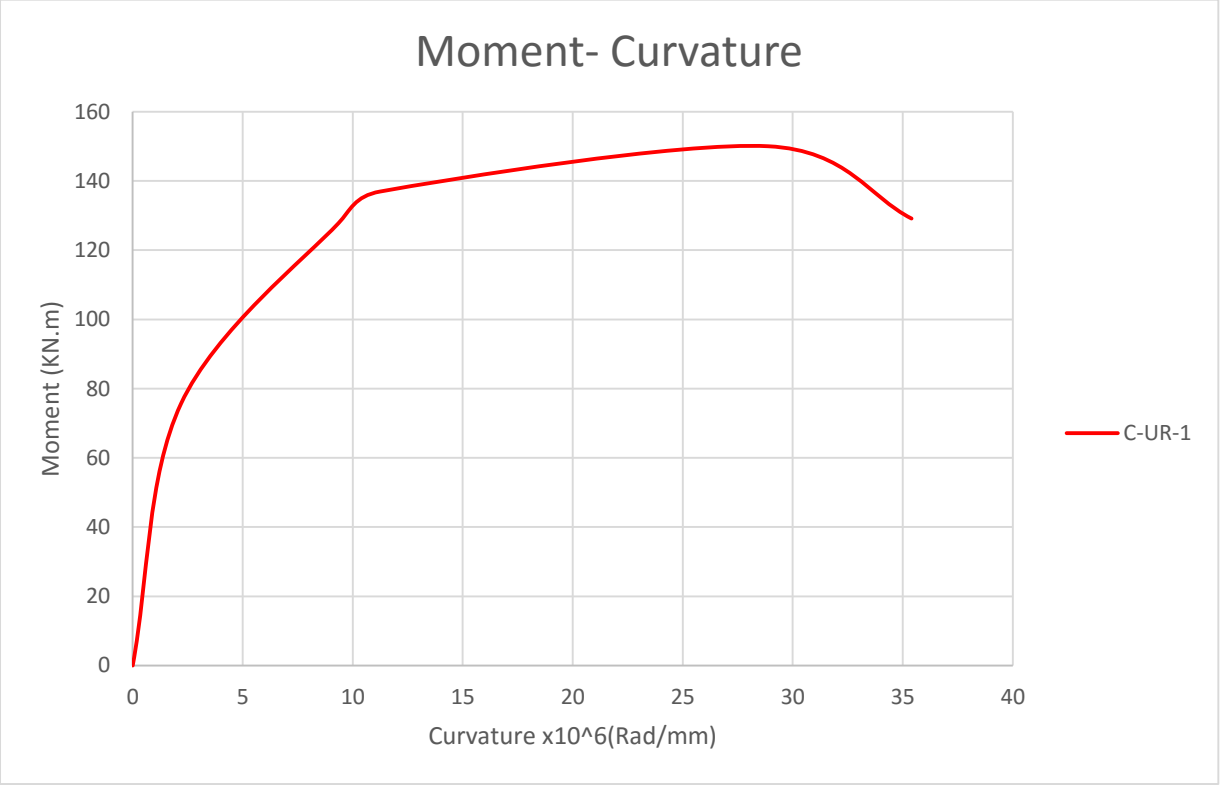

Figure B-44: M-Phi curve for Beam C-UR-1

Table B-22: *M-Phi Table for R-UR-1*

Moment (KN.m)	Curvature (Rad/mm)
0.00	0
36.93	1.66E-06
110.74	1.20496E-05
128.35	2.25409E-05
109.07	3.08515E-05

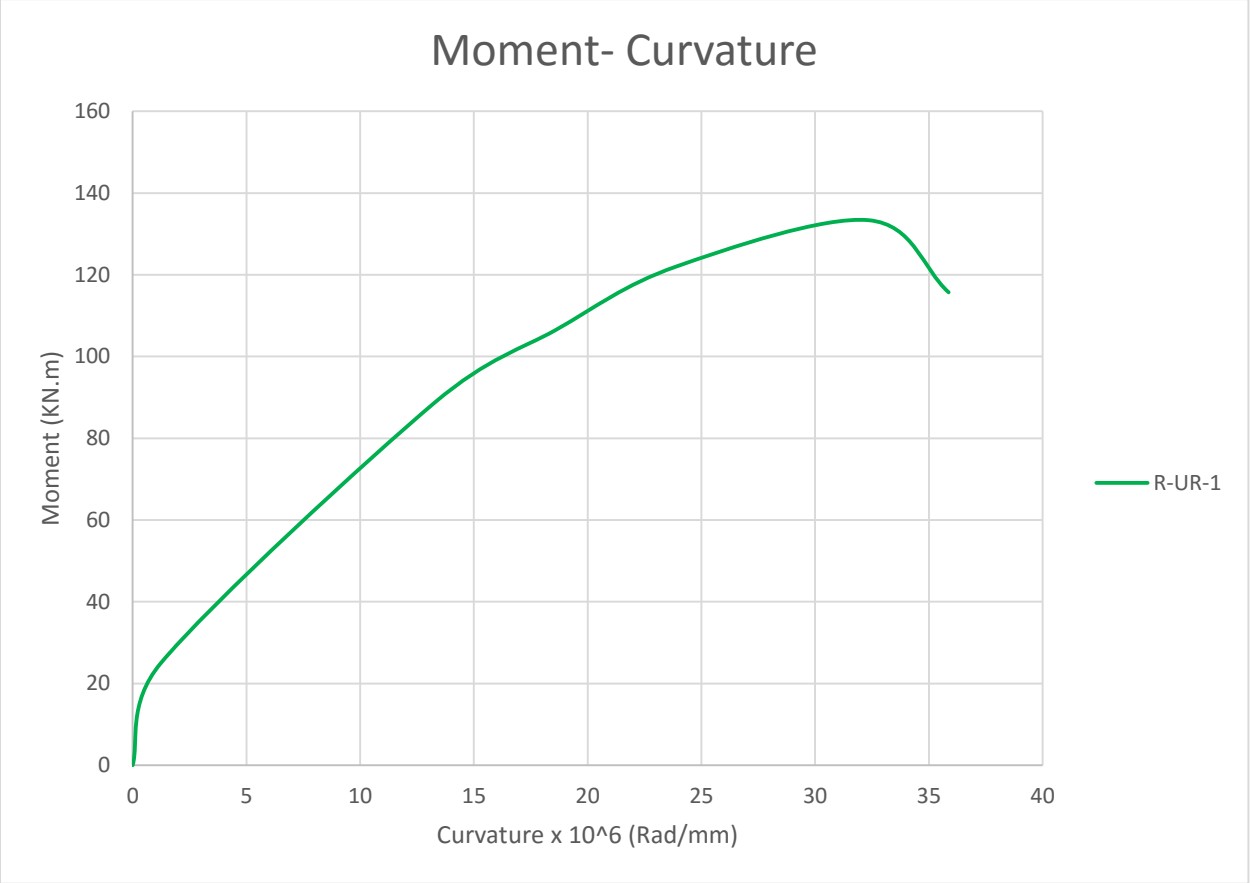

Figure B-45: *M-Phi curve for Beam R-UR-1*

Table B-23 : *M-Phi Table for R-UR-2*

Moment (KN.m)	Curvature (Radians)
0.00	0
24.93	1.23025E-06
88.74	1.48806E-05
106.43	1.85803E-05
121.98	2.38796E-05
133.35	3.236E-05
96.07	3.58702E-05

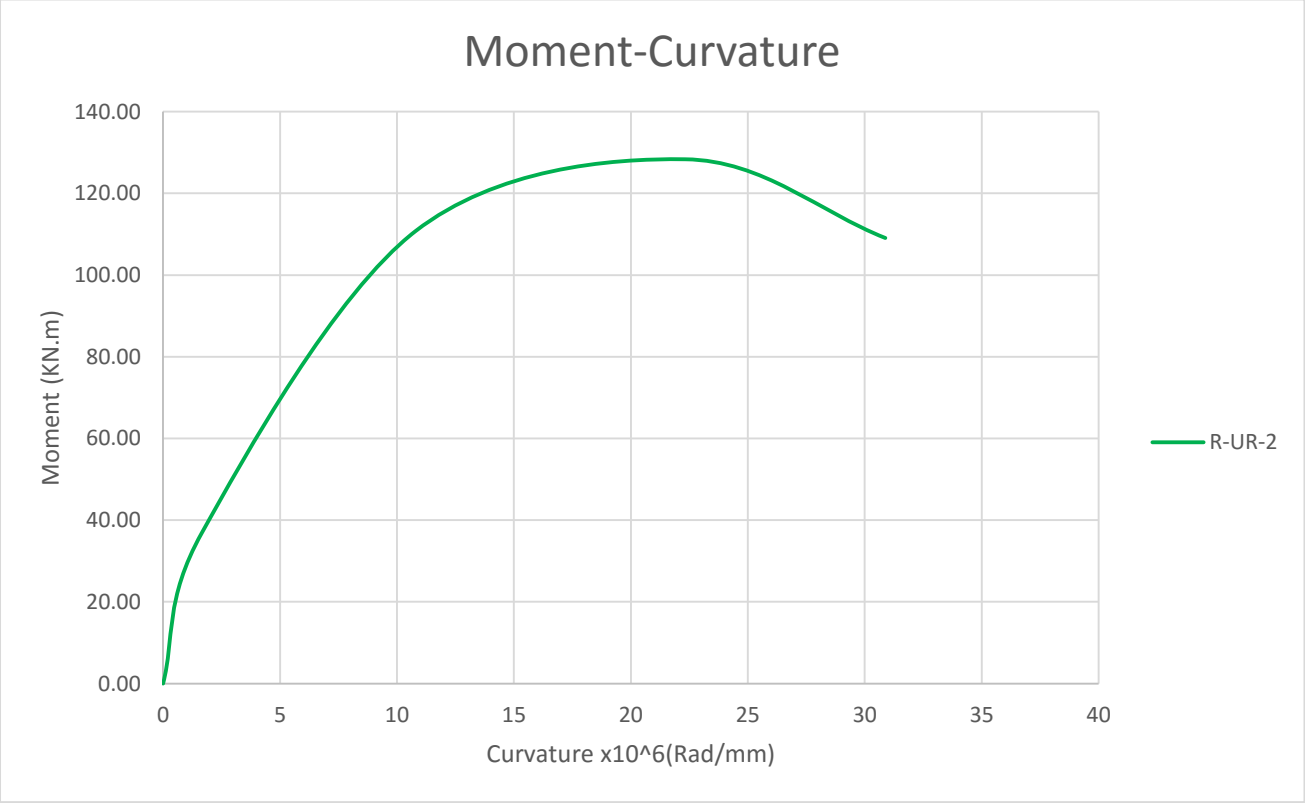

Figure B-46: *M-Phi curve for beam R-UR-2*

Over Reinforced Beams

Table B-24 : M-Phi Table for R-OR-2

Moment (KN.m)	Curvature (rad/mm)
0.000	0
29.115	1.44692E-06
147.072	1.08499E-05
149.288	1.11287E-05
189.285	2.21592E-05
149.144	2.94809E-05

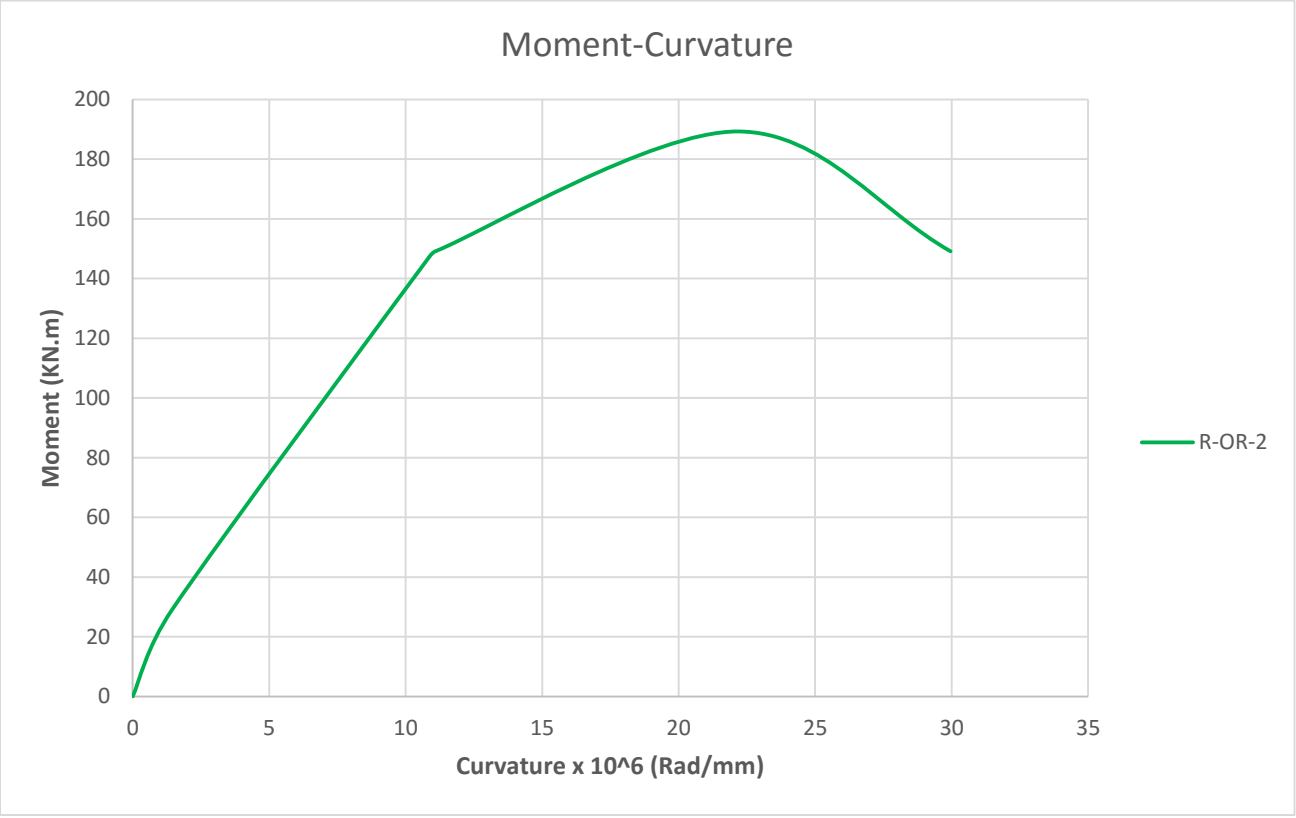

Figure B-47 M-Phi curve for Beam R-OR-2

Table B-25: *M-Phi Table for R-OR-1*

Moment (KN.m)	Curvature (Rad/mm)
0.00	0
59.32	1.44692E-06
141.61	1.11287E-05
171.93	2.21592E-05
139.65	2.88809E-05

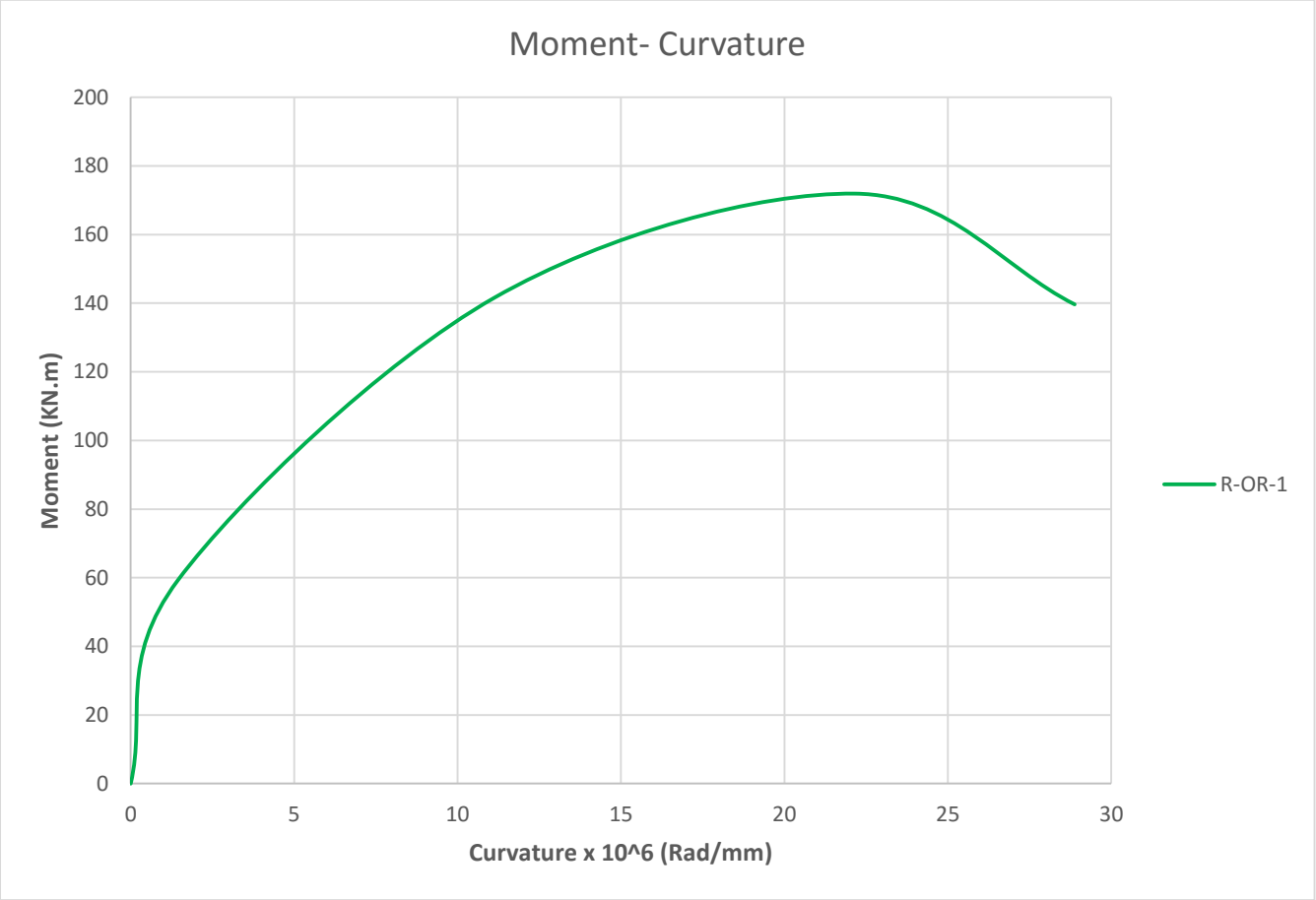

Figure B-48 *: M-Phi Curve for Beam R-OR-1*

Table B-26 : *M-Phi Table for C-OR-3*

Moment (KN.m)	Curvature (Rad/mm)
0.00	0
62.74	6.01395E-06
110.72	1.30558E-05
117.54	1.40363E-05
131.01	1.71152E-05
168.36	2.55867E-05
150.40	4.26089E-05

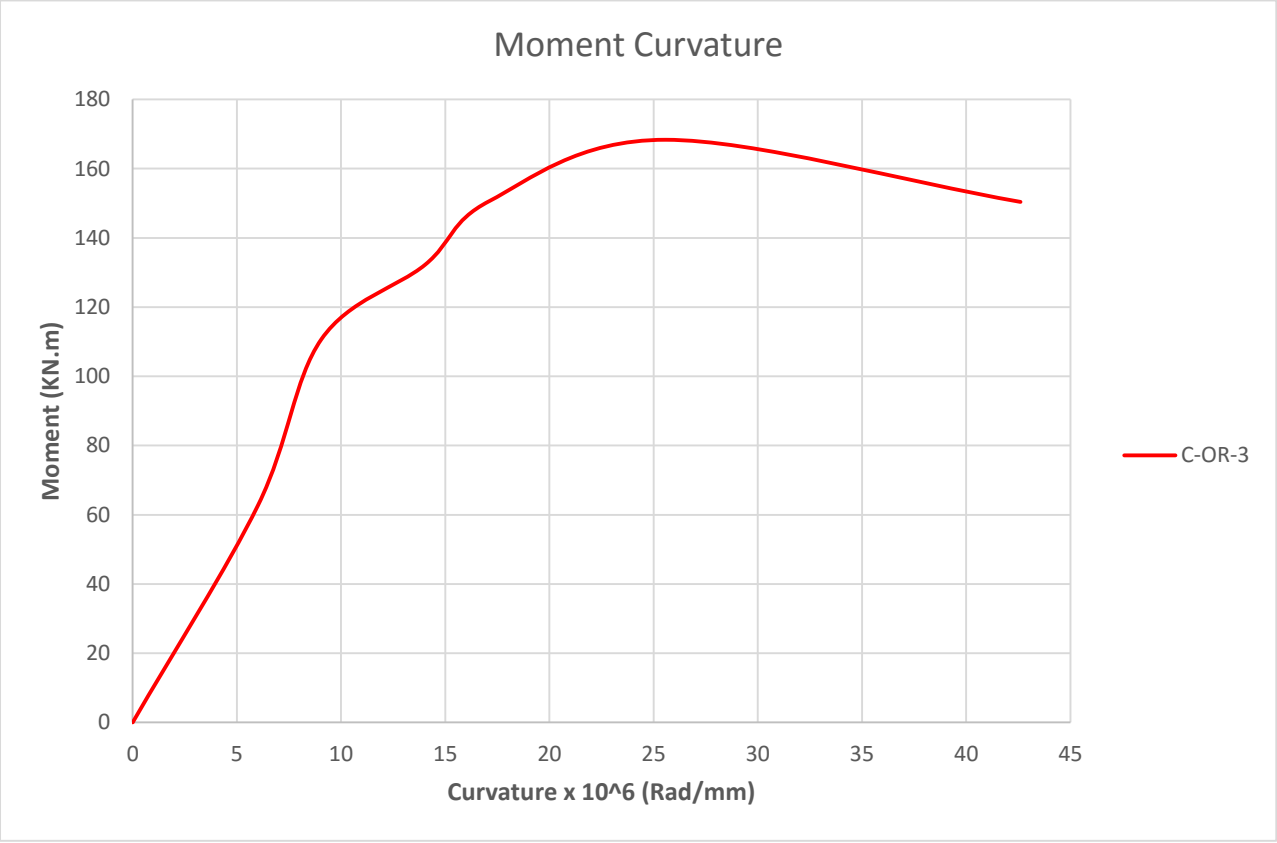

Figure B-49 : *M-Phi curve for Beam C-OR-3*

Table B-27 : *M-Phi Table for C-OR-1*

Moment (KN.m)	Curvature (Rad/mm)
0.00	0
49.45	8.02169E-06
137.31	1.92628E-05
144.29	2.23488E-05
176.15	3.74121E-05
130.30	6.87936E-05

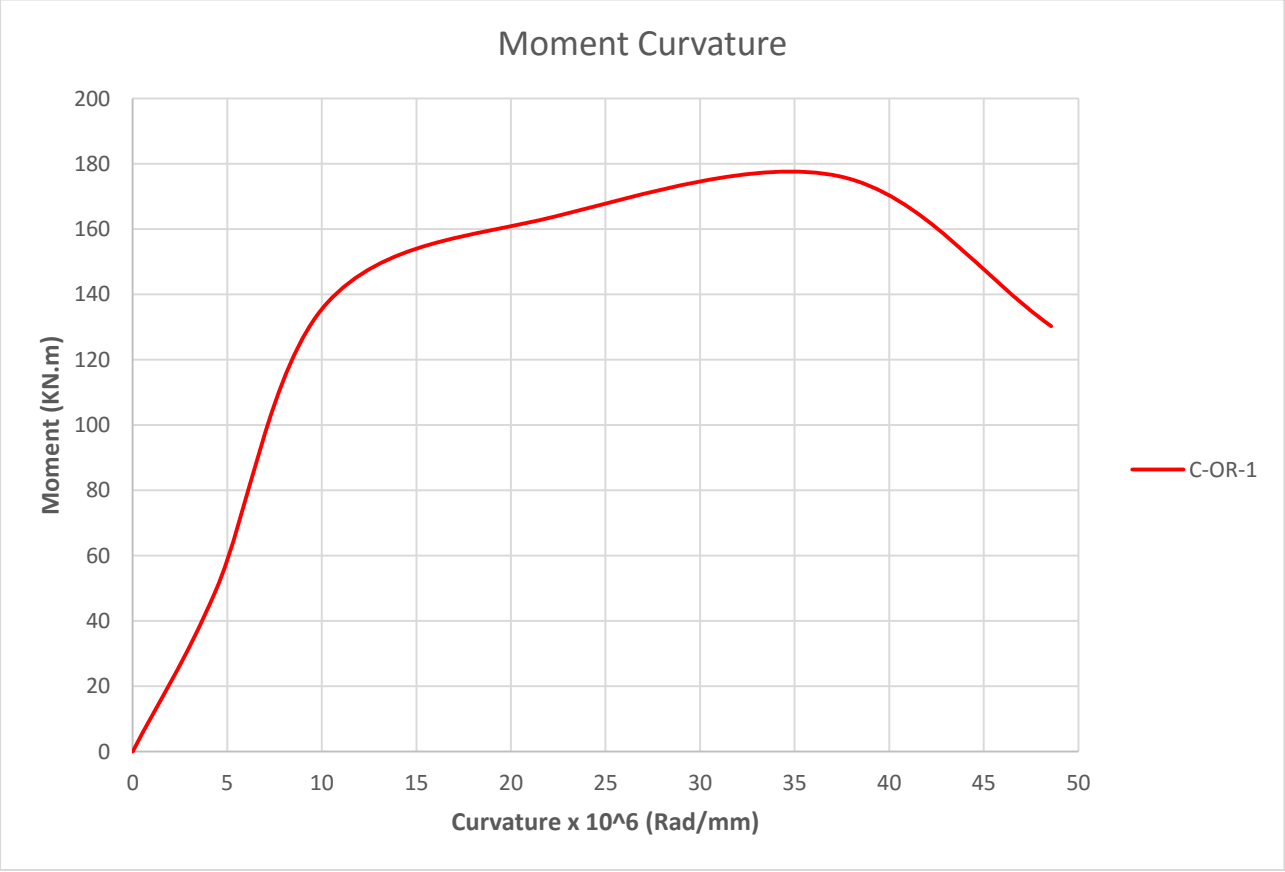

Figure 3-51: M-Phi curve for Beam C-OR-1

Table B-28 : *M-Phi Table for C-OR-2*

Moment (KN.m)	Curvature (Rad/mm)
0.00	0
127.49	1.61E-05
143.32	2.37E-05
159.02	2.85E-05
176.40	4.95E-05
142.89	7.66E-05

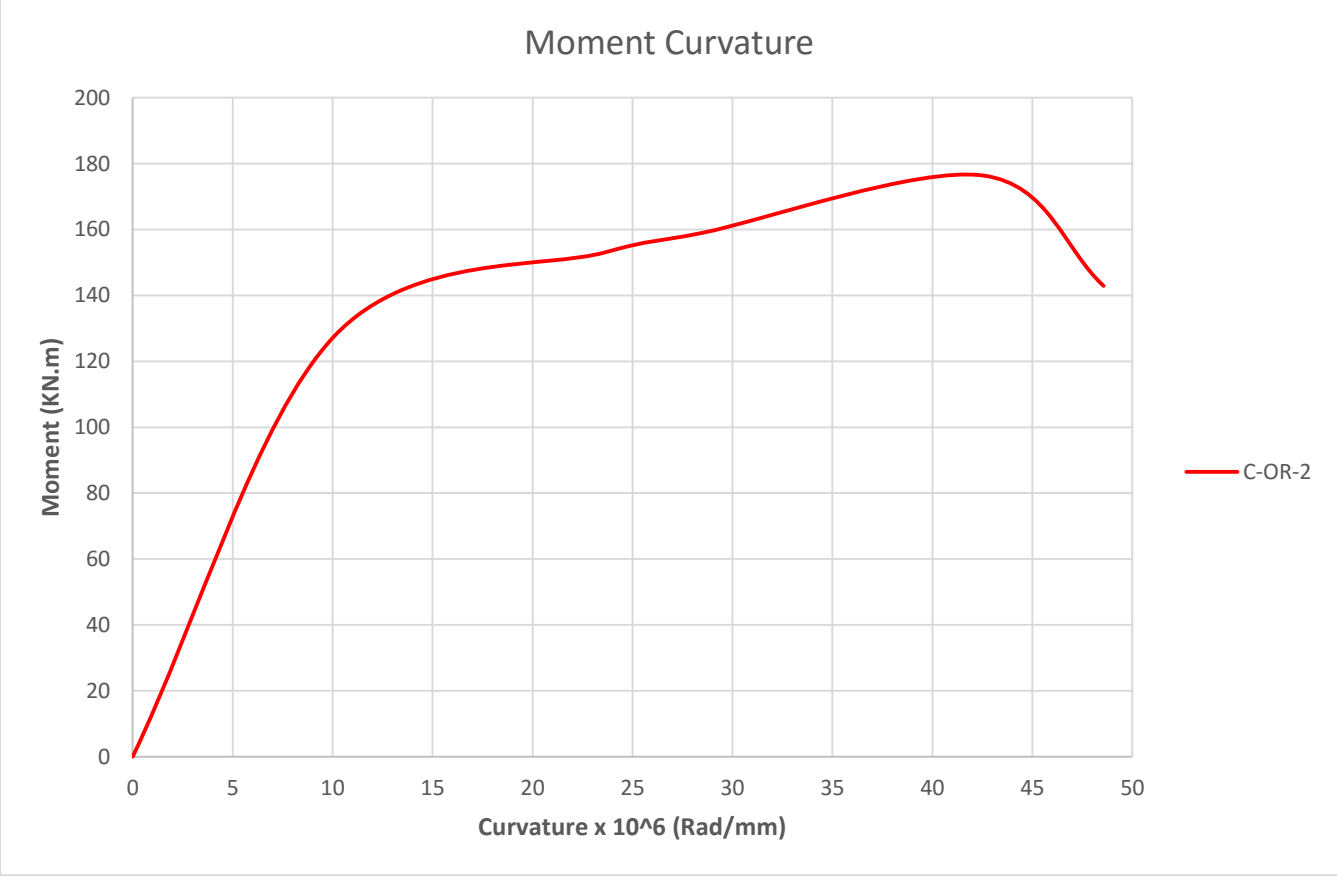

Figure 3-52: M-Phi Curve for Beam C-OR-2

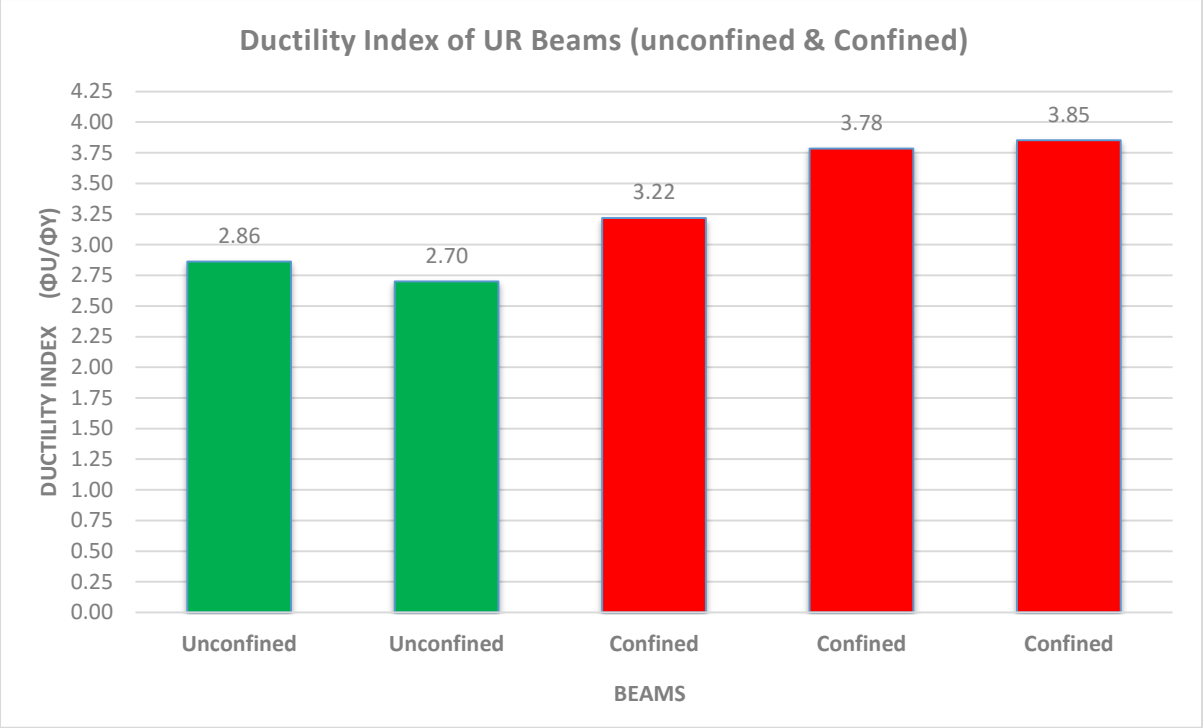

Figure 3-54 Ductility Index of Under Reinforced Unconfined & Confined

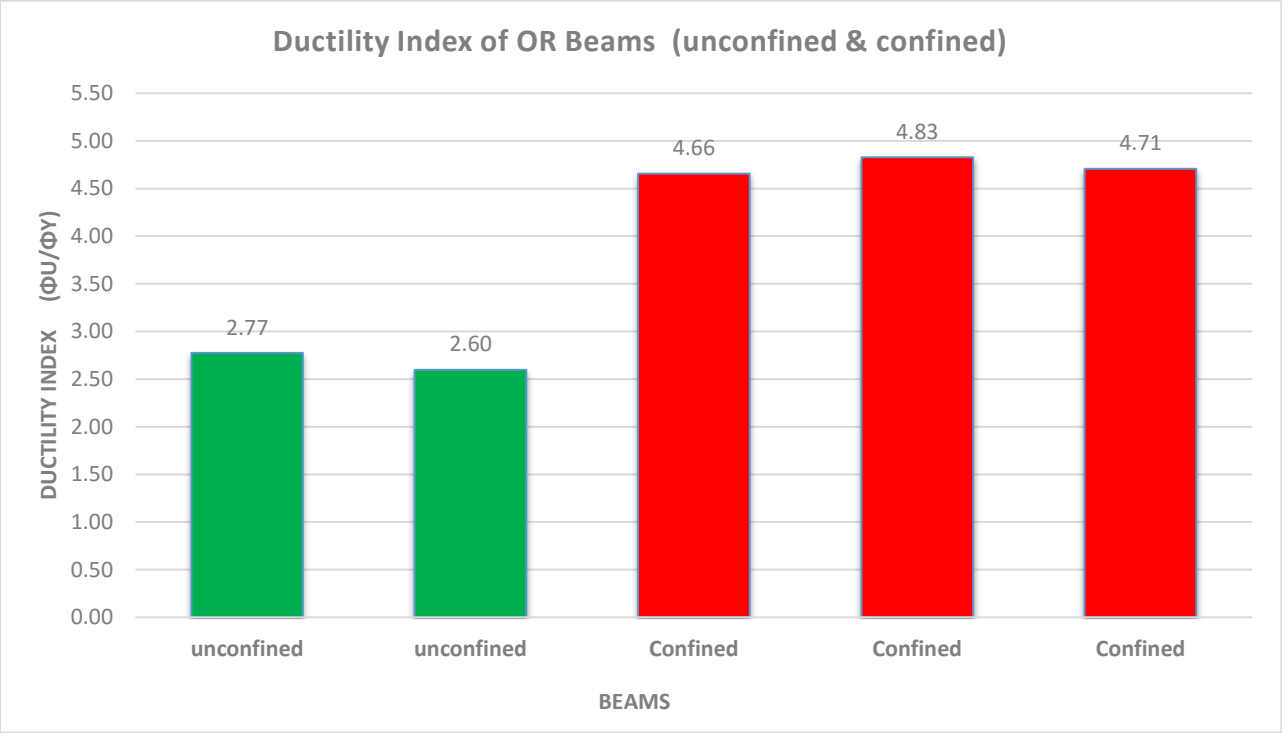

Figure 3-55 Ductility Index of Under Reinforced Unconfined & Confine

APPENDIX-IV

Comparison of Mid Span Deflections of Under and Over reinforced Beams

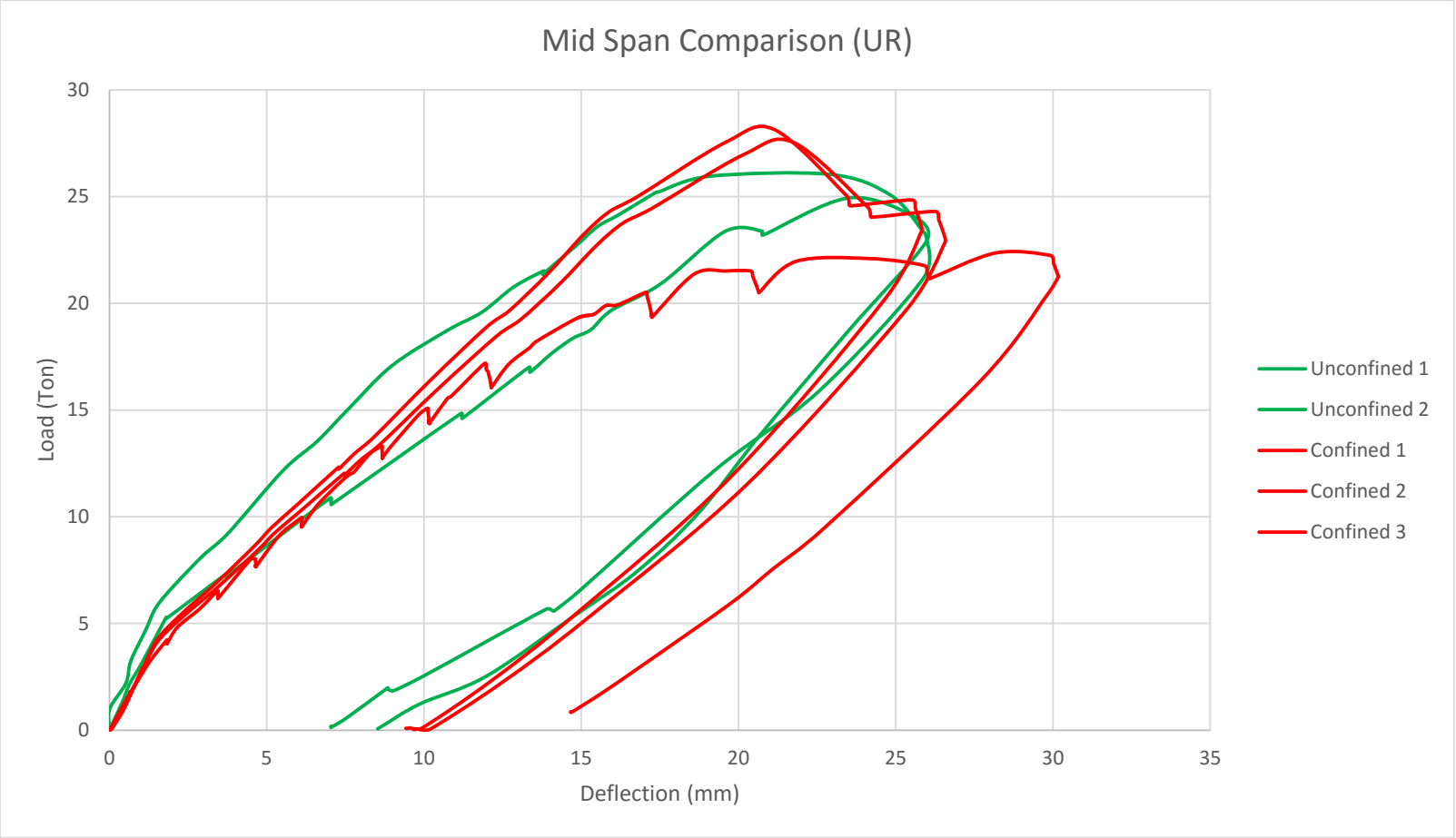

Figure 0-1: ***Load Deflection Comparison of Under reinforced confined and unconfined Beams***

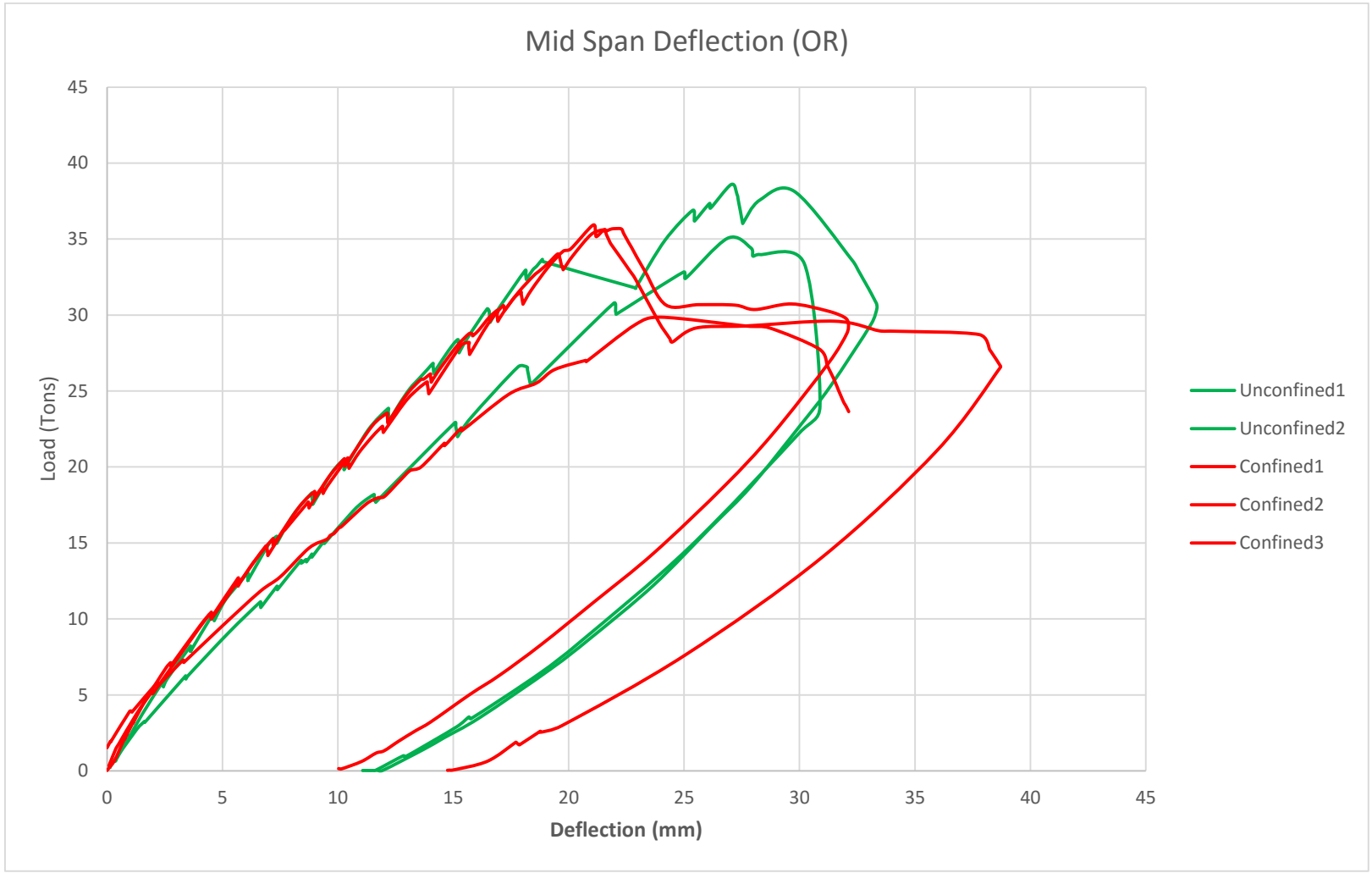

Figure 0-2: *Load Deflection Comparison of Over reinforced confined and unconfined Beams*

Comparison of Moment Curvature relation of Under and Over Reinforced Beams

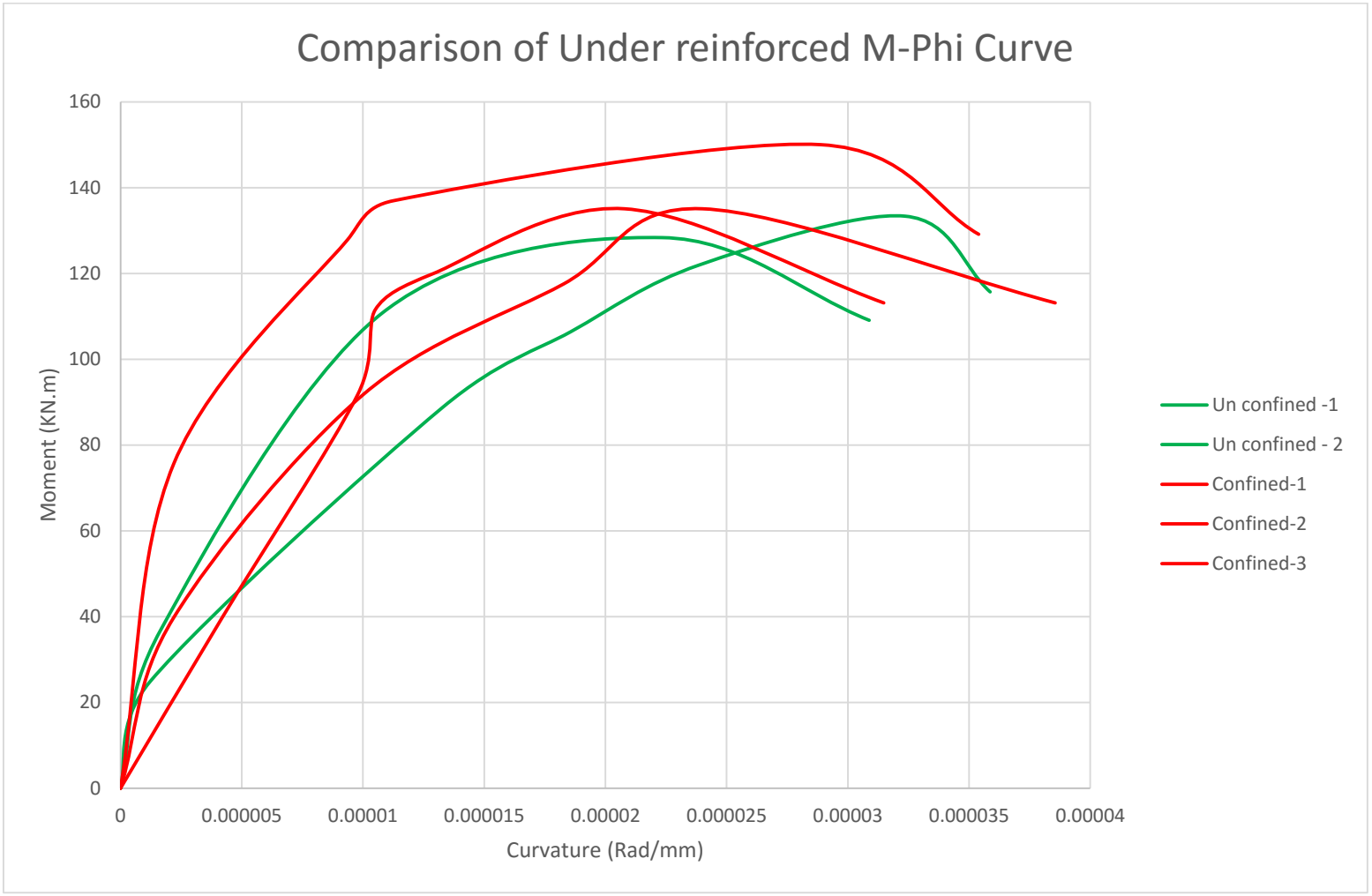

Figure 0-3: M-Phi Relation Comparison of Under Reinforced Confined and Un-Confined Beams

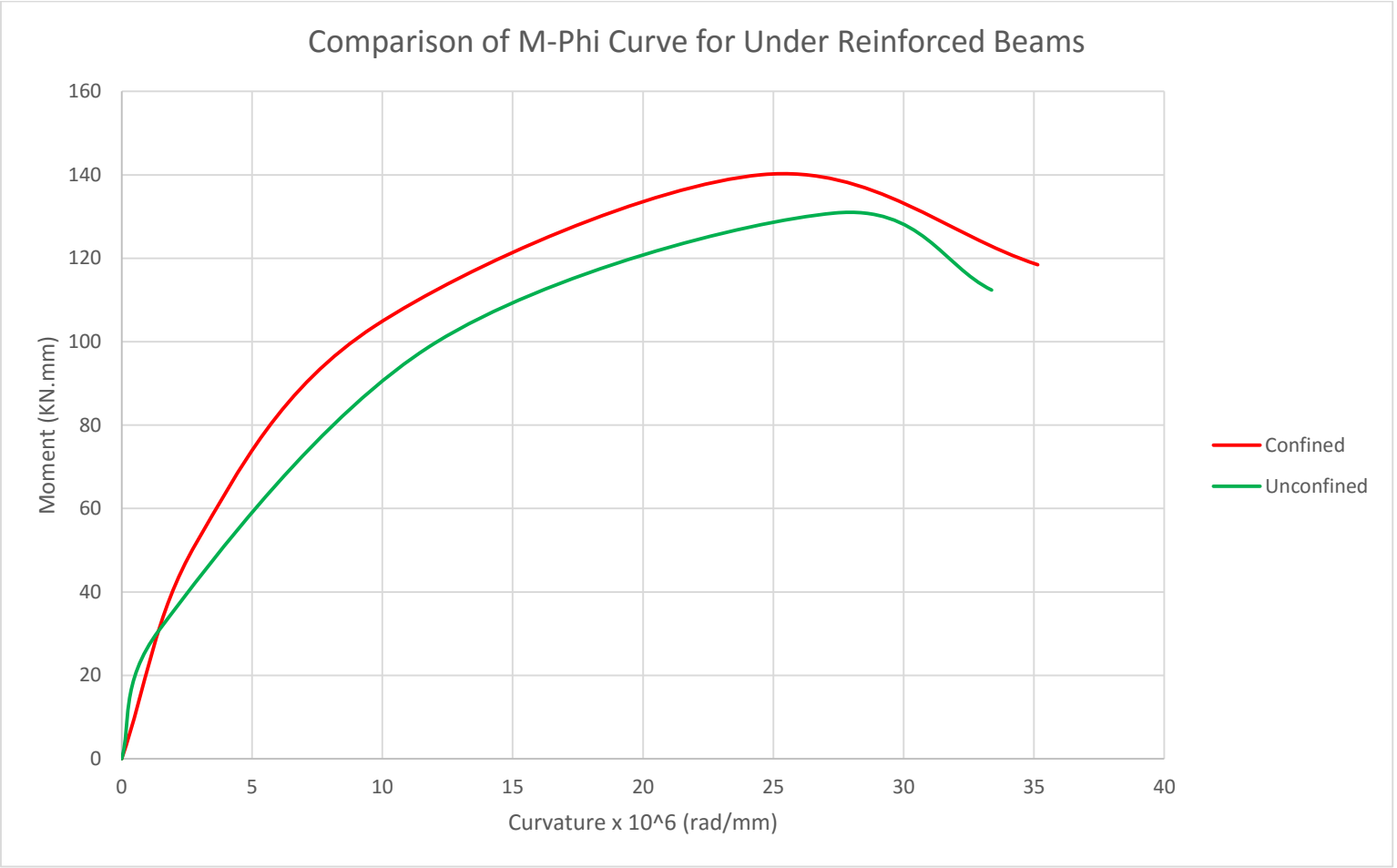

Figure 0-4: *Mean M-Phi graph for Under Reinforced Un- Confined and Confined Beams*

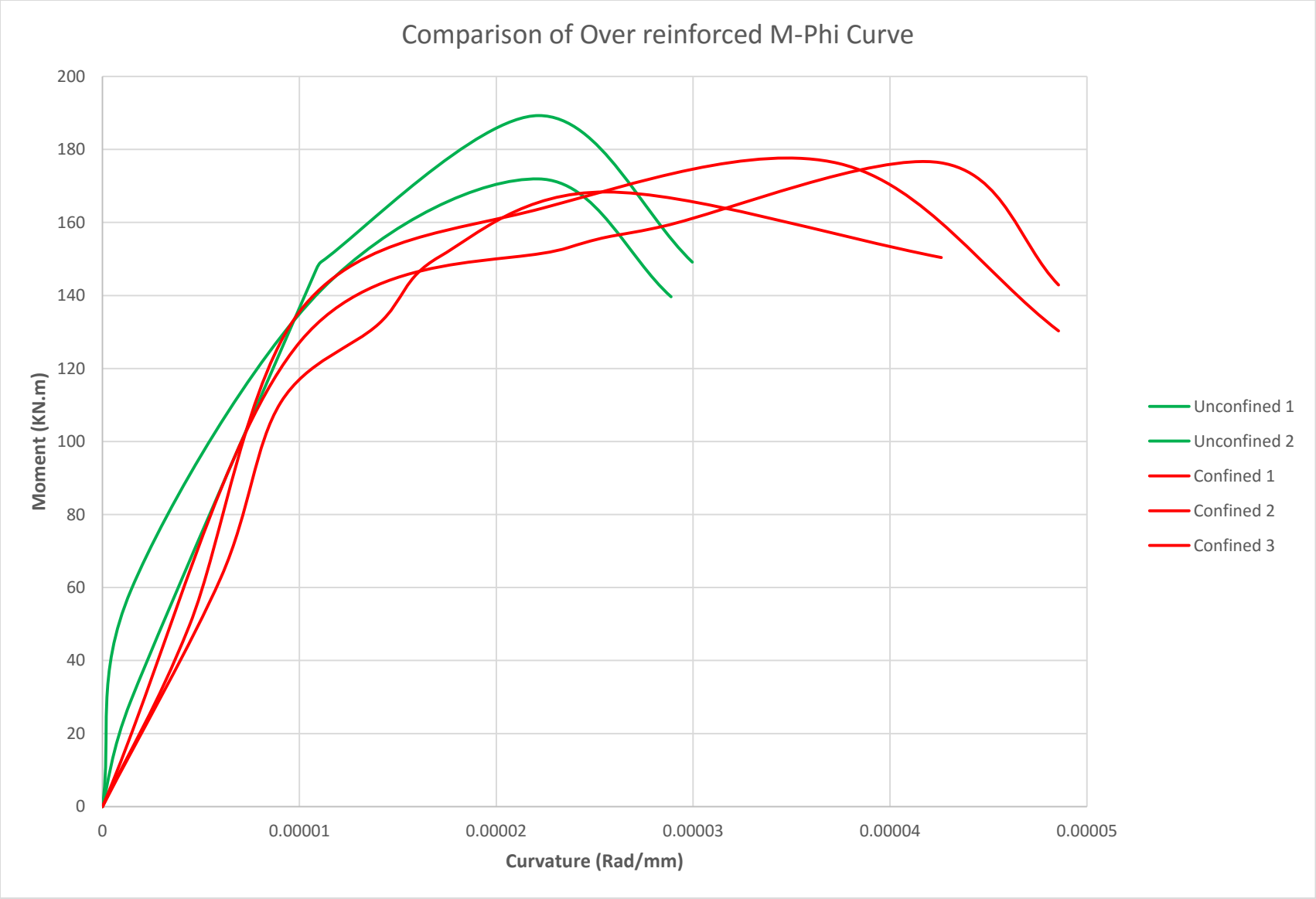

Figure 0-5: *Comparison of M-Phi Relation of Over Reinforced Un-Confined and Confined Beams*

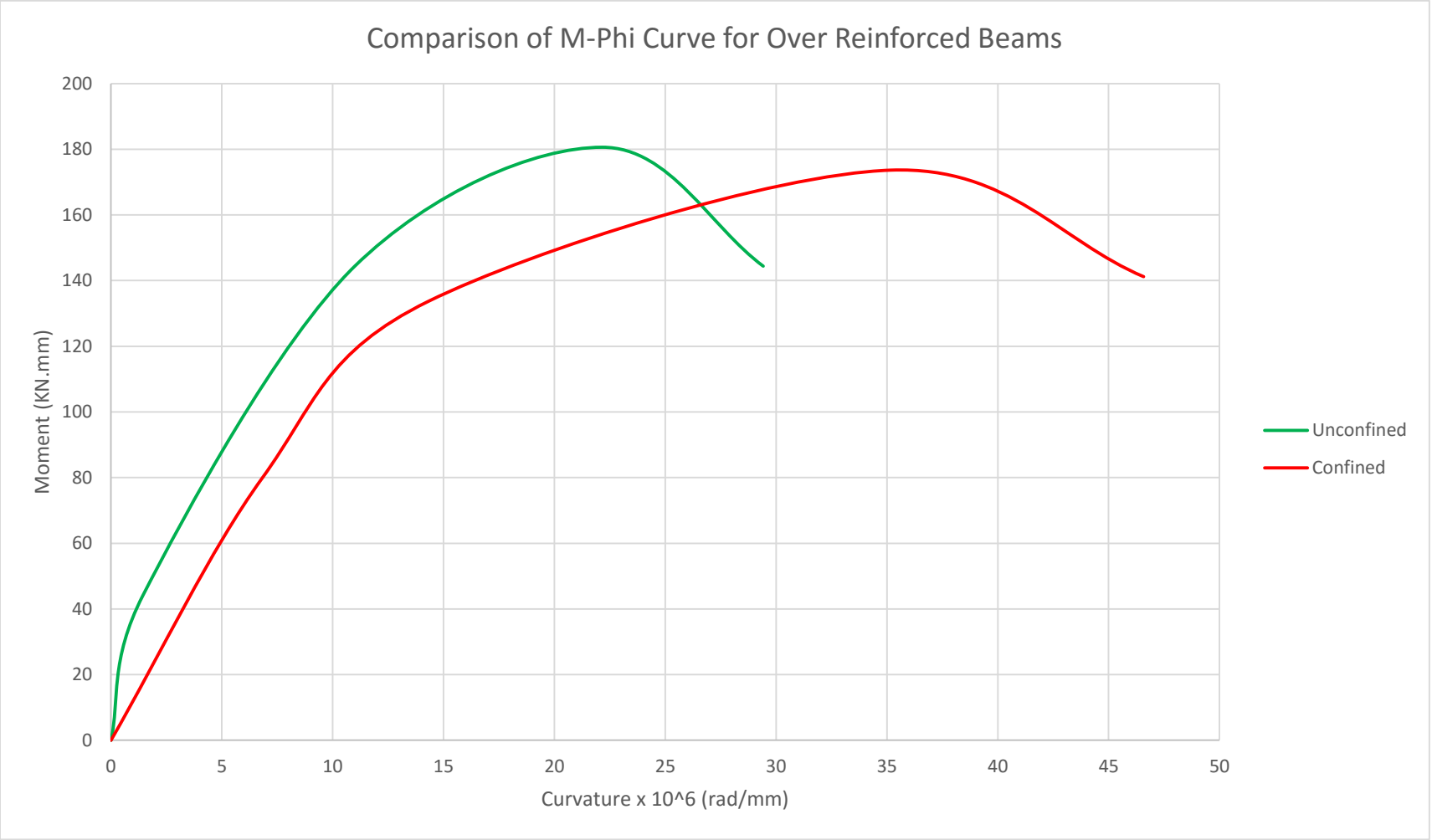

Figure 0-6: *Mean M-Phi graph for Under Reinforced Un- Confined and Confined Beams*

4A- Calculation of predicted flexural capacity of confined under and over-reinforced beams

Under-Reinforced Confined Beam

a. Input Data

fc′= 30 Mpa, f_y = 510 Mpa, As = 1020 mm^2 (2#25 bars), s_v = 63.5 mm,

Asv = 71 mm^2, H = 150 mm, B= 140 mm, ρ_t = 0.022 (Eq.2.9)

b. Strength Gain Factor (K_s)

A_{co} = B*H = 21000 mm^2 , P_{occ} = (21000*30)/1000 = 630 KN

$$K_s = 1.0 + \frac{BH}{PoCC}\left[(1 - \sum_{i=1}^{n} ci^2)\left(1 - \frac{0.5s\tan\theta}{B}\right)\left(1 - \frac{0.5s\tan\theta}{H}\right)\right]\beta\,(\rho_t\, f_{sv})^{\gamma}$$

K_s = 1.38

c. Confined Concrete Strength

f_{cc} = K_s f_{cp} = 1.38*30 = 41.4 MPa

d. Confined Flexural Capacity

Assuming that the tensile force (T) is balanced by the compressive force (C). Total compressive force (C) is the sum of compressive forces in confined core, side cover and top cover

C = T (C_{core}+C_{side}+C_{top} = T)

Assume Ɛc = 0.005, Ɛs1 = .0022K_s = 0.00277, Ω = Ɛc/ $Ɛ_{s1}$ = 1.646,

ɑ = 0.823 ,T= As f_y = 1020*510 = 520.2 KN,

C_{core} = ɑƁf_{cc}Bx = 0.75*.889*41.4*140*x = 3874.21*x

C_{side} = ɑƁ$_1 f_c'$ (2b′)x = 0.837*0.85*30*2*30*x = 1259.06x (b′ = side cover)

C_{top} = Ɓ$_1 f_c'$ (d′)b = 0.85*30*17.5*140 = 62.475 KN (d′ = top cover)

x = 89.16 mm (x =depth of neutral axis)

$$Mcon1 = C_{core}\left(d'' - \frac{\alpha x}{2}\right) + C_{side}\left(d - \frac{\beta 1 x}{2}\right) + Ctop\,(d - \frac{d'}{2}), \quad (d'' = d\text{-}d')$$

Mcon1 = 120.79 kN.m

Over-Reinforced Confined Beam

Flexural capacity of confined over-reinforced beam is calculated by the same procedure as given below:

Mcon2 = 176.2 kN.m

Table 0-1: Comparison of Predicted and measured flexural capacities of Unconfined and confined beams

Beam Designation	Description	Predicted Moment (kN.m)	Predicted Mean Moment (kN.m)	Measured Moment (kN.m)	Measured Mean Moment (kN.m)
Under Reinforced Beams					
R-UR-1	**Reference Beam**	116.52	116.52	128.27	130.81
R-UR-2		116.52		133.35	
C-UR-1	**Confined Beam**	120.79	120.79	134.06	139.71
C-UR-2		120.79		150.01	
C-UR-3		120.79		135.06	
Over Reinforced Beams					
R-OR-1	**Reference Beam**	175.65	175.65	171.93	180.60
R-OR-2		175.65		189.28	
C-OR-1	**Confined Beam**	176.29	176.29	176.15	173.63
C-OR-2		176.29		176.4	
C-OR-3		176.29		168.36	

Table 0-2: Comparison of Ductility Index of unconfined and confined beams

Beam Designation	Description	Curvature Ductility Index	Average Ductility Index	Area Under Curve (kNmm)	Average
Under Reinforced Beams					
R-UR-1	**Reference Beam**	2.86	2.78	4789.34	4417.44
R-UR-2		2.7		4045.64	
C-UR-1	**Confined Beam**	3.22	3.62	4579.89	4677.51
C-UR-2		3.78		4837.21	
C-UR-3		3.85		4612.5	
Over Reinforced Beams					
R-OR-1	**Reference Beam**	2.59	2.68	6246.91	7262.14
R-OR-2		2.77		8277.28	
C-OR-1	**Confined Beam**	4.65	4.72	9214.43	7733.61
C-OR-2		4.82		7537.90	
C-OR-3		4.7		6448.79	

Comparison Summary of Average Ductility Index of under and over reinforced Beams

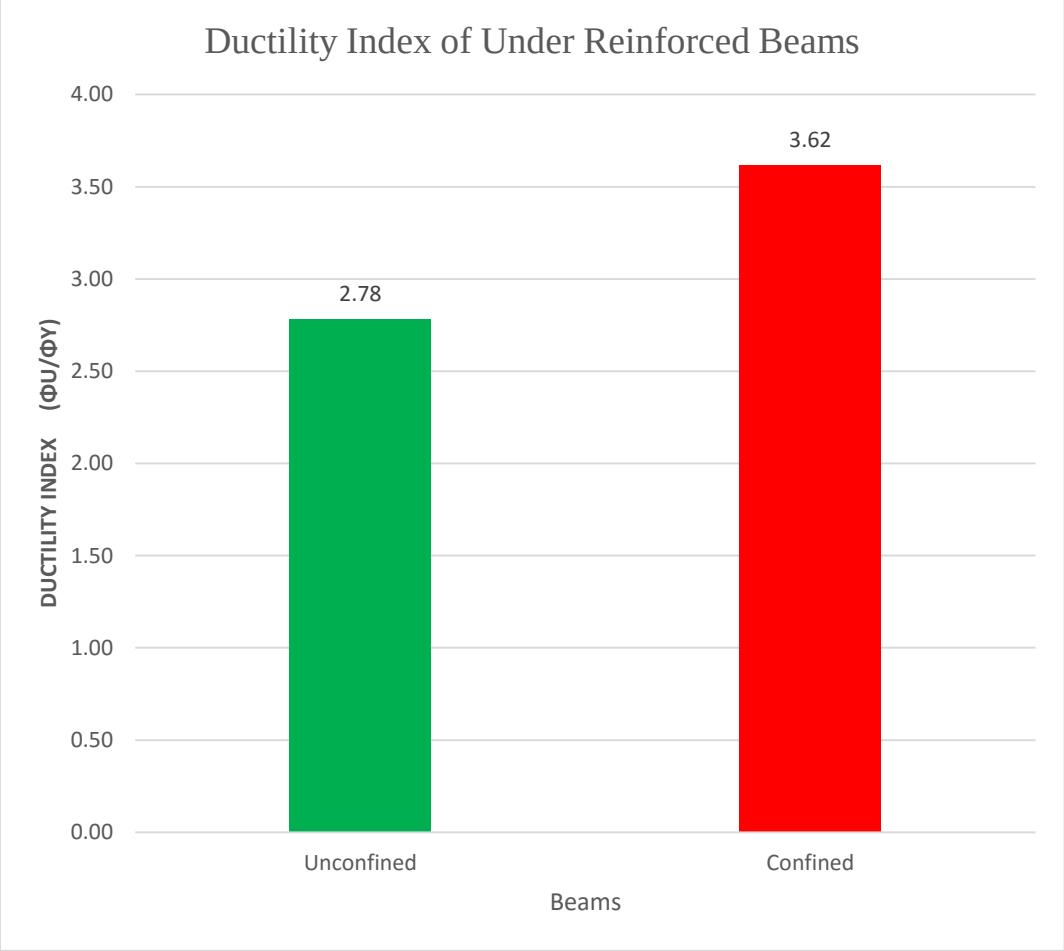

Figure 0-7: Average Ductility Index of Confined & Un-Confined Under Reinforced Beams

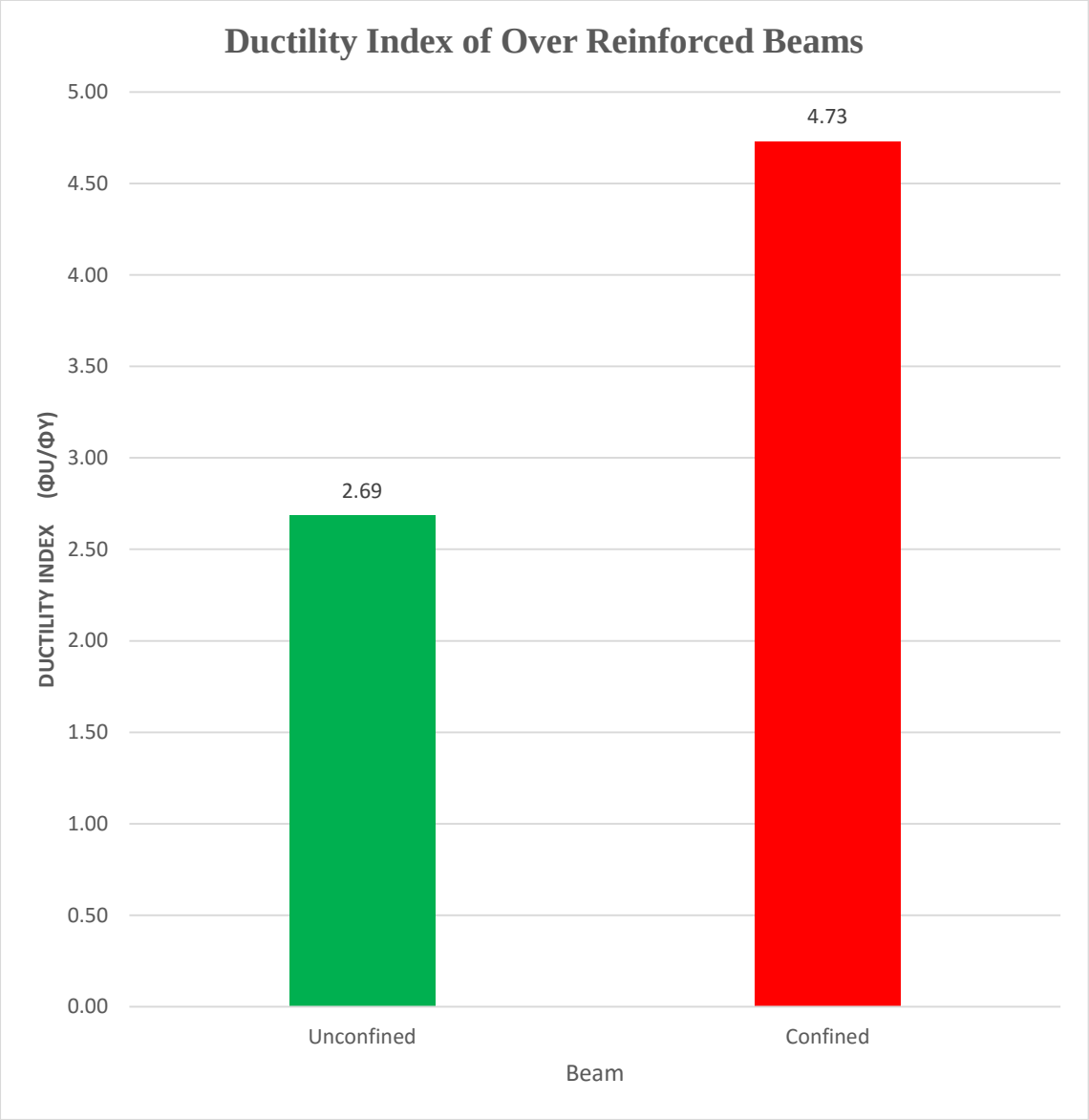

Figure 0-8: Average Ductility Index of Confined & Un-Confined Over Reinforced Beams